

Probe Report

Title: Hepatitis C Virus NS3 Helicase Inhibitor Discovery

Authors: Kelin Li^a, Kevin J. Frankowski^a, Alicia M. Hanson^b, Jean Ndjomou^b, Matthew A. Shanahan^b, Sourav Mukherjee^b, Rajesh Kolli^b, William R. Shadrack^b, Noreena L. Sweeney^b, Craig A. Belon^c, Ben Neuenswander^a, Jill Ferguson^d, Jeffrey Aubé^{a,e}, Frank J. Schoenen^a, Brian S. J. Blagg^{a,e} and David N. Frick^{b*}

^a University of Kansas Specialized Chemistry Center, University of Kansas, Lawrence, KS 66047; ^b Department of Chemistry and Biochemistry, University of Wisconsin-Milwaukee, 3210 N. Cramer St., Milwaukee, WI 53211; ^c Department of Biochemistry and Molecular Biology, New York Medical College, Valhalla, NY 10595; ^d Scripps Research Institute Molecular Screening Center, 10550 N. Torrey Pines Rd, La Jolla, CA 92037 and ^e Department of Medicinal Chemistry, University of Kansas, Lawrence, KS, 66047

*David N. Frick, Ph.D. – E-mail frickd@uwm.edu

Assigned Assay Grant #: 1 R03 MH085690-01

Screening Center Name & PI: None

Chemistry Center Name & PI: Jeffrey Aubé, University of Kansas Specialized Chemistry Center (KU SCC)

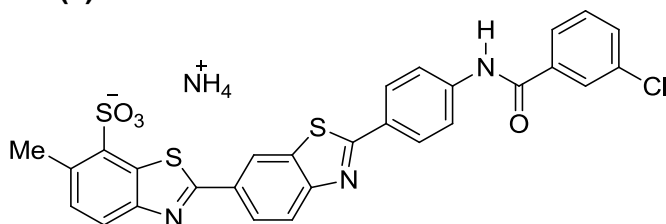
Assay Submitter & Institution: David N. Frick, University of Wisconsin-Milwaukee

PubChem Summary Bioassay Identifier (AID): 1830

Abstract

The Hepatitis C virus (HCV) is a major cause of liver failure and hepatocellular carcinoma, with about 170 million people infected worldwide. Replication of HCV in human cells requires the action of the HCV non-structural protein 3 (NS3), which exhibits both protease and helicase activities. Since there are numerous NS3 protease inhibitors but few NS3 helicase inhibitors, the goal here was to develop specific NS3 helicase inhibitors. During assay development, we discovered that trace components in the dye mixtures thioflavine S and primuline were potent inhibitors of the NS3 helicase. Based on the common structure of these components we designed **ML283**. The probe candidate is a potent inhibitor of the NS3 helicase enzyme and can be synthesized in the necessary quantities for further investigation. **ML283** is more potent and specific than other recently reported NS3 helicase inhibitors under the same assay conditions, allowing a direct comparison. Preliminary experiments indicate that this compound is able to penetrate cells and inhibit HCV replication with no significant cytotoxicity. Thus the probe would be a useful tool for the investigation of viral helicases.

Probe Structure(s) & Characteristics



CID 50930730
SID 114279600
ML283

CID/ML#	Target Name	IC50/EC50 (μM) [SID, AID]	Anti-target Name(s)	IC50/EC50 (μM) [SID, AID]	Fold Selective	Secondary Assay(s) Name: (% at 10 μM) [SID, AID]
CID 50930730/ ML283	Helicase 1b(con1)	2.6 ± 1 μM [SID 114279600, AID 602275]	SYBR Green I stained DNA	>100 μM [SID 114279600, AID 623970]	>38-fold	Replicon inhibition: 54 ± 10 [SID 114279600, AID 623962]
	Helicase 2a(JFH1)	3.9 ± 1 μM [SID 114279600, AID 602275]	<i>E. coli</i> SSB	201±119μM [SID 114279600, AID 623966]	77-fold	cell viability: 112 ± 4 [SID 114279600, AID 623961]

Recommendations for Scientific Use of the Probe

NS3 is a multifunctional protein encoded by HCV that is both a protease and a helicase. NS3 protease inhibitors are an important new class of antiviral drugs but they generally do not affect NS3 helicase activity, and few specific NS3 helicase inhibitors have been reported. The goal of this study is to find chemical probes that more specifically target NS3 helicase. Such compounds are needed to understand why the virus encodes a helicase, and they might be useful to design better drugs that could be combined with drugs that inhibit the NS3 protease.

Many of the potent HCV helicase inhibitors already reported in the literature also bind the helicase nucleic acid substrate. Helicase inhibitors that interact with DNA or RNA could also inhibit cellular nucleic acid enzymes like RNA polymerase. Starting with a compound that inhibits HCV helicase, in part, by binding nucleic acids, we have designed a series of compounds that bind DNA less tightly but still retain an ability to potently inhibit HCV helicase. These more specific compounds are less likely to disrupt the interaction of unrelated proteins with DNA or RNA, as is shown by the fact that they are over 50 times less active in assays with the unrelated *E. coli* single stranded DNA binding protein than the parent molecule.

In addition to possessing enhanced specificity, the probe reported here is more active than other recently reported compounds in assays performed under conditions where NS3 helicase is most active. The probe is also fluorescent, which could be a useful property of a tool molecule, it appears to enter cells, and it inhibits cell HCV replication. The probe is a less potent NS3 protease inhibitor than some of its analogues, suggesting they could be used together to reveal how the NS3 helicase and protease coordinate their actions.

Virologists could use the compounds reported here to study when, where, and why the NS3 helicase acts in cells. If the probe specifically stains NS3 in cells, it could also be used to diagnose HCV infection. Biochemists studying how NS3 unwinds RNA and DNA could use the probe to understand how the protein moves along nucleic acids and disrupts bonds holding the double helix together. Finally, the probe might be a useful starting point to design a new class of direct acting antivirals for future use in HCV treatment.

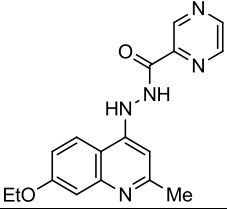
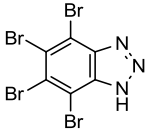
1 Introduction

The Hepatitis C virus (HCV) is a major cause of liver failure and hepatocellular cancer, with about 170 million people infected worldwide. The proteins encoded by HCV have all been intensely studied as drug targets (1). HCV has a small RNA genome that is directly translated by the infected host cell into a single precursor polyprotein that is processed by enzymatic cleavage into 10 proteins of diverse function. The nonstructural proteins include p7, NS2, NS3, NS4A, NS4B, NS5A, and NS5B, and are responsible for the replication and packaging of the HCV genome into capsids formed by the structural proteins (core, E1, E2) (2). NS3 is a multifunctional protein that cleaves viral and host proteins and rearranges nucleic acid duplexes in a reaction fueled by ATP hydrolysis. Newly approved HCV drugs target the NS3 protease (3, 4), but few specific compounds have been reported that inhibit the NS3 helicase function. Replication of HCV in human cells requires the action of the NS3 helicase (5), suggesting that specific helicase inhibitors could be used with the NS3 protease inhibitors as antiviral agents. Specific NS3 helicase inhibitors would also be valuable reagents to study the precise role that NS3 and related proteins play in viral replication.

Unlike other helicases that prefer either RNA or DNA, the HCV helicase unwinds DNA/DNA, RNA/RNA, and RNA/DNA duplexes (6). The HCV NS3 helicase mediates this relatively promiscuous ATP-dependent “active” duplex unwinding because the interaction between the enzyme and the DNA or RNA substrate is mediated by phosphate groups and not by the nucleotide base or sugar moieties (7). *In vitro*, HCV helicase unwinds DNA more efficiently and rapidly than RNA (8), but why NS3 prefers DNA remains a mystery since the virus has no DNA stage and there are still conflicting reports regarding whether NS3 enters the nucleus during the viral lifecycle. Nevertheless, DNA is typically used as a surrogate for RNA in high throughput screens (HTS) used to discover and characterize helicase inhibitors. Any compound that binds DNA to stabilize or disrupt the double helix could therefore influence helicase action, and we find that most of the reported potent HCV helicase inhibitors seem to exert their action through the DNA substrate. Some of these compounds might inhibit HCV in cells, but they have limited utility as chemical probes because their lack of specificity might lead to numerous off-target effects. As one example, several potent HCV helicase inhibitors have been shown to affect transcription by cellular RNA polymerase (9). The identification of specific inhibitors of HCV NS3 helicase will therefore add insights into the biology of HCV infection and replication, and would serve as valuable tools for inhibiting HCV replication in human cells.

At the time of the grant award for this project a few potent inhibitors of NS3 helicase were known (**Table 1.**), but they either did not inhibit helicase under our assay conditions or were found to bind DNA, casting doubt on their selectivity for the NS3 enzyme itself (10). For example, neither the halogenated benzotriazole (CID 1694) (11), nor the “nucleotide mimic” (12) inhibited NS3 helicase in the assays described here. A peptide based inhibitor (13) was a more potent inhibitor in the assay used here (14) than was previously reported (15), but we later

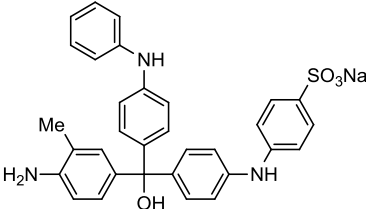
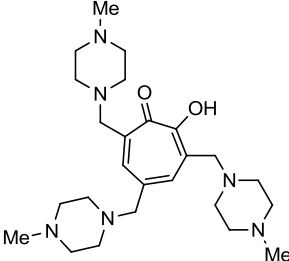
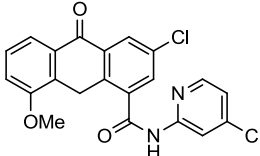
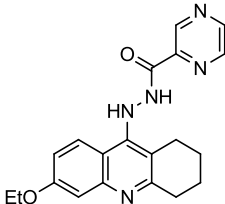
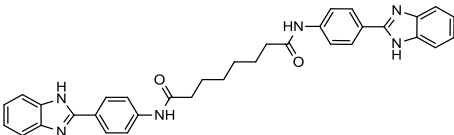
found that this arginine-rich peptide binds nucleic acid more tightly than it binds NS3 helicase (data not shown).

Table 1. Inhibitors of NS3 helicase known at the time of grant award					
Entry	CID	Name	Structure	Potency IC ₅₀ (μM)*	
	SID			NS3 helicase (literature)	NS3 helicase (assay provider lab) [†]
1	Not assigned in PubChem	QU663		75	>100
2	1694	4,5,6,7-tetetrabromo-benzotriazole		60	>100
	multiple				
3	Not assigned in PubChem	NS3pep	RRGRTGRGRRGLYR	0.7	0.1

* IC₅₀ values unless otherwise noted.

[†] IC₅₀ value is using the 1b(con1) genotype.

Since there is currently broad interest in investigating NS3 helicase as a target, during the course of the project several additional compounds were reported to inhibit or bind NS3 helicase (**Table 2.**). Again, some more recently reported helicase inhibitors such as the fluoroquinolones (16) and pyrrolo derivatives (17) had no effect on NS3h reactions catalyzed in vitro by the proteins used here. Only the five previously reported helicase inhibitors that affected NS3h or HCV replicons used here were, therefore, included in all the assays to provide a direct comparison for potential probe candidates. The compounds used for comparison included another nucleotide-mimic CID 50904396 (18), an acridone CID 46202556 (19), a triphenylmethane CID 3084034 (20) a tropolone CID 46913723 (21), and a symmetrical benzimidazole CID 486270 (27).

Table 2. Inhibitors of NS3 helicase disclosed since the time of grant award					
entry	CID	synthesized (S) or purchased (P)	structure	potency IC ₅₀ (μM)*	
	SID			NS3 helicase (literature)	NS3 helicase (assay provider lab) [†]
1	3084034	S		12.6	29 ± 16
	110923084				17 ± 7
2	46913723	S		3.4	24 ± 30
	110923085				19 ± 8
3	46202556	S		1.5	28 ± 25
	110923083				25 ± 6
4	50904396	S		K _i = 0.02 μM	>100
	110923082				>100
5	486270	S		nd	7.5 ± 0.1
	124349743				4.7 ± 1.6

* IC₅₀ values unless otherwise noted.

[†] Top IC₅₀ value is using the 1b(con1) genotype and the bottom value is using the 2a(JFH1) genotype.

2 Materials and Methods

Material and Methods are provided in Appendix A.

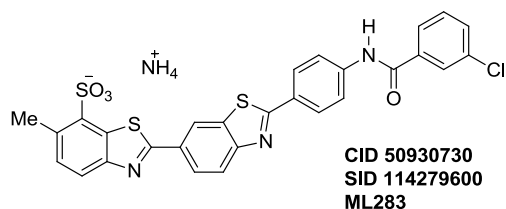
2.1 Assays

Details for the assays listed in **Table 3.** are provided in Appendix A.

Table 3. List of Assays and AIDs for this Project				
PubChem BioAssay Name	AID	Assay Type	Assay Format	Assay Detection and Plate Density
Summary of probe development efforts to identify benzothiazole inhibitors of non-structural protein 3 helicase (NS3)	1830	N/A	N/A	N/A
Fluorescence-based biochemical dose response assay to identify inhibitors of the Hepatitis C Virus non-structural protein 3 helicase (NS3h_con1) [Primary Screening]	602275	Enzymatic	Biochemical	Fluorescence Intensity; 384-well
Fluorescence-based biochemical dose response assay to identify inhibitors of the Hepatitis C Virus non-structural protein 3 helicase (NS3h_JFH1) [Primary Screening]	602275	Enzymatic	Biochemical	Fluorescence Intensity; 384-well
Counterscreen for HCV NS3 helicase inhibitors: Fluorescence-based biochemical dose response assay for compounds that cause fluorescent intercalator displacement (FID) using ethidium bromide. [Confirmatory]	623972	Binding	Biochemical	Fluorescence Intensity; 96-well
Counterscreen for HCV NS3 helicase inhibitors: Fluorescence-based biochemical dose response assay for compounds that cause fluorescent intercalator displacement (FID) using SYBR Green I. [Confirmatory]	623970	Binding	Biochemical	Fluorescence Intensity; 96-well
Counterscreen for HCV NS3 helicase inhibitors: Fluorescence-based biochemical dose response binding assay for single stranded DNA binding protein (SSB) to single stranded DNA. [Confirmatory]	623966	Binding	Biochemical	Fluorescence Polarization; 384-well
Fluorescence-based counterscreen assay for HCV NS3 helicase inhibitors: biochemical screening assay to identify compounds that inhibit the NS3 protease activity [Confirmatory]	623964	Protease	Biochemical	Fluorescence Intensity; 384-well
Fluorescence-based counterscreen assay for HCV NS3 helicase inhibitors: biochemical screening assay to identify compounds that inhibit ATPase activity [Confirmatory]	623973	Enzymatic	Biochemical	Fluorescence Intensity; 384-well
Luciferase cell-based assay to determine inhibition of HCV RNA replication [Confirmatory]	623962	Protein Expression	Cell Lysate Assay	luminescence; 96-well
Cell-based assay to determine general cytotoxicity [Confirmatory]	623961	Viability	Cell Lysate Assay	luminescence; 96-well
Cellular HCV RNA quantification assay [Confirmatory]	623968	RNA expression	Cell Lysate Assay	Fluorescence Intensity; 96-well

2.2 Probe Chemical Characterization

Probe Chemical Structure, Physical Parameters, and Probe Properties



Physiochemical Parameters:

Molecular Formula: C₂₈H₂₁ClN₄O₄S₃

Molecular Weight: 609.1387

Exact mass: 608.0413

ClogP: 5.3

Topological Polar Surface Area: 108

Probe Properties:

Purity (LCMS, 214 nm): 93.6%

Physical State: yellow solid

Figure 1. Property summary of probe compound **ML283**/SID 114279600 (CID 50930730)

Structure verification and Purity: ¹H NMR, ¹³C NMR, LCMS and HRMS

For probe ML283:

Proton and carbon NMR data for SID 114279600 (CID 50930730): Detailed analytical methods and instrumentation are described in section 2.3, entitled “Probe Preparation” under general experimental and analytical details. The numerical experimental proton and carbon data are presented below. Associated spectra are included in Appendix B.

SID 114279600 (CID 50930730) Proton NMR Data: ¹H NMR (500 MHz, DMSO) δ 10.69 (s, 1H), 8.93 (d, *J* = 1.8 Hz, 1H), 8.26 (dd, *J* = 1.8, 8.5 Hz, 1H), 8.18 – 8.15 (m, 3H), 8.08 – 8.01 (m, 3H), 7.97 (d, *J* = 8.2 Hz, 1H), 7.91 (d, *J* = 8.0 Hz, 1H), 7.74 – 7.67 (m, 1H), 7.61 (t, *J* = 7.9 Hz, 1H), 7.38 (d, *J* = 8.6 Hz, 1H), 7.19 (s, 1H), 7.09 (s, 1H), 6.99 (s, 1H), 2.71 (s, 3H).

SID 114279600 (CID 50930730) Carbon NMR Data: ¹³C NMR (126 MHz, DMSO) δ 169.3, 168.6, 164.4, 155.2, 152.2, 142.1, 140.1, 136.5, 135.4, 133.23, 133.17, 132.3, 131.7, 130.5, 130.3, 130.1, 128.1, 128.0, 127.5, 126.6, 125.4, 123.0, 122.6, 121.2, 120.5, 20.3.

LCMS and HRMS data for SID 114279600 (CID 50930730): Detailed analytical methods and instrumentation are described in section 2.3, entitled “Probe Preparation” under general experimental and analytical details. Purity assessment by LCMS at 214 nm for SID114279600 (CID50930730) revealed purity at 214 nm of 93.6 % (retention time = 2.68 minutes). The experimental LCMS and HRMS spectra are included in Appendix B. HRMS (*m/z*): calcd for C₂₈H₁₉ClN₃O₄S₃ (neutral M+H) 592.0226; found 592.0228.

Solubility:

For probe ML283:

Aqueous solubility was measured in a mock assay matrix (25 mM MOPS, 1.25 mM MgCl₂, 0.05 mM DTT, 5 μg/mL BSA, 0.01% v/v final [Tween 20] and 5% v/v final [DMSO], pH = 6.5) at room temperature (23 °C). These modified conditions were chosen to better mimic the environment of the assay. The solubility of probe SID 114279600 (CID 50930730) under the assay conditions was determined to be 29.2 μM at pH 6.5.

Stability

For probe ML283:

The aqueous stability of ML283 was measured with and without the addition of acetonitrile cosolvent (**Figure 2**.) and found to be 100% at 48 hours in the presence of the cosolvent, which is not as prone to interference from compound precipitation during the experiment.

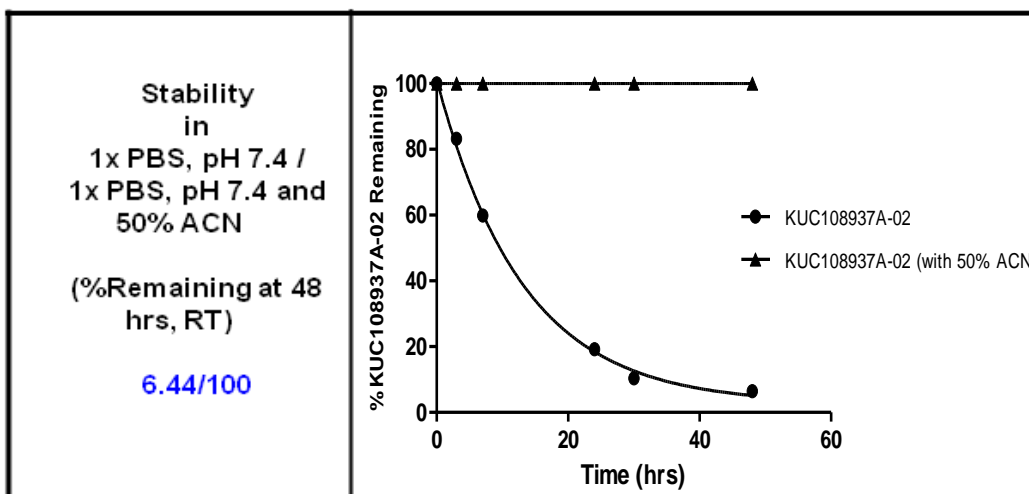


Figure 2. Effect of cosolvent on the apparent stability of **ML283**.

Synthetic Route

For probe ML283:

The probe compound SID 114279600 (CID 50930730) and numerous analogues were synthesized by the reaction sequence shown in **Figure 3**. Thus, the isolated, pure dimeric component from the dye primuline, **P2** (CID 44251428) was diversified with various acid chlorides or other activated coupling partners.

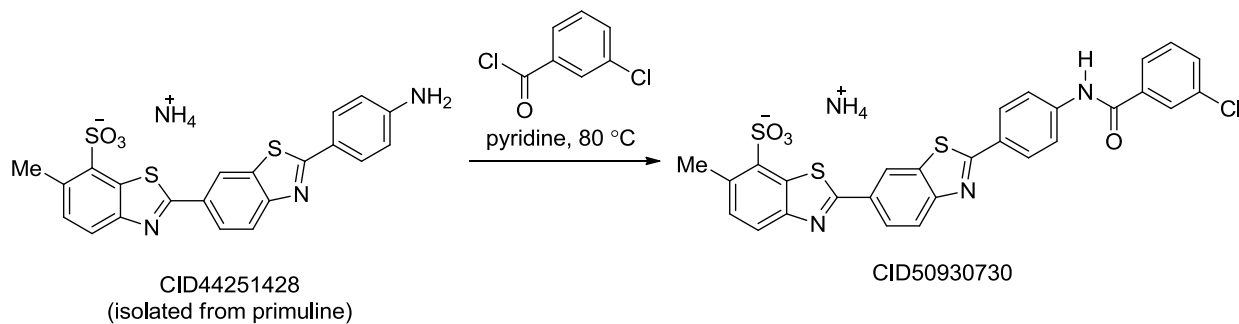


Figure 3. General synthetic route for preparing probe compound SID 114279600 (CID 50930730) and associated analogues

Submission of Probe and Five Related Analogues to the MLSMR

For probe ML283:

Samples of the probe compound and supporting analogues were shipped to the MLSMR on December 12, 2011.

Table 4. Probe and analogue submissions to MLSMR (BioFocus DPI) for NS3 helicase inhibitor discovery							
Probe - ML283 (CID 50930730)							
Probe /Analogue	Internal KU ID	MLS_ID (MLSMR)	CID	SID	Source (vendor or KU syn)	Amt (mg)	Date ordered/ Submitted
Probe ML283	KUC108937A-02	MLS003882779	50930730	131341901	KU syn	21.8	12/12/11
Analogue 1	KUC107956A-02	MLS003882780	49849293	131341962	KU syn	21.2	12/12/11
Analogue 2	KUC107965A-03	MLS003882781	49849294	131341963	KU syn	23.3	12/12/11
Analogue 3	KUC108938A-02	MLS003882782	50930749	131341964	KU syn	21.4	12/12/11
Analogue 4	KUC108934A-02	MLS003882783	50930737	131341965	KU syn	23.0	12/12/11
Analogue 5	KUC110001N-02	MLS003882784	53356656	131341966	KU syn	23.3	12/12/11

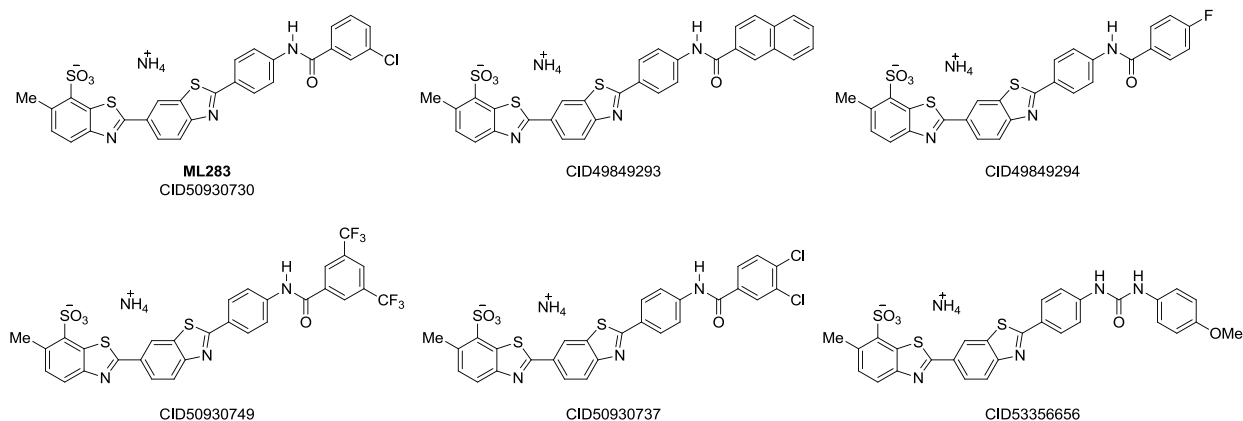


Figure 4. Structures of the probe candidate and supporting analogues.

2.3 Probe Preparation

General synthesis and analysis experimental details: All reagents were used as received from commercial suppliers. The ^1H and ^{13}C spectra were recorded on a Bruker Avance 400 MHz or 500 MHz spectrometer. Chemical shifts are reported in parts per million and were referenced to residual proton solvent signals. Flash column chromatography separations were performed using the Teledyne Isco CombiFlash R_F using RediSep R_F silica gel columns. TLC was performed on Analtech UNIPLATE silica gel GHLF plates (gypsum inorganic hard layer with

fluorescence). TLC plates were developed using iodine vapor. HPLC/MS analysis was carried out with gradient elution (5% CH₃CN to 100% CH₃CN) on an Agilent 1200 RRLC with a photodiode array UV detector and an Agilent 6224 TOF mass spectrometer (also used to produce high resolution mass spectra). Purification was carried out by Mass Directed Fractionation with gradient elution (a narrow CH₃CN gradient was chosen based on the retention time of the target from LCMS analysis of the crude sample) on an Agilent 1200 instrument with photodiode array detector, an Agilent 6120 quadrupole mass spectrometer, and a HTPAL LEAP autosampler. Fractions were triggered using an MS and UV threshold determined by HPLC/MS analysis of the crude sample. The conditions for HPLC analysis included the following: Waters BEH C-18, 1.7 μm, 2.1 x 50mm column; 0.6 ml/min flow rate; and pH 9.8 NH₄OH aqueous mobile phase. The conditions for purification included: Waters XBridge C18 5μm, 19 x 150mm column; 20 ml/min flowrate pH 9.8 NH₄OH aqueous mobile phase.

The probe compound was synthesized using the following protocols:

For probe ML283:

2'-(4-(3-Chlorobenzamido)phenyl)-6-methyl-[2,6'-bibenzo[d]thiazole]-7-sulfonic acid: To a solution of **P2** (CID 44251428) (9.9 mg, 0.022 mmol) in pyridine (1 mL) at 80 °C, was added 3-chlorobenzoyl chloride (5.8 mg, 0.033 mmol, 1.5 equiv.). The reaction mixture was stirred at 80° C overnight. The product was isolated via reverse phase preparative HPLC to give a yellow solid (6.6 mg, 0.011 mmol, 51% yield).

Submitted Probe Analogues:

Analytical data for the five analogues submitted in support of the probe can be found in Appendix C.

3 Results

3.1 Assay Development and Screening

To facilitate HCV helicase inhibitor identification, Belon & Frick developed a new helicase assay that simultaneously identifies compounds that interact with the helicase substrate and compounds that inhibit helicase action (14). This molecular beacon-based helicase assay (MBHA) uses a dual-labeled hairpin-forming DNA oligonucleotide annealed to a longer oligonucleotide, which forms a tail for the helicase to load (**Figure 5**). Once ATP is added, the helicase displaces the molecular beacon, resulting in a decrease in substrate fluorescence. By comparing substrate fluorescence before ATP is added (F_0), one can identify compounds that bind the MBHA substrate. At the same time, compounds that inhibit helicase action can be identified by fluorescence changes in an MBHA before and 30 (or 60) minutes after ATP addition (F_{30}/F_0 or F_{60}/F_0 ratio). In other words, the MBHA can be used as an “internal” counter-screen to identify compounds that appear to affect unwinding because they interfere with the assay. The most common types of interfering compounds are those that fluoresce or absorb light at the same wavelengths as the MBHA Cy5-labeled substrate. Alternatively, other

compounds may bind the DNA substrate and distort it to change how the quenching moiety on the beacon is oriented relative to the Cy5 fluorophore.

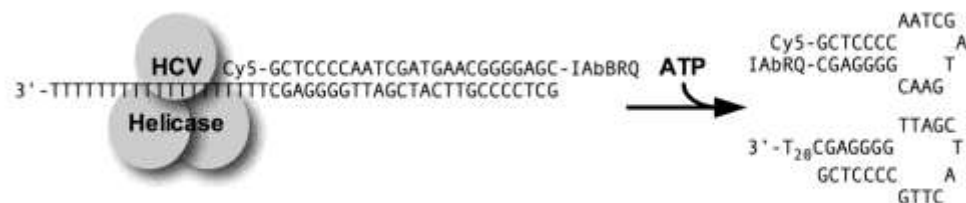


Figure 5. Schematic drawing of the MBHA mechanism

To identify HCV helicase inhibitors, the MBHA was used to screen the National Cancer Institute Developmental Therapeutics Program's Mechanistic Set Library (http://dtp.nci.nih.gov/branches/dscb/mechanistic_explanation.html). In total, 827 compounds (at 20 μM) were screened using a MBHA with a DNA substrate (**Figure 6.** and Appendix D). When compound interference is plotted versus percent inhibition (**Figure 7.**), it is clear that the majority of compounds that appeared to inhibit HCV helicase also quenched fluorescence of the MBHA substrate. Compound interference in the MBHA was evaluated by comparing the fluorescence of assays containing each compound to the fluorescence of DMSO-only negative controls before the addition of ATP. Hits were therefore defined as those compounds that did not interfere with the assays more than 20%, of which twelve were identified. These twelve hits were then subjected to a counterscreen that was designed to independently identify compounds that exhibit DNA-binding properties using a modified fluorescent intercalator displacement (FID) assay (22). The FID counterscreen used ethidium bromide to determine a molecule's ability to bind DNA, and is based on the assumption that a DNA binding compound would displace a fluorescent DNA intercalating agent, leading to an observable decrease in observed fluorescence. Compounds were tested at 1.5 μM in the presence of the 25 base pair substrate used in the helicase assays (**Figure 7**). Results showed that even at a compound concentration 13-times lower than that used in the MBHA, most of the hit compounds decreased the fluorescence of an ethidium bromide-DNA complex by more than 10%, indicative of the molecule's ability to bind DNA. The DNA minor groove-binding compound Berenil ($\text{EC}_{50}=1.6\pm 0.1$ μM) was used a positive control in all FID assays (23).

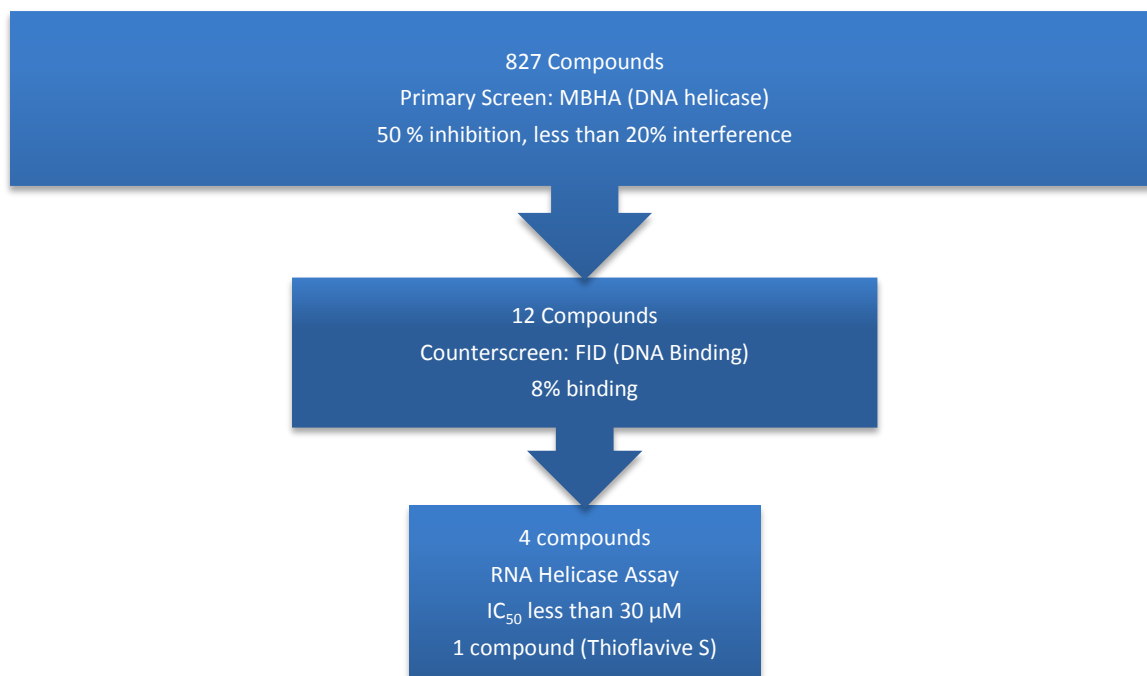


Figure 6. Compound attrition of the NCI Mechanistic Set library during screening phases.

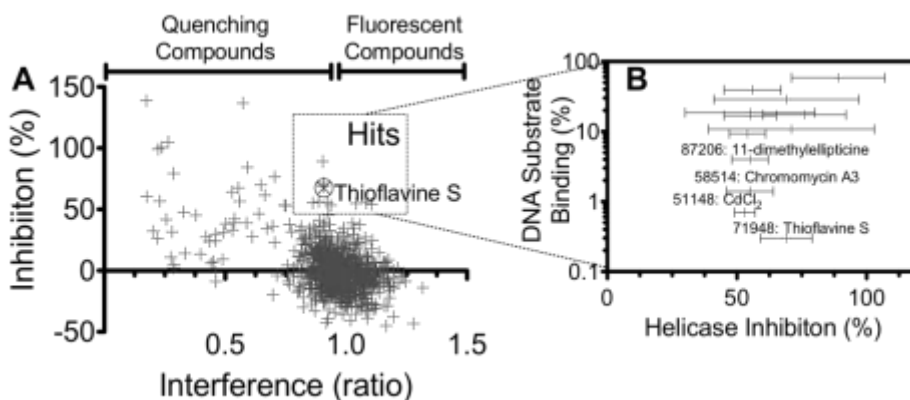


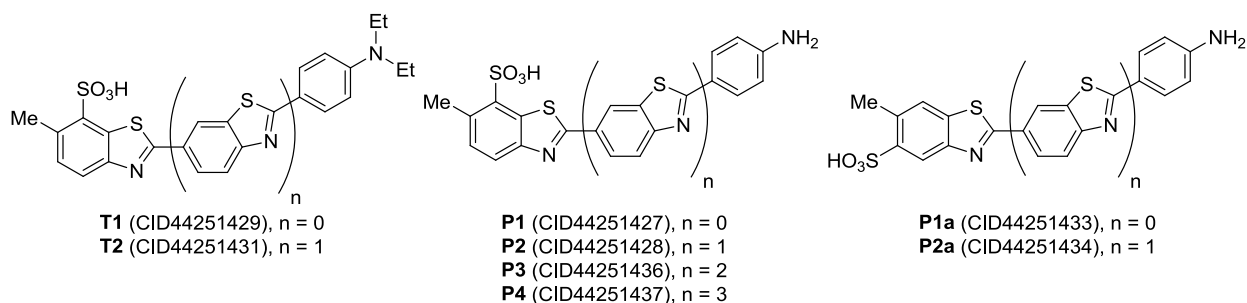
Figure 7. (A) The NCI Mechanistic Set of 827 compounds was screened with an MBHA, each at 20 μM. Fluorescence was read before and 30 minutes after ATP addition and compound inhibition was calculated. Hits were defined as compounds inhibiting more than 50% and interfering less than 20%. (B) The hits from the MBHA primary screen were tested for their DNA binding capacity with an FID counterscreen at 1.5 μM compound concentration, and percent binding was calculated. Numbers refer to Cancer Chemotherapy National Service Center (NSC) numbers.

Four compounds decreased the fluorescence of DNA-bound ethidium bromide less than 8%. The first, CdCl₂, was a known HCV helicase inhibitor that binds in place of the magnesium ion needed for ATP hydrolysis to fuel unwinding (24). The second, ellipticine, was found to fully quench DNA-bound ethidium bromide fluorescence at higher concentrations, and the IC₅₀ value

for ellipticine in MBHAs ($5.6 \pm 0.8 \mu\text{M}$) was similar to its apparent affinity for DNA, suggesting that it inhibited the helicase by interacting with the substrate. Chromomycin A3 inhibited HCV helicase catalyzed-DNA unwinding with an IC_{50} of $0.15 \pm 0.03 \mu\text{M}$, but had no effect on HCV helicase catalyzed RNA unwinding (data not shown). This false positive can be explained by the fact that Chromomycin A3 functionally resembles ethidium bromide as they both represent fluorescent DNA binding compounds (25). This result also demonstrates that not all DNA binding compounds will decrease DNA-bound ethidium bromide fluorescence in an ethidium bromide-based FID assay. The final sample, thioflavine S (CID 415676), did not affect DNA-bound ethidium bromide fluorescence until its concentration exceeded $100 \mu\text{M}$, at which point a 20% fluorescence decrease was observed (**Figure 11.A**). In dose response experiments, thioflavine S (CID 415676) inhibited HCV-helicase catalyzed DNA unwinding with an IC_{50} of $16 \pm 4 \mu\text{M}$, and it inhibited HCV catalyzed RNA unwinding with an IC_{50} of $12 \pm 2 \mu\text{M}$.

Thioflavine S (CID 415676) is not a single compound but rather a heterogeneous dye that is structurally related to another heterogeneous yellow dye, primuline (CID 415713) (24, 26). Primuline (CID 415713) inhibited HCV helicase in MBHAs with similar potency ($11 \pm 1 \mu\text{M}$) as thioflavine S (CID 415676). To better understand how these dyes inhibit HCV helicase, both mixtures were separated using reverse-phase preparative HPLC or a combination of normal phase silica gel column chromatography and reverse-phase preparative HPLC.

The structure of commercial samples of thioflavine S (CID 415676) is not reported consistently, or is left intentionally vague, creating confusion over the chemical identity of the screening hit. For instance, the MSDS (Sigma Aldrich) for thioflavine S describes the compound only as “methylated, sulfonated primuline base.” In the NCI and PubChem online databases, thioflavine S (CID 415676, SID 550242, NSC71948) was reported as a mixture of methylated benzothiazoles, and Packham’s group also reported the same structure (27). To identify the components of commercially obtained thioflavine S (CID 415676) responsible for the observed activity, we purified the commercial sample (Sigma cat. #T1892) via reverse-phase preparative HPLC chromatography to obtain two compounds (**T1** (CID 44251429) and **T2** (CID 44251431)), the structures of which were ascertained using NMR, and LC/MS (**Figure 8**).



thioflavine S (CID415676) = mixture of **T1**, **T2** and minor components (not isolated)

primuline (CID415713) = mixture of **P1**, **P2** and minor components: **P1a**, **P2a**, **P3**, **P4** and others (not isolated)

*All the isolated compounds are ammonium salts except **P4**.

Figure 8. Structures of the isolated components of thioflavine S (**T**) and primuline (**P**).

Contrary to our expectation that the isolated compounds would be methylated primuline derivatives, isolated **T1** (CID 44251429) and **T2** (CID 44251431) were the N, N-diethyl products of the primuline monomeric and dimeric benzothiazoles. Of these, only **T2** (CID 44251431) manifested inhibitory activity against helicase-catalyzed DNA unwinding (**Table 5**). Encouraged by these results, the dye primuline (CID 415713, MP Biomedicals cat. #195454) was also purchased and purified. Primuline (CID 415713) inhibited HCV helicase catalyzed DNA unwinding with about half the potency as **T2** (CID 44251431) (**Table 5**).

In total, six compounds were isolated from primuline (CID 415713). The two major components, **P1** (CID 44251427) and **P2** (CID 44251428), were separated via reverse-phase preparative HPLC in 9.2% and 7.6% isolated yield (by weight) for **P1** (CID 44251427) and **P2** (CID 44251428), respectively. In the MBHA, **P2** (CID 44251428) was equipotent to the primuline mixture (CID 415713), while **P1** (CID 44251427) was inactive. That the purified major active component **P2** (CID 44251428) did not possess increased potency compared to the mixture containing the inactive **P1** (CID 44251427) was unexpected and hinted that highly potent components could be present in the primuline mixture in small amounts. The direct isolation of minor components via reverse-phase preparative HPLC of the dye mixture was not successful. Hence, the purification procedure was modified, enabling the isolation of four minor components. Four chromatographic bands enriched with minor components (UV and LC-MS) were obtained from silica gel chromatography of commercial primuline (CID 415713) upon elution with 20% DCM/MeOH. Subsequent reverse-phase preparative HPLC purification afforded the relatively minor components **P1a** (CID 44251433), **P2a** (CID 44251434), **P3** (CID 44251436) and **P4** (CID 44251437), where **P3** (CID 44251436) and **P4** (CID 44251437) represented 0.49% and 0.23% isolated yield (by weight) of the dye, respectively. All purified compounds were composed of a central benzothiazole oligomer of 1-4 units terminating with a *p*-aminobenzene group (**Figure 8**).

In the MBHA, all of the compounds purified from primuline were helicase inhibitors although **P1** (CID 44251427) and **P1a** (CID 44251433), only partially inhibited unwinding at the highest concentrations tested (**Figure 9.B**). Potency correlated directly with the length of the benzothiazole chain. For **P3** (CID 44251436) or **P4** (CID 44251437), only about 1 μM of either was needed to reduce the rate of helicase catalyzed DNA unwinding by 50% (**Figure 9**, **Table 5**).

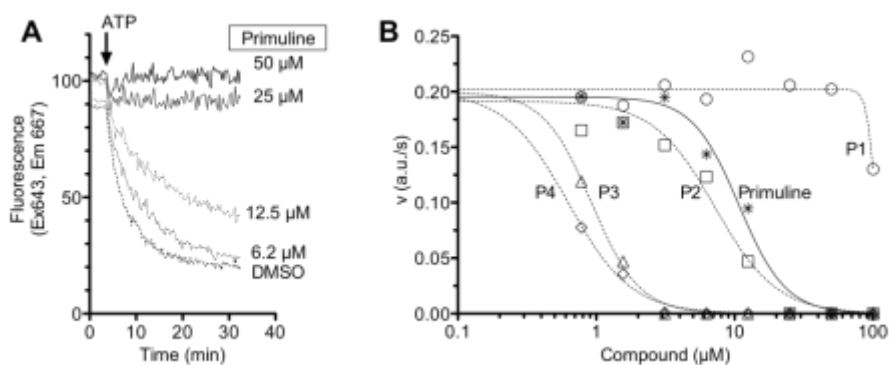


Figure 9. Effects primuline and its components on HCV helicase catalyzed DNA unwinding. (A) MBHAs performed at various concentrations of primuline (CID 415713). Reactions were initiated by adding ATP at the indicated time. (B) Initial rates of DNA unwinding in MBHAs containing indicated concentrations of primuline (CID 415713) (*), compound **P1** (CID 44251427) (circles), **P2** (CID 44251428) (squares), **P3** (CID 44251436) (triangles), or **P4** (CID 44251437) (diamonds). Data are fit to Eq. 3 (methods). IC₅₀'s listed in **Table 5**. are the averages from three separate titrations with each compound.

These purified compounds resemble molecules known to bind DNA, typically along the minor groove, such as the cyanine dye known as BEBO (CID 11741853) (**Figure 10.**), (28, 29) but unlike many DNA binding benzothiazoles, these helicase inhibitors are not positively charged. Instead they are anionic, due to the sulfate groups on the terminal benzothiazole rings.

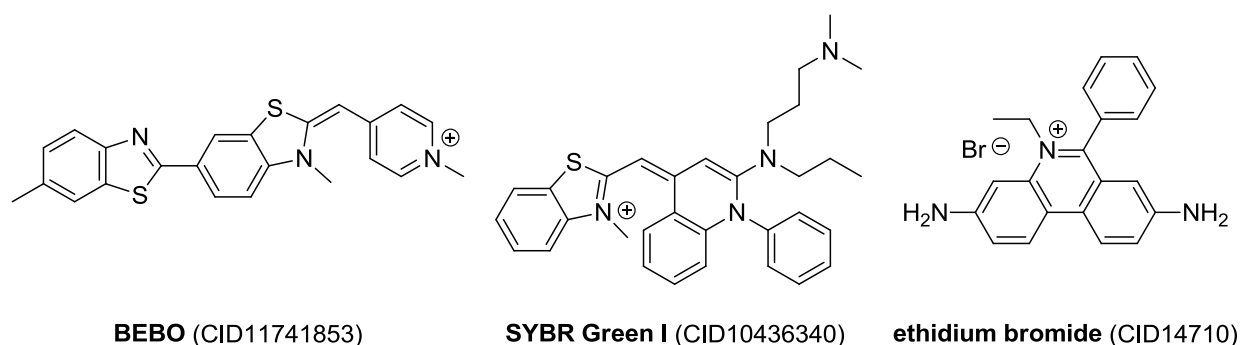


Figure 10. Structures of representative DNA binding agents

To test if the primuline and thioflavine S components interact with DNA, FID assays were repeated with each. Again, ethidium-bromide-stained MBHA-substrate (i.e. the same sequence as that shown in **Figure 5.**, but without the Cy5 and IBQ modifications) fluorescence was read before and after compound addition. Far more thioflavine S was needed in this assay to influence ethidium-bromide-stained DNA fluorescence than known DNA-binding compounds (**Figure 11A**). In contrast to the parent dyes, less of the dye components were needed to effect ethidium-bromide-stained DNA fluorescence. All compounds, except **T1** (CID 44251429), **P1** (CID 44251427) and **P1a** (CID 44251433), decreased the fluorescence of ethidium-bromide-bound DNA by at least 10% when present at 100 μ M. However, only compounds **P3** (CID 44251436) and **P4** (CID 44251437) decreased ethidium-bromide-bound DNA fluorescence more than 50% at the highest concentration tested (**Figure 11B**).

Because **P3** (CID 44251436) and **P4** (CID 44251437) clearly interacted with ethidium-bromide-stained DNA, we suspected that the other dye components might also bind DNA, but in ways that do not displace the intercalated ethidium bromide. We therefore examined the effect of each compound on DNA stained with other dyes, and found that most compounds decreased the fluorescence of DNA stained with SYBR Green I (CID 10436340). The affinity of primuline (CID 415713), thioflavine S (CID 415676) and the purified compounds for the MBHA substrate DNA was therefore estimated using a modified FID assay where ethidium bromide (CID 14710) was replaced with SYBR Green I (CID 10436340). Less of each compound was needed to decrease the fluorescence of SYBR Green I stained DNA, and none of the compounds

appeared to bind DNA more tightly than the potency with which they inhibited the helicase reaction. As seen in other assays **P4** (CID 44251437) bound more tightly than all other compounds (**Figure 11.C, Table 5.**).

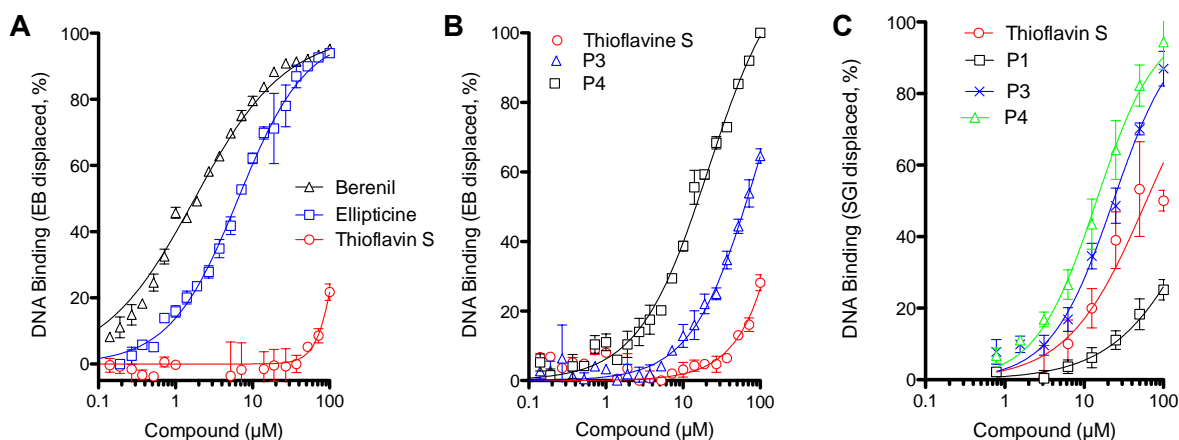


Figure 11. Compound interaction with the partially duplex helicase DNA substrate (A) The ability of thioflavine S to quench the fluorescence of a ethidium bromide-stained DNA substrate. Berenil and another known DNA binding compound, ellipticine, are included for comparison. Each 50 μL FID assay contained 25 mM MOPS pH 6.5, 0.16 μM HCV DNA substrate (4 μM base pairs), 2 μM ethidium bromide, 2% (v/v) DMSO and indicated amounts of each compound. (B) The ability of thioflavine S, and primuline components **P3** (CID 44251436) and **P4** (CID 44251437) to quench the fluorescence of an ethidium bromide stained DNA substrate. (C) The ability of thioflavine S, and primuline components **P1** (CID 44251427), **P3** (CID 44251436) and **P4** (CID 44251437) to quench the fluorescence of a SYBR Green I-stained DNA substrate.

In addition to inhibiting the helicase reaction and binding the helicase substrate, the dye components possess unique properties that make them uniquely useful molecular probes. First they are fluorescent, and their fluorescence can be used to monitor the compounds both *in vitro* and *in vivo* as is done both with thioflavine S (30) and primuline (31). Second, they inhibit other NS3 activities, namely the protein's ability to cleave ATP, the fuel for the helicase reaction, and the peptides via the protease domain. Though numerous NS3 protease inhibitors have been developed, none have yet been reported which inhibit both the NS3 protease and the NS3 helicase functions.

The compounds isolated from the two yellow dyes are all fluorescent, absorbing light around 350 nm, and emitting near 420 nm (**Figure 12.**). Their extinction coefficient and peak absorption wavelengths increase as the length of the benzothiazole oligomer increases. Their relative fluorescence decreases with the length of the benzothiazole chain. None of the compounds absorbed light near the absorption or emission wavelengths of the Cy5-labeled MBHA substrate, or the wavelengths where ethidium-bromide-stained DNA, SYBR Green I (CID

10436340) stained DNA, NS3-catalyzed peptide cleavage, or ATP hydrolysis were measured.

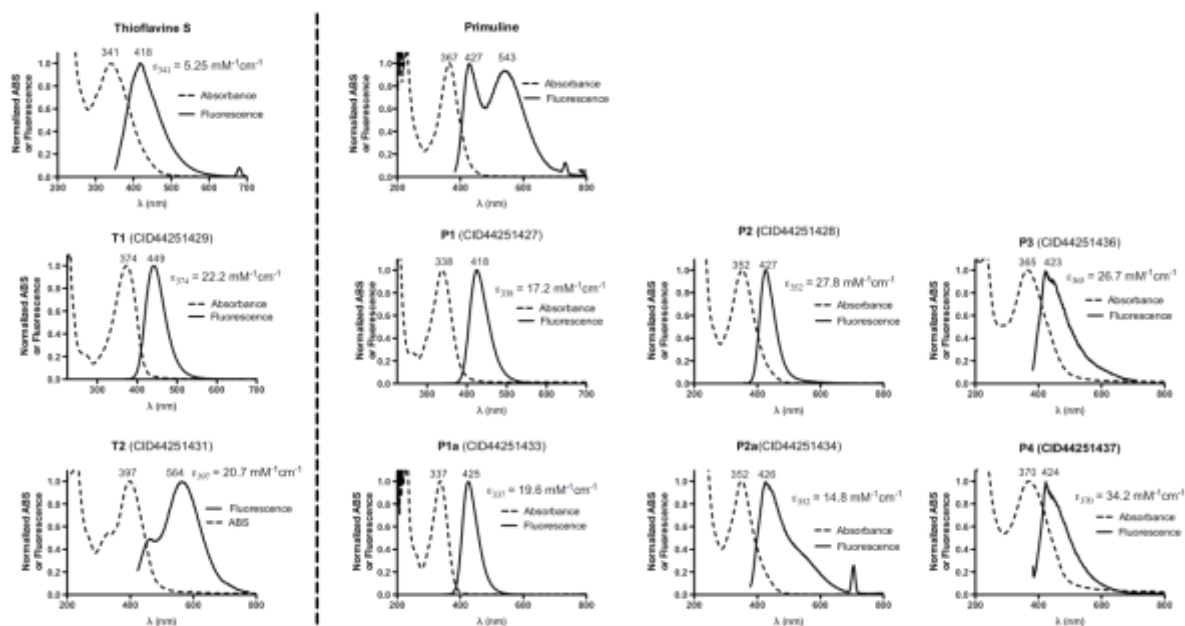


Figure 12. Absorbance and fluorescence emission spectra of primuline, thioflavine S, and their individual components.

Compounds can inhibit HCV helicase-catalyzed ATP hydrolysis by competing with either ATP or the nucleic acid that stimulates ATP hydrolysis. To test if thioflavine S inhibits the ATPase and examine where thioflavine S might act, initial rates of ATP hydrolysis were measured in the presence of various concentrations of ATP, RNA and thioflavine S. Thioflavine S did not compete with ATP (data not shown) but partially compete with RNA (**Figure 13A**). More RNA was needed to stimulate ATP hydrolysis as thioflavine S concentration increased. However, unlike compounds that bind in place of RNA (or DNA), thioflavine S retained inhibitory potential even when the protein was saturated with RNA (32). In addition, thioflavine S inhibited HCV helicase catalyzed ATP hydrolysis even in the absence of RNA, suggesting a direct interaction between the protein and thioflavine S.

The most potent primuline component, **P4** (CID 44251437) was then added to NS3 ATPase assays with and without RNA. **P4** (CID 44251437) inhibited ATP hydrolysis both in the presence and absence of RNA (**Figure 13B**), indicating that the compound is not simply sequestering RNA and preventing activation of ATP hydrolysis. It is also important to note that far more **P4** (CID 44251437) is needed to inhibit ATP hydrolysis in the absence of RNA, indicating that the presence of nucleic acid enhances the enzyme's affinity for the inhibitor (**Figure 13C**). When ATPase assays were performed with compounds isolated from thioflavine S and primuline (**Table 5**.) the same pattern was observed as previously seen in the MBHAs and FIDs (*i.e.* the longer benzothiazole oligomers were always more potent in all assays than the shorter oligomers).

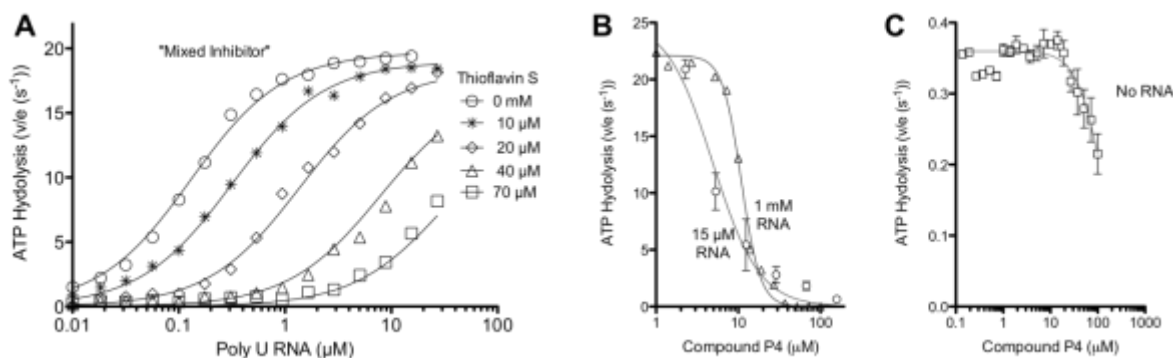


Figure 13. Effects of thioflavine S and the most potent primuline component on HCV helicase catalyzed ATP hydrolysis. (A) ATPase assays were performed in presence of indicated concentrations of thioflavine S and poly(U) RNA (measured as μM UMP). ATP was present at 1 mM, the reactions were initiated by rapidly mixing in NS3h, and the amount of phosphate released was measured after 15 minutes at 26 °C. (B) ATPase assays were performed in presence of 15 μM (circles) or 1 mM (triangles) poly(U) RNA and various concentrations of **P4** (CID 44251437) were present as indicated. (C) ATPase assays were performed in the absence of RNA.

It is not uncommon for helicase inhibitors to inhibit the protein's ability to hydrolyze ATP since ATP hydrolysis is needed to fuel unwinding. However, few compounds have been reported that inhibit the helicase and the protease function of NS3. Surprisingly, **P4** (CID 44251437) and some of the other compounds purified from thioflavine S and primuline also inhibited NS3 catalyzed peptide cleavage (**Figure 14.**). The compounds inhibited the protease if they were added before (**Figure 14.A**) or after the protease substrate. The later experiment demonstrates that inhibition is not simply due to the compound quenching the fluorescence of the protease reaction product. The potency with which the primuline and thioflavine components inhibited the NS3 protease mirrored the potency seen in helicase assays (**Table 5.**).

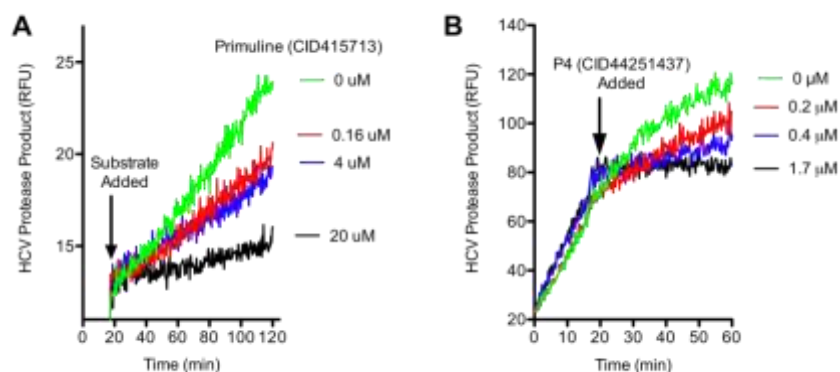


Figure 14. Effects of primuline and **P4** (CID 44251437) on NS3 catalyzed peptide cleavage. Assays were performed at 23 °C using the SensoLyte® 520 HCV Protease Assay Kit (Anaspec)

with 20 nM of a purified recombinant single chain NS3/NS4A protein (33). (A) Indicated concentrations of primuline were added before the protease substrate. (B) Indicated concentrations of **P4** (CID 44251437) were added to ongoing reactions 20 minutes after the reactions were initiated.

Table 5. Isolated thioflavine S and primuline components for NS3 helicase inhibitor discovery								
Compound ID			compound name*	target potency, MBHA (IC ₅₀ , avg, μM)	cell-based assays		antitarget potency (IC ₅₀ , avg, μM)	
#	CID	*		1b(con1)	replicon (% inhibition @ 10 μM)	cell viability (% @ 10 μM)	FID (EtBr)	ATPase
	SID		2a(JFH1)	FID (SYBR Green I)			Protease	
1	415676	P	thioflavine S	24 ± 1.3	-16 ± -2	83 ± 2	nd	>200
				16 ± 5			61 ± 37	nd
2	415713	P	primuline	12 ± 1.3	10	98 ± 3	73 ± 36	nd
				9.6 ± 1.1			43 ± 14	nd
3	44251429	S	T1	33 ± 24	0	99 ± 2	>100	>200
	85285427			25 ± 21.8			>100	nd
4	44251431	S	T2	4.6 ± 1.6	0	96 ± 7	>100	>200
	85285428			4.7 ± 0.6			26 ± 4	nd
5	44251427	S	P1	70 ± 31	0	104 ± 4	>100	>200
	85285425			21 ± 7.7			>200	nd
6	44251428	S	P2	5.6 ± 1.6 45 ± 14 95 ± 14	9 ± 2 55 ± 8 112 ± 4	95 ± 4 85 ± 7 105 ± 5	>100 >100 nd	>200 >200 >200
	85285426 104178066 126920288			7.3 ± 2.2 58 ± 50.7 nd			23 ± 4 >100 >100	nd nd nd
7	44251436	S	P3	0.9 ± 0.02	59 ± 10	91 ± 6	55 ± 20	nd
	85285431			0.6 ± 0.3			nd	nd
8	44251437 44251438	S	P4	0.8 ± 0.2 2.2 ± 0.1	0 45 ± 14	94 ± 3 83 ± 8	15 ± 3 76 ± 1	nd 43 ± 10
	85285432 99438075			0.5 ± 0.4 1.2 ± 0.3			nd 14 ± 3	nd 2 ± 1
9	44251433	S	P1a	>100	0	88 ± 7	>100	>200

	85285429			48.5 ± 54.4			>100	nd
10	44251434	S	P2a	7 ± 3.8	28 ± 5	87 ± 7	>100	>200
	85285430			3.9 ± 0.4			32 ± 3	nd

*Denotes whether the compound was synthesized (S) or purchased (P).
 *Please refer to **Figure 7**. for compound structures. All the isolated compounds are ammonium salts except **P4**.

3.2 Dose Response Curves for Probe

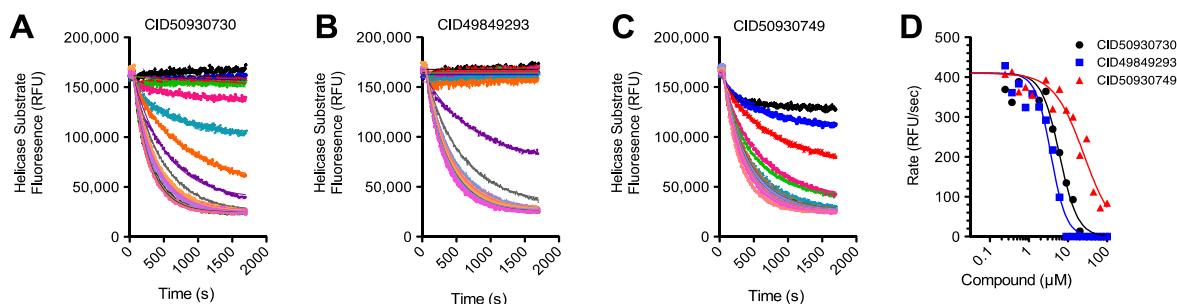


Figure 15. Dose response curves for probe and two analogues. Effect of CID 50930730/**ML283** on standard MBHAs (A) compared with a slightly more active compound CID 49849293 (B) and less active compound CID 50930749 (C). MBHAs were performed in the presence of 16 concentrations of each compound ranging from 100 μM (black), 67 μM (blue), 45 μM (red), 30 μM (green), 20 μM (magenta), 14 μM (light blue), 9 μM (orange), 6 μM (purple), 4 μM (grey), 2.7 μM (pale blue), 1.8 μM (peach), 1.2 μM (dark green), 0.8 μM (pink), 0.5 μM (light purple), 0.4 μM (light orange), and 0.25 μM (pale magenta). Reactions were initiated after 60 seconds by adding ATP to a final concentration of 1 mM. Data obtained after ATP addition are fit to a first order decay equation to calculate initial rates in the presence of various concentrations of each compound. (D) Initial unwinding rates plotted versus compound concentration. Velocities are fit to a dose response equation as described in Appendix A.

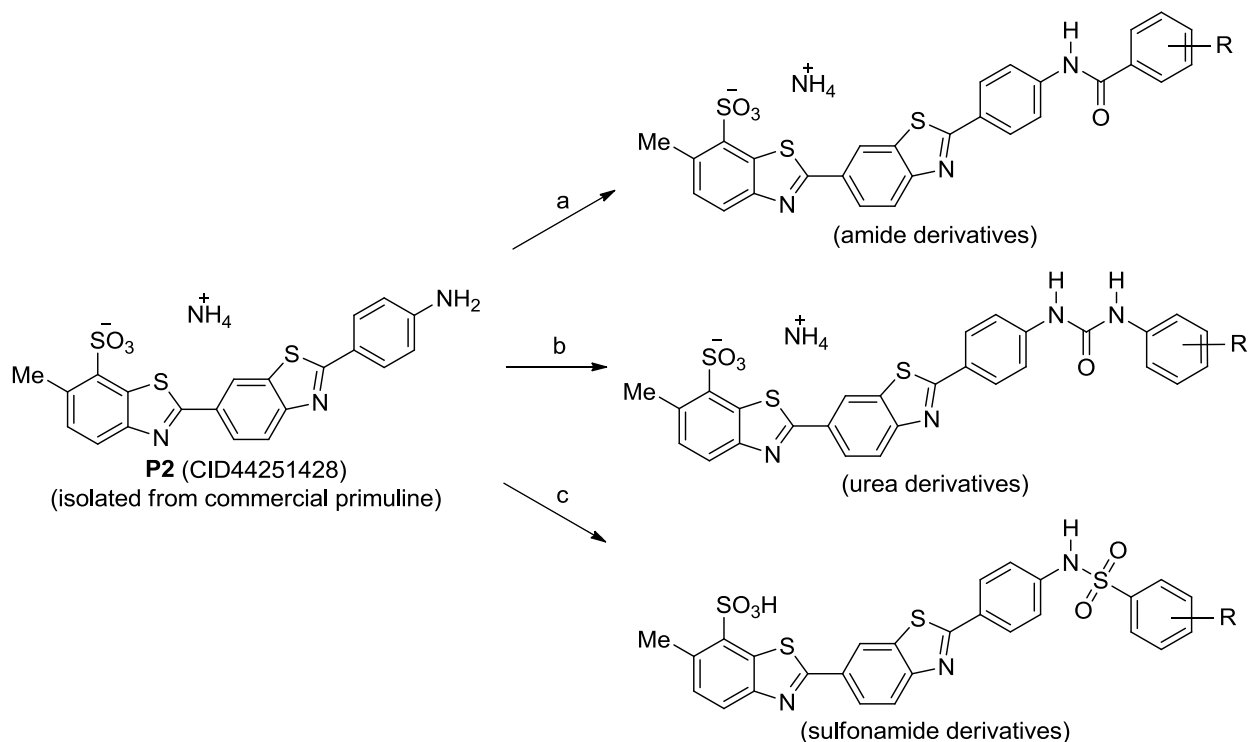
3.3 Scaffold/Moiety Chemical Liabilities

The probe compounds based on an oligomeric benzothiazole scaffold appeared to be relatively stable based on our observations from day-to-day handling related to their synthesis, analysis, dissolution-transfer, lyophilization, and storage. The probe compounds do not contain moieties that are known or expected to be generally reactive.

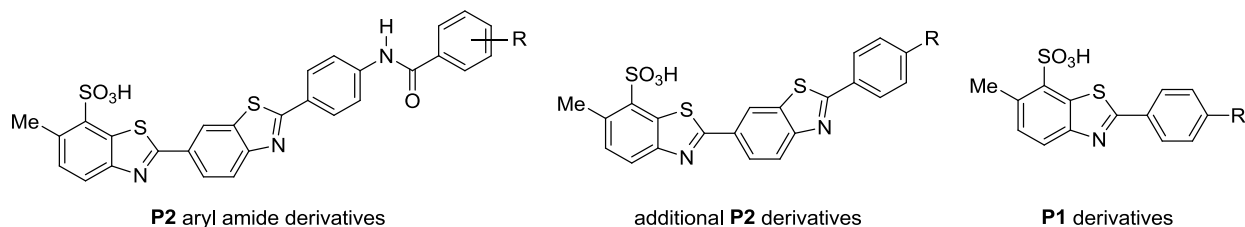
3.4 SAR Tables

The positive results obtained with the higher-order components **P3** (CID 44251436) and **P4** (CID 44251437) isolated from primuline (CID 415713) led us to undertake a structure–activity relationship study based on them. However, difficulties with both isolation of sufficient quantities from the commercial sources and with fully synthetic approaches necessitated that we consider more accessible bioisosteric equivalents. Accordingly, we focused on modification of the amino group at the terminus of **P2** (CID 44251428), which was available in sufficient quantities to serve as a starting material. We envisioned that an appropriately rigid linker could substitute for the third benzothiazole ring of **P3**. Thus, the terminal amine of **P2** (CID 44251428) was acylated to give amides, reacted with isocyanates or sulfonyl chlorides to give urea analogues and sulfonamides, respectively (**Scheme 1.** and **Figure 16.**). **Table 6.** illustrates the effect of various functional groups on substituted phenyl amide derivatives, the most extensively investigated modification strategy. These included electron-donating or -withdrawing groups as well as aliphatic substitutions. The unsubstituted benzamide analogue (CID49849280, entry 11) possessed modest potency in assays employing helicase enzyme from both the 1b(con1) and 2a(JFH1) HCV genotypes ($IC_{50} = 10.7 \pm 1.5 \mu\text{M}$ and $4.6 \pm 1.4 \mu\text{M}$, respectively). Introduction of a diverse range of *para* substitution (e.g. NH_2 (CID 49849300), $\text{N}(\text{CH}_3)_2$ (CID 49849284), OCH_3 (CID 49849282), CO_2CH_3 (CID 49849290), *t*-Bu (CID 49849299) and Br(CID 50930740)) had no significant effect on the potency of helicase inhibition. Improved analogues were obtained when Cl (CID 49849302), F (CID 49849294), CH_3 (CID 49849286) or CF_3 (CID 49849276) were tested in the *para* position. The increased size of alkyl substitution from Me to *t*-Bu resulted in an *ca.* 2-fold activity loss. Altering the Cl position from *para* to *meta* (entries 19 and 22, CID 49849302 and CID 50930730) had no effect on helicase inhibition, although the *meta* substitution displayed weaker DNA binding coupled with promising cell-based HCV replicon values. Increasing, the number of chloro groups as in CID 50930737 (entry 23) showed no improvement. The CF_3 substituted series possessed an intriguing range of activity. The 4- CF_3 (CID 49849276) analogue was the most potent compound in the helicase assays ($IC_{50} = 1.8 \pm 0.4 \mu\text{M}$ and $2.5 \pm 1.0 \mu\text{M}$, for 1b(con1) and 2a(JFH1) HCV genotypes respectively). Moving the CF_3 group from the *para* position to the *ortho* or *meta* position resulted in a loss of inhibitory activity (7-10 fold, entries 24-26, CID 50930748, CID 50930755 and CID 49849276). Introduction of additional fluorine or CF_3 substitution on the derivatives also exhibited no effect on the helicase inhibition when compared to the 4- CF_3 (CID 49849276) substituted compound (see entries 27-33, CID 50930749, CID 50930745, CID 50930751, CID 50930741, CID 50930743, CID 50930732 and CID 50930733). In fact, depending on the position of fluorine or CF_3 substitution, a significant decrease in potency was observed. Alternate amide linked moieties to the substituted benzamides were briefly explored (entries 34-44, **Table 7.**). Replacing substituted phenyl with a methyl alkyl group resulted in complete loss of activity (CID 53239937, entry 44). Analogues targeting improved solubility by replacing the phenyl ring with pyridine ring, produced less potent analogues (2-5 fold decrease in helicase activity, CID 50930756 and CID 50930734, entries 40 and 41). Though significantly less potent, these analogues did possess greatly improved solubility under the assay conditions; for example CID 50930756 was soluble at $> 100 \mu\text{M}$ compared to **ML283**, which possessed a solubility of 29.2

μM (**Table 10**). *N*-methylation of the naphthyl analogue (CID 49849293) also caused a significant drop in activity (5 fold,



Scheme 1. Reagents: (a) substituted benzoyl chloride, pyridine, 80 °C; (b) arylisocyanate, DMF, 80 °C; (c) arylsulfonyl chloride, pyridine, 80 °C.



* Analog substitution is listed in Tables 3.4.1, 3.4.2 and 3.4.3

Figure 16. Structures of derivatives based on the major components in primuline.

CID 52914816), which could indicate the loss of a key hydrogen bond interaction. While none of these analogues possessed improved helicase activity compared to **ML283**, the solubility of the 3-pyridyl analogue (CID 50930756) and nascent potency of the naphthyl analogues (CID 49849293 and CID 53308659) provide inspiration for designing future analogue sets.

In an effort to mimic the tetrameric structure of **P4** (CID 44251437), the more elaborate amide derivatives CID 49849289 and CID 49849287 (entries 38 and 39, **Table 7**.) were synthesized. No improvements in potency were observed for these tetrameric analogues over the previous trimeric analogues. The simple one-step synthesis of the trimeric analogues compared to the

tetrameric analogues prompted us to focus on the former for future studies targeting more potent inhibitors of helicase function and HCV replication.

In DNA binding assays, none of the **P2** derivatives decreased the fluorescence of DNA-bound ethidium bromide by more than 10% even at 100 μ M. However, like **P3** (CID 44251436) and **P4** (CID 44251437), many of the derivatives appeared to bind SYBR-Green-I-stained DNA, and these EC₅₀ values in SYBR Green-based FID assays are reported. Most of the amide derivatives were at least 10-fold more potent in the MBHA than the DNA-binding assay. The 3-Cl analogue (**ML283**, CID 50930730) was chosen for nomination as the probe candidate based on a combination of helicase assay inhibition (both 1b(con1) and 2a(JFH1) HCV genotypes), high percentage of cellular HCV replication (54% at 10 μ M) coupled with no detectable cytotoxicity and low DNA binding in the SYBR Green FID assay (EC₅₀ > 100 μ M).

Two additional classes of chemical linkers were also explored to mimic the benzothiazole moiety (**Table 7.**). The urea analogues, which were synthesized from **P2** (CID 44251428) by reacting it with different isocyanates and the sulfonamide analogues prepared via the sulfonation of **P2** (CID 44251428) with sulfonyl chlorides. The *p*-tolyl urea analogue CID 49849298 (entry 46) has potency in the MBHA and replicon assays approaching that of the probe candidate, although increased DNA binding was observed (17 μ M for CID 49849298 compared to >100 μ M for **ML283**). Slightly less potent analogues were achieved *via* sulfonation (e.g. CID 49849295, 2-fold activity drop) compared to **ML283**.

The other major component isolated from the primuline mixture, **P1** (CID 44251427) was also investigated as a substrate for the synthesis of active analogues. **Table 8.** summarizes the derivatives synthesized based on the monomer **P1** (CID 44251427). None of the compounds showed significant activity in the replicon assay and only the Fmoc-protected amines CID 53377547 and CID 53377543 (entries 56 and 60) and the trifluoromethylphenyl analogue CID 53308658 (entry 58) possessed MBHA potency approaching that of **ML283**. The absence of replicon activity for this series was the primary motivation to pursue derivatives based on the equally abundant **P2** (CID 44251428).

The synthetic diversification strategy of the isolated component **P2** (CID 44251428) allowed us to produce analogues with a diverse range of substitution on the 'eastern' portion of the compounds in quantities > 20 mg in one or two synthetic steps. A strategy capable of incorporating modifications anywhere in the molecule and which did not depend on the separation of a complex dye mixture to obtain starting material would be highly advantageous, if the synthetic manipulations could be minimized. All attempts toward the *de novo* synthesis of oligomeric analogues of **P3** (CID 44251436) and **P4** (CID 44251437) were unsuccessful despite a dedicated effort. Inspired by the success of the amide derivative of **P2** (CID 44251428) in the MBHA and replicon assay, a series of simplified analogues were synthesized. **Table 9.** summarizes the structures and activities of these compounds. Though active in the replicon assay, they were also found to be marginally cytotoxic. The promising results in the semisynthetic series and increasing complexity of the synthetic route to the target analogues prompted us to focus on the semisynthetic series.

The SAR campaign to identify **ML283** was based on a total of 55 compounds in addition to the eight isolated dye components. **Figure 17** illustrates the different structural elements explored in the course of the search for an accessible analogue of **P3** (CID 44251436), and

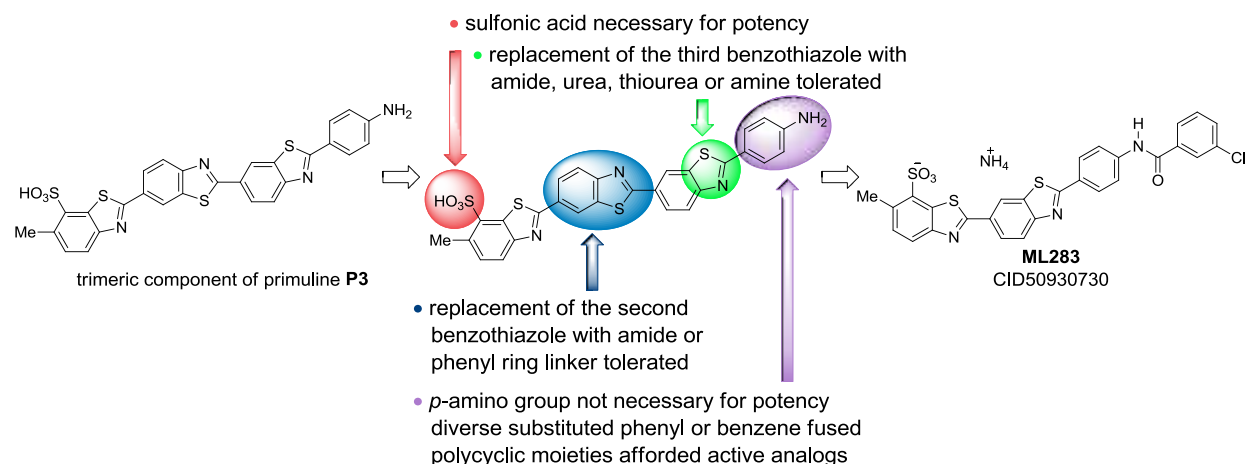
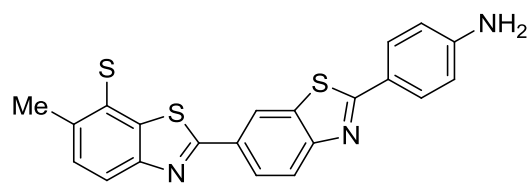
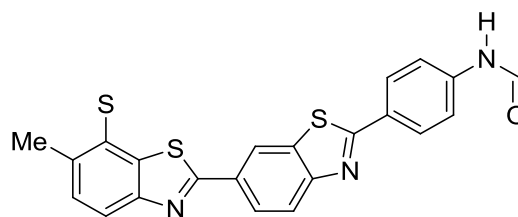


Figure 17. Summary of the SAR strategy to synthesize analogues based on the hit, **P3**.

which positions tolerated modification. While the majority of analogues were based on the derivatization of the primary amine on **P2** (CID 44251428), this was a highly fruitful site for diversity, affording analogues across the potency range of 1.8 to > 100 μ M in the NS3 helicase assay. Furthermore, all compounds were well tolerated in the cell viability assay yet varied in their ability to inhibit the HCV replicon within the range of 0.3 to 64%. All 55 SAR compounds are novel chemical entities and we have filed a provisional patent application for these compounds and their application as inhibitors of helicase function and HCV replication. In fact, a SciFinder substructure search for any carbonyl derivatives of **P2** (CID 44251428) did not return any hits (**Figure 18**), indicating the novelty of this derivatization approach. To more fully assess the novelty of the probe and analogues as inhibitors of the NS3 helicase, we conducted a SciFinder substructure search on the dimeric primuline component **P2** (CID 44251428), which was the starting material for the majority of the analogues. The search results indicated that 116 substances or mixtures contained this substructure, as reported in 88 patents and references. Of these references and patents, 63 focused on the synthesis or use of the substances as inks or dyes for textiles, outside of a biological context. The 25 remaining references were largely focused on utilizing these substances or dye mixtures for the identification of organisms and/or molecular structures and no instances of using primuline components as helicase enzyme inhibitors or for the treatment of HCV were found. The full search results are discussed in Appendix E.

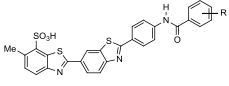


P2 substructure



amide derivative substructure

Figure 18. P2 and amide derivative substructures used in SciFinder searches.

Table 6. SAR analysis of primuline P2 amide derivatives for NS3 helicase inhibitor discovery								
Compound ID			 *structure, R =	target potency, MBHA (IC ₅₀ , avg, μM)	cell-based assays		antitarget potency	
#	CID	*		1b(con1)	replicon (% inhibition @ 10 μM)	cell viability (% @ 10 μM)	FID (SG)	SSB
	SID		2a(JFH1)	%Displaced at 100 μM			%Displaced at 100 μM	
11	49849280	S	H	10.7 ± 1.5	45 ± 5	88 ± 2	31 ± 13	91
	104178051			4.6 ± 1.4			>100	4 ± 1
12	49849300	S	4-NH ₂	10.3 ± 2.4	33 ± 1	93 ± 4	63 ± 15	99
	104178052			5.3 ± 2.5			55 ± 13	3 ± 1
13	46839370	S	4-NHFmoc	5.4 ± 1	57 ± 21	92 ± 4	76 ± 5	53
	99222880			5.8 ± 3.1			6 ± 2	>100
14	49849284	S	4-N(Me) ₂	11.0 ± 6.7	22 ± 2	94 ± 5	44 ± 4	98
	104178064			6.4 ± 1.2			>100	4 ± 1
15	49849286	S	4-methyl	3.3 ± 0.3	52 ± 12	87 ± 4	50 ± 15	96
	104178060			2.5 ± 0.5			>100	5 ± 2
16	49849299	S	4- <i>t</i> -butyl	8.2 ± 1	51 ± 9	87 ± 4	72 ± 19	80
	104178062			5.0 ± 0.7			16 ± 6	32 ± 7
17	49849282	S	4-methoxy	10.0 ± 2.6	64 ± 4	85 ± 5	35 ± 10	92
	104178055			5.4 ± 1.4			>100	2 ± 1

18	49849290	S	4-CO ₂ CH ₃	9.7 ± 4.6	40 ± 1	101 ± 8	28 ± 10	91
	104178057			2.4 ± 0.6			>100	2 ± 0.5
19	49849302	S	4-chloro	3.4 ± 0.3	42 ± 9	84 ± 6	67 ± 17	80
	104178059			2.3 ± 0.5			31 ± 15	46 ± 52
20	50930740	S	4-bromo	5.2 ± 4	7 ± 18	113 ± 5	70 ± 9	91
	114279591			7.4 ± 3			30 ± 13	27 ± 6
21	49849294	S	4-fluoro	5.2 ± 0.6	50 ± 5	94 ± 2	35 ± 15	88
	104178054			3.0 ± 0.8			>100	14 ± 4
22	50930730	S	3-chloro	2.6 ± 1	54 ± 10	112 ± 4	41 ± 11	47
	114279600			3.9 ± 1			>100	>100
23	50930737	S	3,4-dichloro	3.7 ± 1	43 ± 15	114 ± 7	67 ± 12	53
	114279601			4.5 ± 1			30 ± 32	> 100
24	50930748	S	2-trifluoromethyl	14.1 ± 1	0.3 ± 9	112 ± 1	30 ± 15	92
	114279599			24.3 ± 9			>100	13 ± 2
25	50930755	S	3-trifluoromethyl	19.7 ± 12	41 ± 8	121 ± 3	46 ± 10	23
	114279602			15.9 ± 2			>100	>100
26	49849276	S	4-trifluoromethyl	1.8 ± 0.4	44 ± 12	90 ± 4	69 ± 9	80
	104178061			2.5 ± 1.0			29 ± 9	4 ± 2
27	50930749	S	3,5-di(trifluoromethyl)	22.2 ± 4	60 ± 4	122 ± 5	43 ± 13	73
	114279597			28.7 ± 5			86 ± 210	36 ± 7
28	50930745	S	2-fluoro, 6-trifluoromethyl	16.8 ± 6	55 ± 7	122 ± 2	66 ± 40	96
	114279594			54.1 ± 19.7			64 ± 34	13 ± 1
29	50930751	S	2-fluoro, 3-trifluoromethyl	9.2 ± 3	48 ± 18	122 ± 1	49 ± 27	63
	114279595			8.1 ± 2			>100	71 ± 13
30	50930741	S	2-fluoro, 5-trifluoromethyl	6.4 ± 2	39 ± 4	132 ± 14	35 ± 26	69
	114279603			6.7 ± 1			>100	12 ± 8

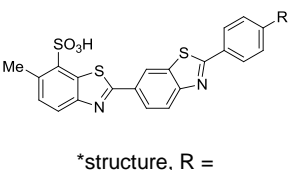
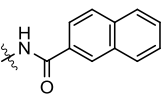
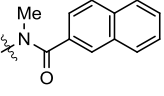
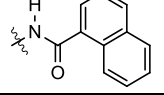
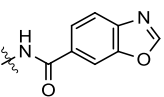
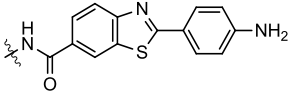
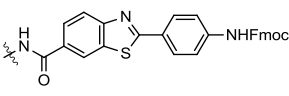
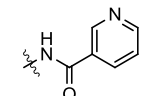
31	50930743	S	3-fluoro, 4-trifluoromethyl	17.4 ± 17	48 ± 4	129 ± 2	66 ± 18	92
	114279596			13.0 ± 2			28 ± 28	10 ± 1
32	50930732	S	3-fluoro, 5-trifluoromethyl	28.4 ± 7	51 ± 9	113 ± 1	48 ± 17	23
	114279605			15.8 ± 2.2			>100	>100
33	50930733	S	3-fluoro, 6-trifluoromethyl	19.0 ± 15	61 ± 14	118 ± 4	35 ± 21	95
	114279604			16.6 ± 2			>100	14 ± 2

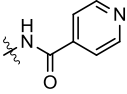
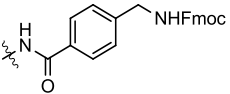
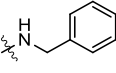
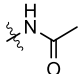
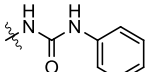
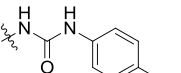
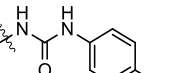
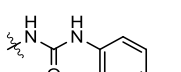
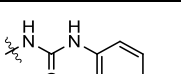
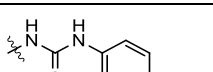
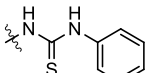
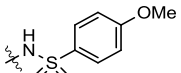
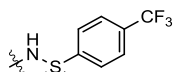
*Denotes whether the compound was synthesized (S) or purchased (P).

*See **Figure 16**. for general compound structure.

* All the compounds are ammonium salts.

Table 7. SAR analysis of additional P2 derivatives for NS3 helicase inhibitor discovery

Compound ID		* #	 *structure, R =	target potency, MBHA (IC ₅₀ , avg, μM)	cell-based assays		antitarget potency (IC ₅₀ , avg, μM)		
#	CID			1b(con1)	replicon (% inhibition @ 10 μM)	cell viability (% @ 10 μM)	FID (SG) %Displaced @ 100 μM	SSB %Displaced @ 100 μM	
	SID	2a(JFH1)			EC ₅₀ (μM)	SSB EC ₅₀ (μM)			
34	49849293	S		2.7 ± 0.7	61 ± 10	87 ± 4	64 ± 7	83	
	104178063			3.6 ± 0.0			21 ± 33	63 ± 11	78
35	52914816	S		14.4 ± 0.04	24 ± 32	101 ± 9	35 ± 23	105	
	123050378			13.5 ± 0.6			>100	9 ± 2	
36	53308659	S		4.5 ± 0.4	-9 ± 8	103 ± 5	80 ± 3	94	
	124767864			3.9 ± 0.3			30 ± 4	9 ± 2	
37	50930738	S		3.6 ± 1	15 ± 11	114 ± 13	59 ± 17	nd	
	114279598			6.4 ± 3			46 ± 36	nd	
38	49849289	S		5.5 ± 2.1	37 ± 4	85 ± 2	59 ± 4	95	
	104178067			3.5 ± 1.2			68 ± 25	±	
39	49849287	S		29 ± 31	44 ± 9	95 ± 3	nd	nd	
	46897855			4.0 ± 2.4			42 ± 5	67 ± 5	95
	99350539			>100				nd	nd
104178065		1.9 ± 0.9		22 ± 4	5 ± 1				
40	50930756	S		22.1 ± 2	51 ± 22	113 ± 6	15 ± 10	48	
	114279592			48 ± 40			>100	>100	

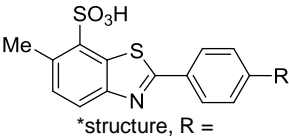
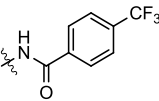
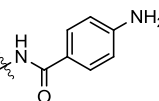
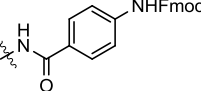
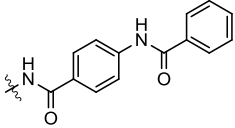
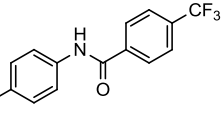
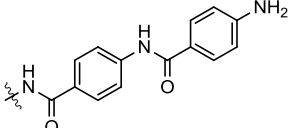
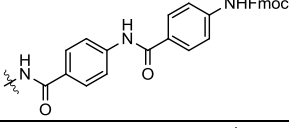
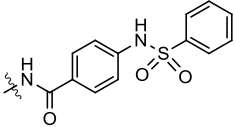
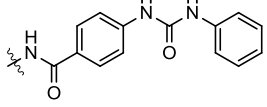
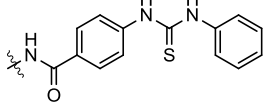
41	50930734	S		52 ± 20	59 ± 13	117 ± 5	19 ± 7	63
	114279593			52 ± 25			>100	55 ± 20
42	53239937	S		4.4 ± 0.3	48 ± 18	102 ± 6	53 ± 25	59
	124349740			4.6 ± 0.3			56 ± 4008	57 ± 16
43	53312458	S		11.0 ± 1.6	-64 ± 25	109 ± 8	92 ± 4	102
	124771944			13.5 ± 0.7			27 ± 3	5 ± 1
44	53255450	S		>100	26 ± 21	102 ± 9	48 ± 5	89
	124391240			>100			>100	17 ± 4
45	53356772	S		4.1 ± 1.3	-18 ± 56	108 ± 4	46 ± 2	95
	125258858			6.0 ± 1.9			>100	6 ± 1
46	49849298	S		5.3 ± 0.9	43 ± 9	93 ± 1	90 ± 9	96
	104178053			4.0 ± 1.9			18 ± 6	10 ± 3
47	53255447	S		5.1 ± 3.3	7 ± 39	99 ± 7	84 ± 22	91
	124391241			4.0 ± 1.3			18 ± 13	15 ± 3
48	53356770	S		7.8 ± 2.2	17 ± 25	93 ± 2	58 ± 3	100
	125258856			9.9 ± 3.4			74 ± 7	11 ± 2
49	53356653	S		3.6 ± 0.9	35 ± 28	98 ± 1	74 ± 4	94
	125258665			4.4 ± 0.4			8 ± 2	5 ± 1
50	53356656	S		4.8 ± 2	21 ± 10	99 ± 9	55 ± 6	95
	125258667			6.4 ± 2.5			73 ± 13	4 ± 1
51	53356771	S		9.3 ± 3.8	9 ± 9	98 ± 10	76 ± 9	98
	125258857			9.6 ± 3.1			30 ± 3	7 ± 1
52	49849295	S		24.4 ± 2.2	44 ± 5	75 ± 3	69 ± 4	98
	104178056			13.4 ± 7.2			42 ± 6	10 ± 2
53	53255448	S		32.0 ± 16	-7 ± 14	101 ± 6	57 ± 20	nd
	124391237			35.0 ± 6.1			82 ± 34	nd

*Denotes whether the compound was synthesized (S) or purchased (P).

*See **Figure 16**. for general compound structure.

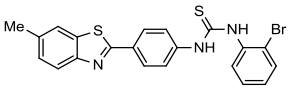
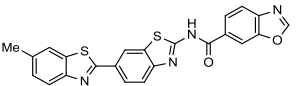
* All the compounds are ammonium salts except entries **35**, **38**, **43** and **52**.

Table 8. SAR analysis of P1 derivatives for NS3 helicase inhibitor discovery

Compound ID			 *structure, R =	target potency, MBHA (IC ₅₀ , avg, μM)	cell-based assays		antitarget potency (IC ₅₀ , avg, μM)	
#	CID	*		1b(con1)	replicon (% inhibition @ 10 μM)	cell viability (% @ 10 μM)	FID (SG) %Displaced @ 100 μM	SSB %Displaced @ 100 μM
	SID		2a(JFH1)			EC ₅₀ (μM)	SSB EC ₅₀ (μM)	
54	53255449	S		>100	11 ± 14	102 ± 9	9 ± 6	nd
	124391238			>100			>100	nd
55	53255452	S		69 ± 26	21 ± 29	103 ± 6	17 ± 6	nd
	124391239			64 ± 2.2			>100	nd
56	53377547	S		12 ± 3.7	31 ± 10	108 ± 2	44 ± 2	93
	125300032			12			>100	27 ± 5
57	53377551	S		81.4 ± 22	-19 ± 42	115 ± 3	18 ± 2	84
	125300033			79.2			>100	57 ± 13
58	53308658	S		10.4 ± 1.9	4 ± 8	97 ± 7	41 ± 2	86
	124767865			14.7 ± 2.9			>100	23 ± 6
59	53377553	S		30 ± 3.8	-42 ± 26	112 ± 5	21	94
	125300037			26			>100	17 ± 5
60	53377543	S		2.5 ± 0.5	-14 ± 26	113 ± 5	22	n/a
	125300038			1.9			>100	7 ± 3
61	53377554	S		>100	-73 ± 50	119 ± 11	25 ± 5	61
	125300035			>100			>100	>100
62	53377548	S		44 ± 12	-64 ± 90	113 ± 4	17 ± 2	96
	125300034			32			>100	20 ± 4
63	53377546	S		29 ± 6.9	-13 ± 2	106 ± 3	37 ± 4	93
	125300036			29			>100	23 ± 5

*Denotes whether the compound was synthesized (S) or purchased (P).
 *See **Figure 16**. for general compound structure.
 * All the compounds are ammonium salts.

Table 9. SAR analysis of selected fully synthetic analogues for NS3 helicase inhibitor discovery

Compound ID			complete structure	target potency, MBHA (IC ₅₀ , avg, μM)	cell-based assays		antitarget potency (IC ₅₀ , avg, μM)	
#	CID	*		1b(con1)	replicon (% inhibition @ 10 μM)	cell viability (% @ 10 μM)	FID (SG) %Displaced @ 100 μM	SSB %Displaced @ 100 μM
	SID		2a(JFH1)	EC ₅₀ (μM)			SSB EC ₅₀ (μM)	
64	49795072	S		>100	80 ± 17	39 ± 10	nd	nd
	103162420			>100			nd	nd
65	49795073	S		60 ± 6.1	90 ± 35	28 ± 5	nd	nd
	103162421			75 ± 32.6			nd	nd

*Denotes whether the compound was synthesized (S) or purchased (P).

3.5 Cellular Activity

Two cell-based assays have been completed to characterize CID 50930730/**ML283** and most analogues, as reported in the SAR tables. These assays were: 1) a *Renilla* luciferase reporter assay to examine the ability of compounds to inhibit replication of a HCV *Renilla* luciferase subgenomic replicon and 2) a *Firefly* luciferase-based viability assay that measures the effect of compounds on cell viability. Both assays were conducted on HCV replicon containing cells treated with compounds at 10 μM. The activity for the probe compound in both cell-based assays is described in detail in Section 3.4, SAR Tables, and detailed assay descriptions are given in Section 3.1.

The HCV replicon chosen (**Figure 19.A**) was derived from the same HCV strain (con1, genotype 1b) as the NS3 protein used for screening and enzyme assays, and was a variant of the replicon first reported by Lohmann *et al.* (34) with two cell culture adaptive mutations (E1202G and S2204I) (35, 36). This subgenomic replicon also had a *Renilla* luciferase gene fused to the 5'-end of the neomycin phosphotransferase gene used for selection, so that the cellular levels of *Renilla* luciferase correlated directly with the amount of HCV RNA present in cells (37). After replicon transfection and selection, cells were treated in parallel in two triplicate sets. One set of cells was used for *Renilla* luciferase assays and the other set was used to determine cell viability using a firefly luciferase-based assay and all compounds were tested at 10 μM.

CID 50930730/**ML283** and many of its close analogues showed some modest activity against the HCV replicon, but effects varied depending on the batch of cells used and the passage number of stably transfected replicon cells. We observed also that cell-based experiments with CID 50930730/**ML283** are difficult due to its limited solubility in PBS and cell culture media (see below) and because of its ability to aggregate at higher concentration in the absence of non-ionic detergents (e.g. Tween20). This observation has limited our efforts to study the dose dependent efficacy of CID 50930730/**ML283** because typically no more than 10 μM of CID 50930730/**ML283** can be administrated before it begins to appear to aggregate in the culture (**Figure 19.A**). Experiments with other, more soluble analogues yielded more reproducible concentration response curves. For example, CID 50930749 showed a concentration-dependent inhibition of replicon luciferase activity with $5 \pm 2 \mu\text{M}$ needed to reduce replicon-encoded luciferase by 50%. Even at the highest concentration tested (50 μM) CID 50930749 was not toxic to Huh7.5 cells (**Figure 19.C**). In the same system, the most potent comparison helicase inhibitor (the symmetrical benzimidazole CID 486270, had a IC_{50} of $8 \pm 4 \mu\text{M}$ but it decreased cell viability with a CC_{50} of $87 \pm 40 \mu\text{M}$ (**Figure 19.D**). An approved HCV drug, Telaprevir, inhibited the replicon with an IC_{50} of $0.62 \pm 0.05 \mu\text{M}$ and reduced cell viability with a CC_{50} value of $28 \pm 5 \mu\text{M}$ (**Figure 19E**).

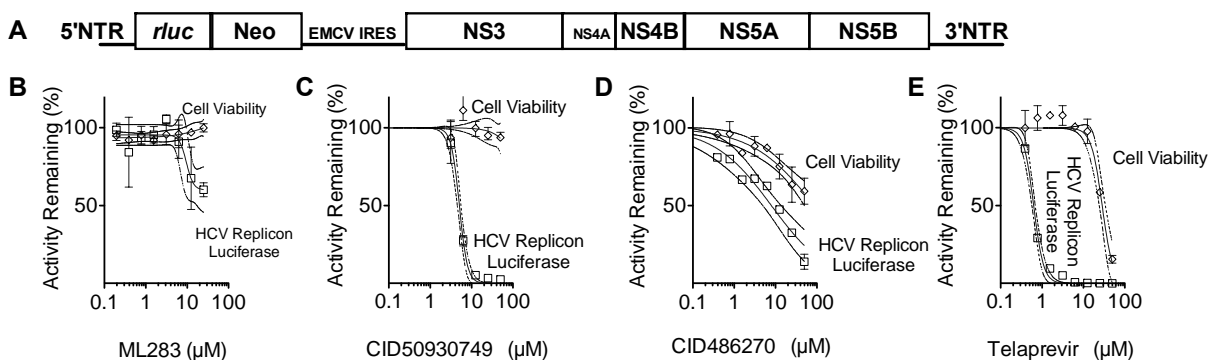


Figure 19. Effect of **ML283**, CID 50930749, CID 486270, and Telaprevir on Huh7.5 hepatoma cells harboring a stably transfected subgenomic *rLuc* HCV replicon. (A) Schematic genome map of the HCV replicon used in this project. Percent *Renilla* luciferase remaining (circles) after 72 hours exposure of replicon containing cells to **ML283** (B) CID 50930749 (C), CID 486270 (D), or Telaprevir (E) when grown in media containing 0.5% DMSO. Cell viability was measured with the Cell Titer-Glo luminescent cell viability kit (Promega) and is also expressed compared to DMSO controls.

To further examine the anti-HCV activity of CID 50930730/**ML283** in cells containing HCV replicons, we examined the effect of CID 50930730/**ML283** and CID 50930749 exposure on HCV RNA levels. Assays with the probe CID 50930730/**ML283** were again confounded by its poor solubility in cell culture media, as evidenced by the fact that concentration dependent reduction of HCV RNA was reversed after the concentration of CID 50930730/**ML283** exceeded 12 μM . In contrast, CID 50930749 exposure reduced HCV RNA levels in replicon cells in a concentration-dependent manner (**Figure 20.A**). To compare the effect of CID 50930749 to that of interferon $\alpha/2\text{b}$, the current standard of HCV care, cells were exposed to each for ten days. Analysis of luciferase activity (not shown) and HCV RNA (**Figure 20.B**) during, and at the end of

treatment, showed that CID 50930749 reduced HCV content in a time-dependent fashion. In repeated experiments CID 50930749 led to a 16-fold decrease in HCV replicon RNA content. This was about one-quarter of the effect seen with interferon.

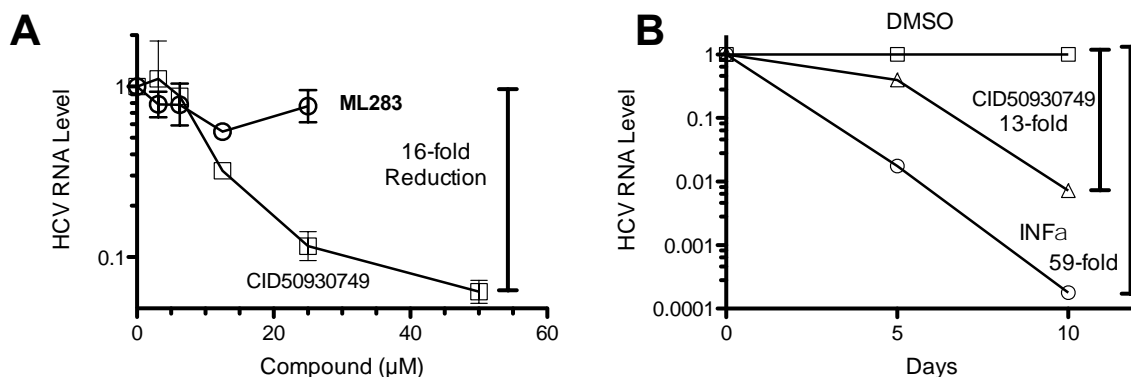


Figure 20. Effect of **ML283**, CID 50930749, and interferon on cellular HCV RNA levels (A) Amount of HCV RNA remaining in cells exposed to indicated amounts of **ML283** or CID 50930749. RNA was measured using 1 µg of total RNA with specific Taq-man probes and quantitative reverse transcriptase PCR (qRT-PCR). (B) Time-dependent clearance of HCV RNA in cells exposed to 10 µM of CID 50930749 (triangles) or 100 units of interferon (circles). RNA levels are expressed relative to RNA levels observed in cells grown in the presence of media and 0.5% DMSO. All assays were performed in triplicate, and error bars mark standard deviations.

More extensive cell based assays have been completed with CID 50930749, which again was the probe analogue that was most active in cells (*In vitro*, CID 50930749 was less potent and less specific than CID 50930730/**ML283**). For example, CID 50930749 was used to investigate how probe treatment might affect the cellular location of HCV replication complexes. In replicon containing Huh7.5 cells, HCV replication occurs in a membranous web associated with the rough endoplasmic reticulum (38). Clear differences in such complexes were observed when mock-treated (DMSO only) cells were compared with cells treated with CID 50930749, primuline, or interferon- $\alpha/2b$. Like interferon, CID 50930749 treatment reduced the number of replication complexes (**Figure 21**). In both cases, only reticular staining of NS5A and no replication complexes were seen. However, mock-treated cells and primuline-treated cells showed no apparent differences in HCV replication complexes. These results support the anti-HCV activity of CID 50930749.

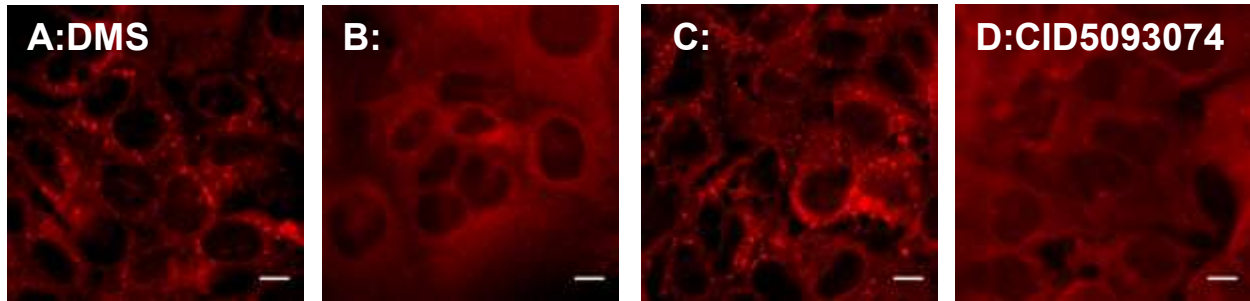


Figure 21. Effect of CID 50930749 on the cellular location of HCV Replication complexes seen in the replicon-containing Huh7.5/Con1sg-Rluc cells. After 72 hours of mock treatment with 0.5% DMSO (A), 100 units of interferon (B), 10 μ M primuline (CID 415713) (C) or 10 μ M of CID 50930749 (D), cells were fixed, permeabilized, and stained with 9E10 α -NS5A antibody (obtained from Charles Rice, Rockefeller University) and Alexa 546 secondary antibody. Scale bar = 10 μ m.

Since CID 50930749 is fluorescent, it can be directly observed in cells as shown in **Figure 22**.. HCV-replicon-bearing Huh7.5 cells were treated with CID 50930749 for 72 hours and cells were fixed, permeabilized, and stained for NS5A. Cells were imaged for CID 50930749 localization and compared with the antibody stained NS5A replication complexes. NS5A and CID 50930749 do not appear to co-localize, but since the viral target of CID 50930749 is HCV helicase, ongoing experiments aim to look at co-localization of CID 50930749 with viral helicase using specific anti-helicase mAb and higher resolution imaging. Interestingly, CID 50930749 showed a diffused and dotted cytoplasmic staining patterns in replicon cells and no evidence of CID 50930749 getting in the nucleus was observed.

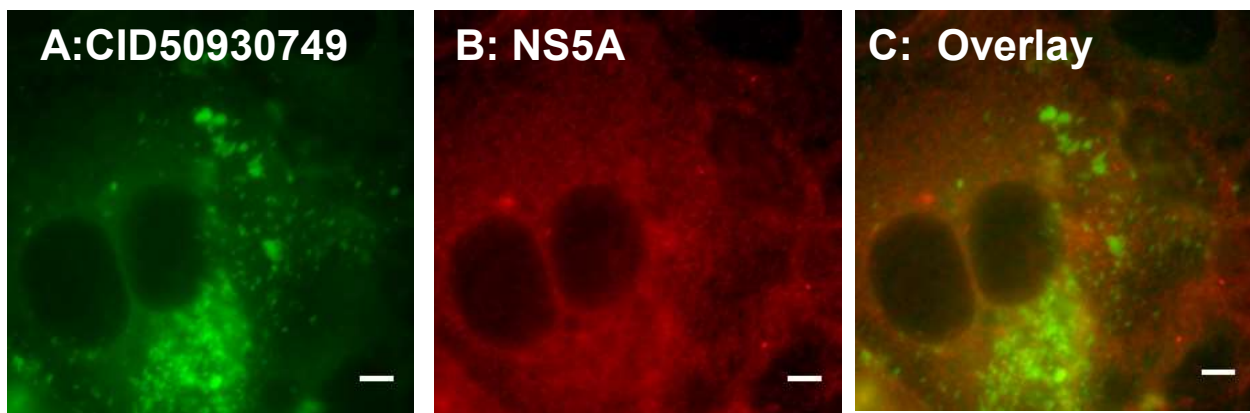


Figure 22. CID 50930749 location in cells. Huh7.5/Con1sg-Rluc cells were treated with CID 50930749 for 72 hours, permeabilized and stained with 9E10 α -NS5A antibody and Alexa 546 secondary antibody. (A) Localization of CID 50930749 fluorescence observed when the cells are excited at 350 nm. (B) NS5A localization observed when the same cells were excited to observe the NS5A replication complexes. (C) Overlay of the images with CID 50930749 colored green and NS5A complexes colored red. Scale bar: 10 μ m.

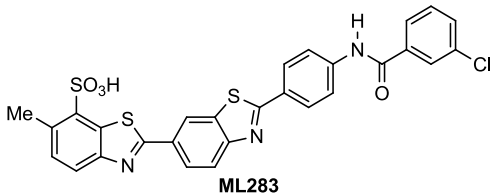
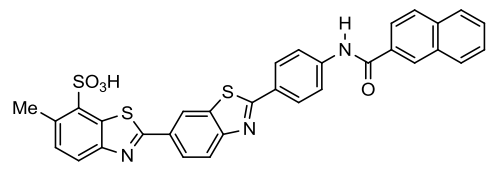
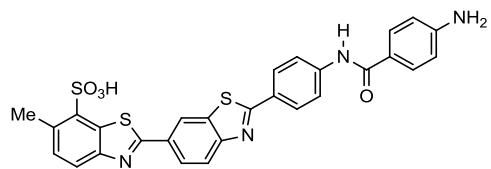
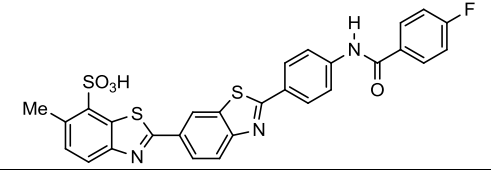
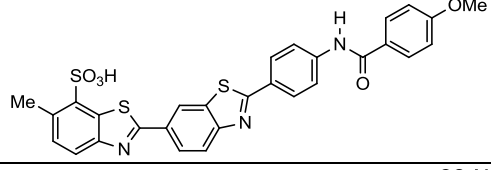
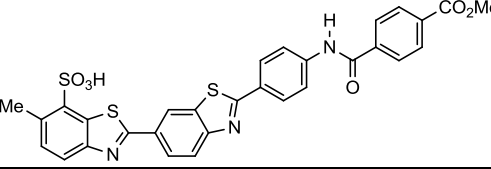
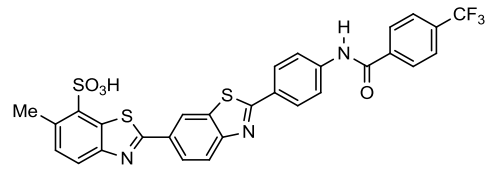
The data above show that cellular experiments with the probe compound, which is a more potent and specific helicase inhibitor, might be possible if administered with a compatible excipient. Once a system is found to deliver the probe to cells, the probe and less specific analogues such as CID 50930749 could serve as a powerful tools to yield insights into when and where the helicase acts in an infected cell, or to test the hypothesis that the helicase activity on RNA or DNA is needed for HCV replication. Furthermore, if our ongoing experiments at investigating direct interaction of HCV helicase and these fluorescent probes in cell are successful, the probe could then be used to directly monitor virus morphogenesis and egress in real time using live cell imaging. Preliminary work with CID 50930730/**ML283** shows that, like CID 50930749, CID 50930730/**ML283** enters cells and specifically stains certain cellular structures (**Figure 23.**).

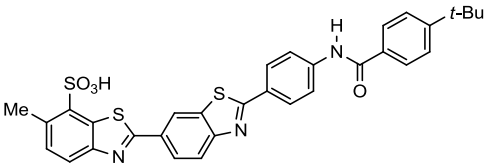
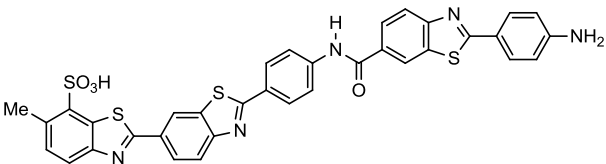
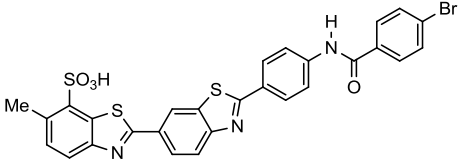
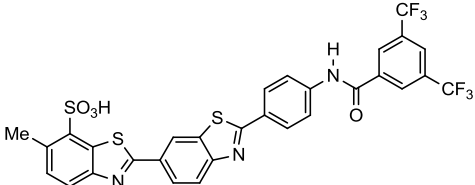
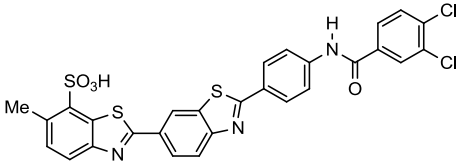
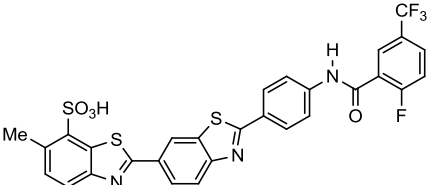
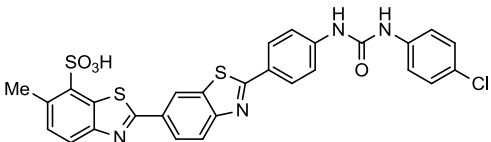
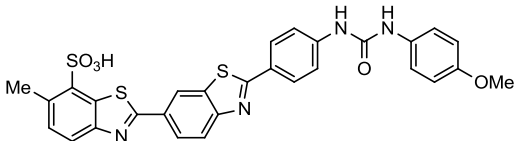


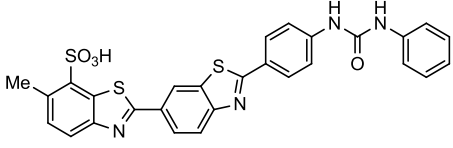
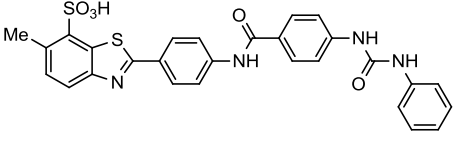
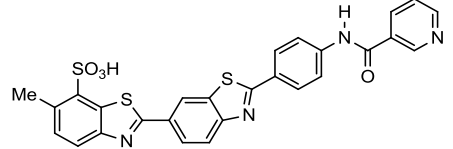
Figure 23. Use of fluorescence microscopy to visualize CID 50930730/**ML283** in cells. (A) Cells exposed to **ML283** show specific cell staining, and the compound appears to stains cytoplasmic structures, with faint or no staining of nucleus. No staining was observed on coverslip. Similar specific cell staining is seen with CID 50930737 (B) and CID 49849293 (C).

3.6 Profiling Assays

The probe **ML283** and a series of analogues were screened for solubility under conditions similar to those used in the MBHAs (**Table 10.**, MOPS buffer). Analogues targeting improved solubility by replacing the phenyl ring with pyridine ring, produced less potent analogues (2-5 fold decrease in helicase activity, CID 50930756 and CID 50930734, entries 40 and 41, **Table 10.**). Though significantly less potent, these analogues did possess greatly improved solubility under the assay conditions; for example CID 50930756 was soluble at > 100 μ M compared to **ML283**, which possessed a solubility of 29.2 μ M (**Table 10**). Future SAR efforts will focus on combining the solubility enhancing structural elements in analogues which retain potency for the NS3 helicase. To exclude the possibility that compound aggregation was the source for the observed helicase inhibition, the solubility of the probe candidate and several analogues was measured in a mock assay medium containing BSA, detergent (Tween 20) and DMSO (**Table 10.**, assay matrix). These data demonstrate that the probe is sufficiently soluble (29.2 μ M) to fully account for the observed helicase inhibition.

Table 10. Comparison of solubility and potency for ML283 and selected analogues				
CID	Structure*	Solubility (μM)	NS3 potency, IC_{50} (μM)	
		MOPS buffer ^a	Helicase 1b(con1)	ATPase
		assay matrix ^b	Helicase 2a(JFH1)	Protease
50930730	 ML283	0.39	2.6 ± 1	74 ± 7
114279600		29.2	3.9 ± 1	>100
49849293		4.5	2.7 ± 0.7	30 ± 6
104178063		3.7	2.3 ± 0.6	>100
49849300		42.4	10 ± 2	194 ± 30
104178052			5.3 ± 2.5	39 ± 17
49849294		0.4	5.2 ± 0.6	67 ± 30
104178054		129.4	3.0 ± 0.8	89 ± 47
49849282		2.8	10 ± 3	50 ± 7
104178055		nd	5.4 ± 1.4	83 ± 44
49849290		2.7	9.7 ± 4.6	nd
104178057		nd	2.4 ± 0.6	>100
49849276		1.1	1.8 ± 0.4	24 ± 5
104178061		nd	2.5 ± 1.0	5 ± 1

49849299		5.4	8.2 ± 0.99	150 ± 21
104178062		nd	5.0 ± 0.7	56 ± 23
49849289		0.3	5.5 ± 2.1	>200
104178067		nd	3.5 ± 1.2	7 ± 1
50930740		0.8	5.2 ± 4	50 ± 4
114279591		nd	7.4 ± 3	6 ± 1
50930749		0.2	22.2 ± 4	141 ± 28
114279597		180.1	28.7 ± 5	23 ± 15
50930737		1.3	3.7 ± 1	44 ± 12
114279601		2.6	4.5 ± 1	13 ± 4
50930741		0.3	6.4 ± 2	61 ± 13
114279603		nd	6.7 ± 1	51 ± 25
53356653		0.1	3.6 ± 0.9	86 ± 24
125258665		nd	4.4 ± 0.4	13 ± 4
53356656		0.4	4.8 ± 2	73 ± 46
125258667		25.2	6.4 ± 2.5	>100

53356772		0.8	4.1 ± 1.3	70±13
125258858		nd	6.0 ± 1.9	>100
53377548		1.8	43.8 ± 12	>200
125300034		nd	32.1	>100
50930756		>100	22.1 ± 2	>200
114279592		nd	48 ± 40	nd
^a Measured in MOPS buffer (25 mM MOPS, 1.25 mM MgCl ₂ and 2% v/v final [DMSO], pH 6.5) ^b Measured in 25 mM MOPS, 1.25 mM MgCl ₂ , 0.05 mM DTT, 5 µg/mL BSA, 0.01% v/v final [Tween 20] and 5% v/v final [DMSO], pH 6.5 * All the compounds are ammonium salts except CID49849289				

Another physical property of the probe and all its analogues that has been examined is their optical properties. Compared to **P4** (CID 44251437), CID 50930730/**ML283** has a sharper absorbance peak centered at 360 nm (**Figure 24.A**). When excited at 350±12 nm, CID 50930730/**ML283** is also more fluorescent than **P4** (CID 44251437).

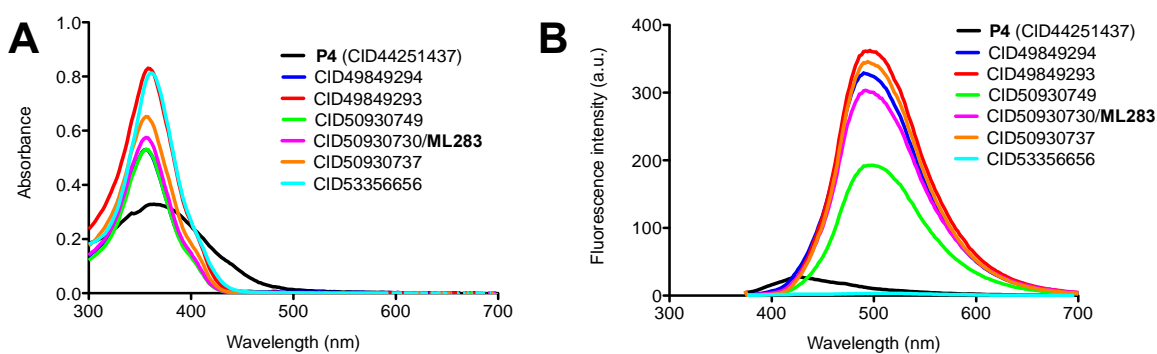


Figure 24. Spectra of CID 50930730/**ML283** and some analogues. (A) Absorbance of 20 µM aliquots of the indicated compounds. (B) Fluorescence emission spectra of compounds when excited at 350 ± 12 nm.

To uncover other off-target effects, the probe has been analyzed for its ability to influence the interaction of an unrelated nucleic-acid-binding-protein with DNA. The protein chosen was the

single-stranded DNA binding protein (SSB) encoded by *E. coli*. SSB has been widely studied because of its ability to coordinate DNA replication and recombination and is commercially available (New England Biolabs). We designed a fluorescence polarization-based assay to monitor the binding of SSB to single-stranded DNA (**Figure 25A**). In the SSB assay, the polarization of a Cy5-labeled oligonucleotide is monitored. Oligonucleotide polarization increases when SSB is added to the assay. SSB increased the fluorescence polarization of Cy5-dT15, with about 20 nM SSB needed to saturate the oligonucleotide with a $K_{0.5}$ of 9.6 ± 2 nM in the presence of 5 nM Cy5-dT15. DNA-binding compounds like **P4** (CID 44251437) cause SSB to fall from the DNA. The probe and its analogues were added to this assay each in a 16 point 1.5-fold dilution series starting at 100 μ M, in order to calculate an IC_{50} value for each. Clear differences are apparent with CID 50930730/**ML283** displacing far less SSB than all other compounds tested (**Figure 25.B**). Concentration response curves reveal that about 67-times more CID 50930730/**ML283** (IC_{50} =200 μ M) is needed to displace the same amount of SSB from DNA than is needed to inhibit HCV helicase in an MBHA (**Figure 25.C**). These assays further support the notion that CID 50930730/**ML283** is more specific than **P4** (CID 44251437), or any other analogue, with regard to its ability to inhibit NS3 helicase. All data using this counterscreen are reported in the SAR tables.

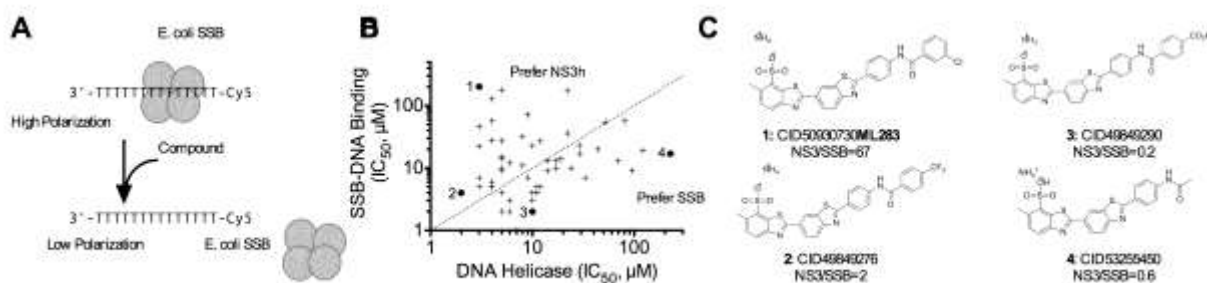


Figure 25. Effect of compounds on the polarization of a Cy5-dT15-*E. coli* single-stranded DNA binding protein (SSB) complex. (A) FP based assay to monitor SSB binding to Cy5-dT15. (B) Ability of various primuline derivatives to inhibit HCV helicase (x-axis) and decrease polarization of a Cy5-dT15-SSB complex. The dotted line shows where hypothetical compounds that inhibit both assays with the same potency would lie on the plot. (C) Structures of the four compounds with the most extreme properties are shown on the right, along with the ratios of IC_{50} values obtained in the two different assays.

We have also analyzed the ability of most of the compounds in **Table 10**. to inhibit NS3 catalyzed ATP hydrolysis and peptide cleavage. IC_{50} values for each assay are reported in **Table 5**. and **Table 10**.. Importantly, the probe (CID 50930730/**ML283**) maintains an ability to inhibit the ATP hydrolysis that fuels unwinding, but it is a 50-fold less potent protease inhibitor than **P4** (CID 44251437).

The pharmacokinetic (PK) properties of the probe (CID 50930730/**ML283**) were profiled using a standard panel of assays (**Table 11**). The most striking result is the solubility variation depending on the buffer system used. While the aqueous solubility is low in the PBS--based

solvent system, in both the detergent-containing (Tween 20) assay matrix and the proprietary Prisma HT buffer system the compound is readily soluble. The unknown identity of the components in the Prisma HT buffer system complicates further speculation into the solubility discrepancy. The solubility results have inspired us to pursue improving compound solubility through formulation with other solubilizing agents and these experiments are currently in progress. The low solubility and permeability of the probe (CID 50930730/**ML283**) were not surprising for a polycyclic aromatic compound of molecular weight 592 g/mol. Encouragingly, the probe (CID 50930730/**ML283**) was highly stable under the various conditions screened and possessed no detectable hepatic toxicity. Analogues possessing improved solubility and PAMPA properties will be the aim of future efforts.

Table 11. Summary of <i>in vitro</i> ADME properties of ML283 CID 50930730						
Aqueous Solubility ($\mu\text{g/mL}$) ^a (@ pH 5.0/6.2/7.4)	PAMPA Pe ($\times 10^{-6}$ cm/s) ^b (@ Donor pH)	Plasma Protein Binding (% Bound)		Plasma Stability ^d Human Mouse/ 1:1 Plasma:PBS	Hepatic Microsome Stability ^e Human/ Mouse	Hepatic Toxicity ^f LC50 (μM)
		Human 1 μM / 10 μM	Mouse 1 μM / 10 μM			
36.7/>60/>60	0 (5.0) 0.22 (6.2) 0 (7.4)	97.7/ 99.0	98.2/ 99.0	96.7/95.0	83.6/83.1	>50
^a in aqueous buffer (phosphate-free), pH's 5.0/6.2/7.4 @ RT (23-25°C) ^b in aqueous buffer (pION); Donor compartment pH's 5.0/6.2/7.4; Acceptor compartment pH 7.4 @ RT ^c in aqueous buffer (pION); Donor compartment pH 7.4; Acceptor compartment pH 7.4 @ RT ^d % remaining at 3 hr @ 37°C ^e % remaining at 1 hr @ 37°C ^f towards Fa2N-4 immortalized human hepatocytes						

4 Discussion

4.1 Comparison to existing art and how the new probe is an improvement

One of the challenges in developing chemical probes that target helicases is that potent helicase inhibitors often exert their actions by binding nucleic acid helicase substrates. Such compounds lack specificity because they can inhibit any protein that needs to access the genetic material. We attempted to discover more specific helicase inhibitors that do not target nucleic acids using high throughput helicase and DNA-binding assays, but even the most promising compounds, which were purified from the most active library sample, interacted with the DNA substrate in the absence of protein. We have, nevertheless, been able to engineer potent analogues that interact with DNA less tightly yet still retain an ability to inhibit helicase catalyzed nucleic acid strand rearrangements. Some of these compounds retain the important ability to inhibit HCV replication in cells, and could therefore prove useful for antiviral drug development.

To discover helicase inhibitors that do not bind nucleic acids, we screened a compound library using a helicase assay that simultaneously detects a compound's ability to interact with the

helicase substrate and its ability to interfere with the movement of HCV helicase through DNA. The results of the screen confirmed that most library samples that block helicase movements also interact with the helicase substrate. We confirmed that most of the newly uncovered HCV helicase inhibitors interact with DNA using a DNA binding assay (**Figure 7.**). The binding assay was based on a FID assay (22) that monitors fluorescence changes that occur when a compound interacts with DNA stained with ethidium bromide. The most active sample in the screened library that least affected the fluorescence of ethidium bromide-stained DNA was the yellow dye thioflavine S (CID 415676), and potent benzothiazole oligomers were purified from this dye and its relative, primuline (CID 415713). When the most active benzothiazole oligomers purified from primuline (CID 415713) were found to interact with SYBR Green I stained DNA, we learned that the ethidium bromide-based FID failed to detect the interaction of thioflavine S (CID 415713) with DNA. A more sensitive SYBR Green I assay was therefore developed and used to chemically optimize the probe by aiding the design of the more specific **P2** derivatives. The observation that DNA-interactions escaped detection in the ethidium bromide-based FID reinforces the notion that care needs to be taken when using FID assays because DNA-binding compounds might not displace the bound intercalator. There is likewise still some uncertainty as to whether or not the derivatives that failed to influence the fluorescence of SYBR Green-stained DNA interact with nucleic acids. Preliminary results using isothermal titration calorimetry support the relative affinities reported here, but more extensive DNA- and RNA-binding experiments clearly need to be done with these compounds.

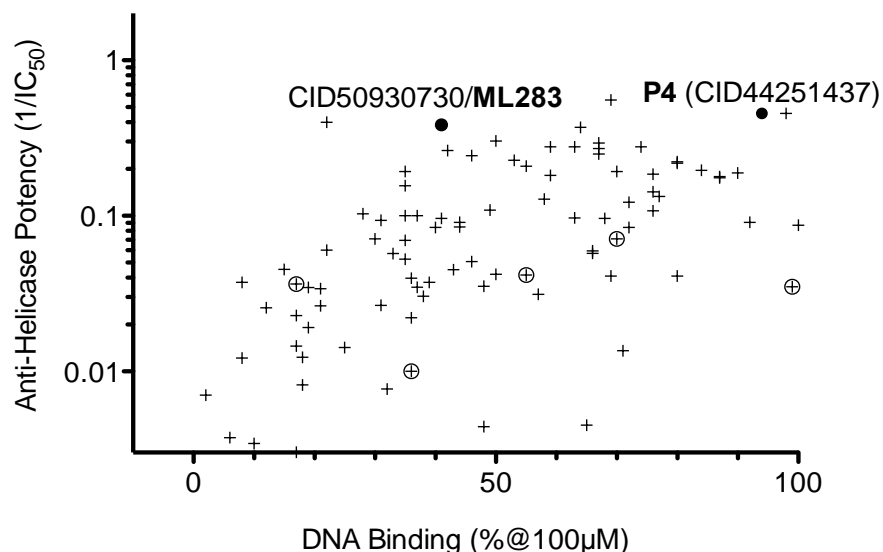


Figure 26. Comparative effects of benzothiazoles in HCV helicase assays. Potency of each compound tested in the study in MBHAs is plotted against percent ethidium bromide DNA fluorescence quenched (FID) at 100 µM. Filled circles mark CID 50930730/ML283 and P4 (CID 44251437). Open Circles mark published helicase inhibitors used for comparison.

The most potent benzothiazoles were notably more effective than the recently reported helicase inhibitors used for comparison, two of which appeared to function primarily by interacting with the DNA substrate (CID 3084034 and CID 46913723). CID 50930730/ML283 was nearly as

potent as **P4**, and it eliminated the HCV replicon without apparent toxicity similar to both **P3** (CID 44251436) and **P4** (CID 44251437). Also like **P4** (CID 44251437), CID 50930730/**ML283** inhibited HCV helicase catalyzed RNA unwinding and ATP hydrolysis (data not shown).

CID	helicase ^a 1b(con1) IC ₅₀ (μM)	DNA Binding (ethidium bromide) ^a EC ₅₀ (μM)	Cell Based Assays		NS3 ATPase ^a IC ₅₀ (μM)	NS3 protease IC ₅₀ (μM)
	helicase ^a 2a(JFH1) IC ₅₀ (μM)	DNA Binding (SYBR Green I) ^{a,b} EC ₅₀ (μM)	replicon (% inhibition @ 10 μM)	cell viability (% @ 10 μM)		
50904396	>100	>100	81 ± 7	31 ± 4	>200	>100
	>100	>100				
46202556	28 ± 25	>100	73 ± 49	79 ± 4	>200	85 ± 62
	25 ± 6	>100				
3084034	29 ± 16	4 ± 2	23 ± 2	73 ± 5	>200	72 ± 27
	17 ± 7	17 ± 2				
46913723	24 ± 30	31 ± 9	46 ± 13	69 ± 3	>200	>100
	18 ± 8	72 ± 14				
486270	7.5 ± 0.1	nd	96 ± 4	31 ± 11	>200	49 ± 17
	5 ± 2	14 ± 10				

^aHelicase (MBHA), DNA binding (FID), ATP hydrolysis, and protease were monitored in the presence of 8 different concentrations of each compound (2-fold dilution series starting at 100 μM). IC₅₀ values were determined from dose-response curves. Dissociation constants were calculated with equation 5. All values are means ± standard deviations from three independent titrations with inhibitor. ND, not determined.
^bAverage (±SD) percent bound at 100 μM is reported for compounds that did not decrease the fluorescence of SYBR Green I stained DNA more than 50% at the highest concentration tested.

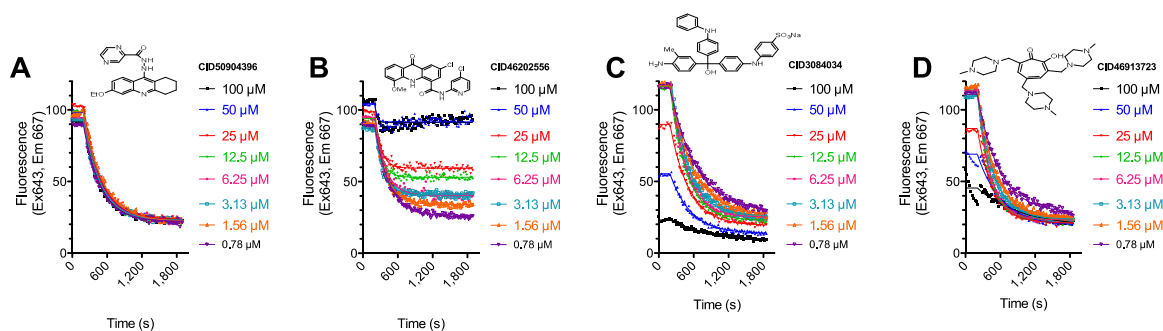


Figure 27. Dose response curves for helicase inhibitors used for comparison. MBHAs were performed in the presence of the indicated concentrations of each compound. Reactions were initiated after 210 seconds by adding ATP to a final concentration of 1 mM. Data obtained after ATP addition are fit to a first order decay equation to calculate initial rates in the presence of various concentrations of each compound. IC₅₀ values in **Table 12.** are calculated by fitting initial rates to Eq. 3 (Methods).

The compounds reported here are more potent and specific than other recently reported HCV helicase inhibitors (**Table 12.**, **Figure 27.**). Only CID 3084034 and CID 486270 inhibited MBHAs with potency similar to **ML283**, although the precise effects of CID 3084034 and CID 46913723 on HCV helicase action were difficult to assess because both interfered with the MBHA. In cells,

some of comparison compounds inhibited the replicon like the probe and its analogues. Only CID 46202556 was more effective than the probe analogue that was most active in cells (CID 50930749). None of the comparison helicase inhibitors were particularly toxic at 10 μ M except for CID 50904396.

We have also not been able to reproduce all of the results previously reported for the comparison helicase inhibitors. For example, the nucleotide mimic CID 50904396, which had been reported to have a K_i of 20 nM (18) had almost no detectable effect on the MBHA at 5,000 times higher concentration (**Table 12.**). While it had some antiviral activity, the activity was coupled with notable toxicity at 10 μ M (**Table 12.**). The acridone CID 46202556 was about 17-times less potent in our helicase assay than it was in a previously reported assay, but yet it still was one of the most effective compounds in eliminating the HCV replicon. Similarly, although its interaction with the helicase substrate obscured effects in our MBHA, the triphenylmethane CID 3084034 displayed no inhibition at its previously reported IC_{50} of 12 μ M, although the compound did not appear as cytotoxic as had been reported (20). CID 46913723 had antiviral activity as previously reported, but again, compound interference in the MBHA made its effect on the helicase *in vitro* difficult to judge (21).

To test if our different results were due to different assay conditions, we have repeated helicase assays with the above inhibitor using a helicase assay that did not rely on molecular beacons. Using the same assay that was designed by Boguszewska-Chachulska *et al.* (39) we found that all four comparison compounds were about 5 times more potent, but they were still 5-10 times less potent than the probe or its most potent analogues. Interestingly, we found that the activity for the acridone (CID 46202556) was pH dependent and it only inhibited unwinding above pH 7. Also the nucleotide mimic (CID 50904396) only appears to inhibit the reaction when $MgCl_2$ was substituted with $MnCl_2$. The effect of all four comparative compounds is enhanced when reaction temperatures are increased from 23 $^{\circ}C$ to 37 $^{\circ}C$ where the DNA is less stable and more easily unwound by the helicase. In contrast, temperature does not seem to affect the IC_{50} of the probe or its more potent analogues.

In conclusion, we have found that the commercial dyes thioflavine S (CID 415676) and primuline (CID 415713) contain potent compounds for the inhibition of the NS3 helicase of HCV. We show here that minor components of primuline (CID 415713) inhibit both the HCV helicase and HCV replicon replication. The antiviral potential of these trimeric and tetrameric benzothiazoles inspired the derivatization of the more abundant dimeric constituent. Several derivatives were found to be close in potency to the isolated trimer or tetramer in the MBHA and to possess improved DNA-binding profiles. Importantly, the antiviral potential of this class of helicase inhibitors does not appear to depend entirely on either their ability to inhibit HCV helicase or bind DNA. We speculate that the ability to inhibit HCV replication results from a compound's ability to enter Huh7.5 cells, which can be monitored by examining compound fluorescence when they are administered to cells. In cell culture, both thioflavine S (CID 415676) and primuline (CID 415713) do not stain Huh7.5 cells, but preliminary data suggest that some of the derivatives enter cells. As described below, effects of the most potent replicon inhibitors of HCV replication (e.g. **ML283**) are presently being examined in more detail. The

results of these studies will be used to inform additional chemistry efforts toward helicase inhibitors, which is an ongoing concern of our laboratories.

4.2 Mechanism of Action Studies

Experiments geared towards understanding how the probe inhibits the helicase reaction *in vitro* and how the probe disrupts cellular HCV replication are presently in progress in our laboratories.

Biochemical assays are being performed similar to the ones done with primuline, thioflavine S, and other helicase inhibitors (32). Briefly, steady state kinetics is being used to test if the probe competes with other known NS3 ligands like ATP, RNA, the NS4A peptide, and a variety of NS3 protease inhibitors. Intrinsic protein fluorescence and the fluorescence of the probe itself are being used to examine the direct interaction of the protein and probe, with Förster resonance energy transfer being used to estimate atomic distances. Some of the more soluble analogues are being used with isothermal titration calorimetry to better understand the thermodynamics explaining interaction between the probe, NS3 and nucleic acids.

Cellular experiments in progress include more detailed studies of the kinetics of HCV inhibition using both HCV replicons and cells infected with the JFH1 strain virus, which is uniquely capable of replication in cell culture. We are also examining methods to best deliver the probe in the cells to yield a more potent and reproducible antiviral effect. The probe and its more potent analogues are also being added to cells with HCV protease inhibitors and other drugs in clinical trials to examine for synergistic and antagonistic effects that might occur when helicase inhibitors are combined with other direct acting antivirals.

4.3 Planned Future Studies

The obvious next experiment to be done with this probe would be to test its effect on the replication of authentic HCV. All the work here was done using purified, recombinant HCV proteins and modified HCV subgenomic replicons. Such systems are HTS compatible, but they fail to recapitulate the complete HCV lifecycle. Future studies should therefore involve HCV capable of replicating in cell culture (47). We suspect that the probe will be more effective with authentic HCV because the helicase has been recently shown to interact with the HCV structural protein, core, which is not present in subgenomic replicons (48). The fact that the probe analogue most active in cells, *CID 50930749*, is less selective than the probe raises the interesting possibility that the antiviral effect seen with other helicase inhibitors is not due to a direct attack on NS3h but rather a non-specific attack on related helicase or nucleic acid binding proteins. This is an interesting hypothesis that could be rigorously tested using *CID 50930749*, the probe, and some of the other compounds reported here. Since probe solubility might still limit its use in such studies, future efforts will also be devoted to synthesizing and testing more soluble analogues.

In other studies, the probe and analogues will also be tested against RNA helicases encoded by other organisms, as well as a panel of ATPase and proteases. If the probe lacks specificity in such experiments, more analogues will be designed to enhance specificity. Planned future

studies that could enhance specificity include more detailed structural studies using X-ray crystallography, followed by structure-based design of more specific derivatives of the probe.

Acknowledgments. This work was supported by National Institutes of Health grants U54 HG005031, R03 MH085690-01 and RO1 AI088001 and a Research Growth Initiative Award from the UWM Research Foundation. We thank Dmitriy Minond; Peter Hodder and Katharine Emery of the Scripps Research Institute, Florida for help with assay development and for uploading the screening results into PubChem. We are also grateful to Doreen Badheka, Kelley-Anne Cyaeski, Yoji High, and John J. Hernandez for their help with various enzymatic assays and to Cihan Aydin and Charles Rice for reagents. Finally, we thank Arianna Mangravita-Novo, Michael Vicchiarelli and Layton H. Smith of the Sanford-Burnham Medical Research Institute at Lake Nona for providing the solubility measurements.

5 References

1. Garber K (2011) Hepatitis C: move over interferon. *Nat Biotechnol* 29:963–966.
2. Lindenbach BD, Rice CM (2005) Unravelling hepatitis C virus replication from genome to function. *Nature* 436:933–938.
3. Zeuzem S, Andreone P, Pol S, Lawitz E, Diago M, Roberts S, Focaccia R, Younossi Z, Foster GR, Horban A *et al.* (2011) Telaprevir for retreatment of HCV infection. *N Engl J Med* 364:2417–2428.
4. Bacon BR, Gordon SC, Lawitz E, Marcellin P, Vierling JM, Zeuzem S, Poordad F, Goodman ZD, Sings HL, Boparai N *et al.* (2011) Boceprevir for previously treated chronic HCV genotype 1 infection. *N Engl J Med* 364:1207–1217.
5. Lam AM, Frick DN (2006) Hepatitis C virus subgenomic replicon requires an active NS3 RNA helicase. *J Virol* 80:404–411.
6. Frick DN (2007) The hepatitis C virus NS3 protein: a model RNA helicase and potential drug target. *Curr Issues Mol Biol* 9:1–20.
7. Gu M, Rice CM (2010) Three conformational snapshots of the hepatitis C virus NS3 helicase reveal a ratchet translocation mechanism. *Proc Natl Acad Sci U S A* 107:521–528.
8. Frick DN, Rypma RS, Lam AM, Gu B (2004) The nonstructural protein 3 protease/helicase requires an intact protease domain to unwind duplex RNA efficiently. *J Biol Chem* 279:1269–1280.
9. Stankiewicz-Drogon A, Palchykovska LG, Kostina VG, Alexeeva IV, Shved AD, Boguszewska-Chachulska AM (2008) New acridone-4-carboxylic acid derivatives as potential inhibitors of hepatitis C virus infection. *Bioorg Med Chem* 16:8846–8852.

10. Belon CA, Frick DN (2009) Helicase inhibitors as specifically targeted antiviral therapy for hepatitis C. *Future Virol* 4:277–293.
11. Borowski P, Deinert J, Schalinski S, Bretner M, Ginalski K, Kulikowski T, Shugar D (2003) Halogenated benzimidazoles and benzotriazoles as inhibitors of the NTPase/helicase activities of hepatitis C and related viruses. *Eur J Biochem* 270:1645–1653.
12. Maga G, Gemma S, Fattorusso C, Locatelli GA, Butini S, Persico M, Kukreja G, Romano MP, Chiasserini L, Savini L *et al.* (2005) Specific Targeting of Hepatitis C Virus NS3 RNA Helicase. Discovery of the Potent and Selective Competitive Nucleotide-Mimicking Inhibitor QU663. *Biochemistry* 44:9637–9644.
13. Borowski P, Heising MV, Miranda IB, Liao CL, Choe J, Baier A (2008) Viral NS3 helicase activity is inhibited by peptides reproducing the Arg-rich conserved motif of the enzyme (motif VI). *Biochem Pharmacol* 76:28–38.
14. Belon CA, Frick DN (2008) Monitoring helicase activity with molecular beacons. *Biotechniques* 45:433–40, 442.
15. Gozdek A, Zhukov I, Polkowska A, Poznanski J, Stankiewicz-Drogon A, Pawlowicz JM, Zagorski-Ostojka W, Borowski P, Boguszevska-Chachulska AM (2008) NS3 Peptide, a novel potent hepatitis C virus NS3 helicase inhibitor: its mechanism of action and antiviral activity in the replicon system. *Antimicrob Agents Chemother* 52:393–401.
16. Khan IA, Siddiqui S, Rehmani S, Kazmi SU, Ali SH (2011) Fluoroquinolones inhibit HCV by targeting its helicase. *Antivir Ther, in press*.
17. Kandil S, Biondaro S, Vlachakis D, Cummins AC, Coluccia A, Berry C, Leyssen P, Neyts J, Brancale A (2009) Discovery of a novel HCV helicase inhibitor by a de novo drug design approach. *Bioorg Med Chem Lett* 19:2935–2937.
18. Gemma S, Butini S, Campiani G, Brindisi M, Zanolli S, Romano MP, Tripaldi P, Savini L, Fiorini I, Borrelli G *et al.* (2011) Discovery of potent nucleotide-mimicking competitive inhibitors of hepatitis C virus NS3 helicase. *Bioorg Med Chem Lett* 21:2776–2779.
19. Stankiewicz-Drogon A, Dorner B, Erker T, Boguszevska-Chachulska AM (2010) Synthesis of new acridone derivatives, inhibitors of NS3 helicase, which efficiently and specifically inhibit subgenomic HCV replication. *J Med Chem* 53:3117–3126.
20. Chen CS, Chiou CT, Chen GS, Chen SC, Hu CY, Chi WK, Chu YD, Hwang LH, Chen PJ, Chen DS *et al.* (2009) Structure-based discovery of triphenylmethane derivatives as inhibitors of hepatitis C virus helicase. *J Med Chem* 52:2716–2723.
21. Najda-Bernatowicz A, Krawczyk M, Stankiewicz-Drogon A, Bretner M, Boguszevska-Chachulska AM (2010) Studies on the anti-hepatitis C virus activity of newly synthesized tropolone derivatives: identification of NS3 helicase inhibitors that specifically inhibit subgenomic HCV replication. *Bioorg Med Chem* 18:5129–5136.

22. Boger DL, Fink BE, Brunette SR, Tse WC, Hedrick MP (2001) A simple, high-resolution method for establishing DNA binding affinity and sequence selectivity. *J Am Chem Soc* 123:5878–5891.
23. Brown DG, Sanderson MR, Garman E, Neidle S (1992) Crystal structure of a berenil-d(CGCAAATTTGCG) complex. An example of drug-DNA recognition based on sequence-dependent structural features. *J Mol Biol* 226:481–490.
24. Frick DN, Banik S, Rypma RS (2007) Role of divalent metal cations in ATP hydrolysis catalyzed by the hepatitis C virus NS3 helicase: magnesium provides a bridge for ATP to fuel unwinding. *J Mol Biol* 365:1017–1032.
25. Jensen RH (1977) Chromomycin A3 as a fluorescent probe for flow cytometry of human gynecologic samples. *J Histochem Cytochem* 25:573–579.
26. Horobin RW, Kiernan JA, Conn HJ (2002) Conn's biological stains: a handbook of dyes, stains and fluorochromes for use in biology and medicine. (BIOS, Oxford), pp 357-358.
27. Sharp A, Crabb SJ, Johnson PW, Hague A, Cutress R, Townsend PA, Ganesan A, Packham G (2009) Thioflavin S (NSC71948) interferes with Bcl-2-associated athanogene (BAG-1)-mediated protein-protein interactions. *J Pharmacol Exp Ther* 331:680–689.
28. Karlsson HJ, Lincoln P, Westman G (2003) Synthesis and DNA binding studies of a new asymmetric cyanine dye binding in the minor groove of [poly(dA-dT)]₂. *Bioorg Med Chem* 11:1035–1040.
29. Bengtsson M, Karlsson HJ, Westman G, Kubista M (2003) A new minor groove binding asymmetric cyanine reporter dye for real-time PCR. *Nucleic Acids Res* 31:e45.
30. Guntern R, Bouras C, Hof PR, Vallet PG (1992) An improved thioflavine S method for staining neurofibrillary tangles and senile plaques in Alzheimer's disease. *Experientia* 48:8–10.
31. Graham RK, Caiger P (1969) Fluorescence staining for the determination of cell viability. *Appl Microbiol* 17:489–490.
32. Belon CA, High YD, Lin TI, Pauwels F, Frick DN (2010) Mechanism and specificity of a symmetrical benzimidazolephenylcarboxamide helicase inhibitor. *Biochemistry* 49:1822–1832.
33. Frick DN, Ginzburg O, Lam AM (2010) A method to simultaneously monitor hepatitis C virus NS3 helicase and protease activities. *Methods Mol Biol* 587:223–233.
34. Lohmann V, Korner F, Koch J, Herian U, Theilmann L, Bartenschlager R (1999) Replication of subgenomic hepatitis C virus RNAs in a hepatoma cell line. *Science* 285:110–113.

35. Krieger N, Lohmann V, Bartenschlager R (2001) Enhancement of hepatitis C virus RNA replication by cell culture-adaptive mutations. *J Virol* 75:4614–4624.
36. Blight KJ, McKeating JA, Rice CM (2002) Highly permissive cell lines for subgenomic and genomic hepatitis C virus RNA replication. *J Virol* 76:13001–13014.
37. Huang Y, Chen XC, Konduri M, Fomina N, Lu J, Jin L, Kolykhalov A, Tan SL (2006) Mechanistic link between the anti-HCV effect of interferon gamma and control of viral replication by a Ras-MAPK signaling cascade. *Hepatology* 43:81–90.
38. Gosert R, Egger D, Lohmann V, Bartenschlager R, Blum HE, Bienz K, Moradpour D (2003) Identification of the hepatitis C virus RNA replication complex in Huh-7 cells harboring subgenomic replicons. *J Virol* 77:5487–5492.
39. Boguszevska-Chachulska AM, Krawczyk M, Stankiewicz A, Gozdek A, Haenni AL, Stokovskaya L (2004) Direct fluorometric measurement of hepatitis C virus helicase activity. *FEBS Lett* 567:253–258.
40. Lam AM, Keeney D, Eckert PQ, Frick DN (2003) Hepatitis C virus NS3 ATPases/helicases from different genotypes exhibit variations in enzymatic properties. *J Virol* 77:3950–3961.
41. Heck JA, Lam AM, Narayanan N, Frick DN (2008) Effects of mutagenic and chain-terminating nucleotide analogues on enzymes isolated from hepatitis C virus strains of various genotypes. *Antimicrob Agents Chemother* 52:1901–1911.
42. Belon CA, Frick DN (2009) Fuel specificity of the hepatitis C virus NS3 helicase. *J Mol Biol* 388:851–864.
43. Wakita T, Pietschmann T, Kato T, Date T, Miyamoto M, Zhao Z, Murthy K, Habermann A, Krausslich HG, Mizokami M *et al.* (2005) Production of infectious hepatitis C virus in tissue culture from a cloned viral genome. *Nat Med* 11:791–796.
44. Lanzetta PA, Alvarez LJ, Reinach PS, Candia OA (1979) An improved assay for nanomole amounts of inorganic phosphate. *Anal Biochem* 100:95–97.
45. Wolk B, Buchele B, Moradpour D, Rice CM (2008) A dynamic view of hepatitis C virus replication complexes. *J Virol* 82:10519–10531.
46. Lindenbach BD, Evans MJ, Syder AJ, Wolk B, Tellinghuisen TL, Liu CC, Maruyama T, Hynes RO, Burton DR, McKeating JA *et al.* (2005) Complete Replication of Hepatitis C Virus in Cell Culture. *Science* 309:623–626.
47. Lindenbach, B. D., Evans, M. J., Syder, A. J., Wolk, B., Tellinghuisen, T. L., Liu, C. C., Maruyama, T., Hynes, R. O., Burton, D. R., McKeating, J. A. & Rice, C. M. (2005) Complete Replication of Hepatitis C Virus in Cell Culture. *Science* **309**, 623-626.

48. Mousseau, G., Kota, S., Takahashi, V., Frick, D. N. & Strosberg, A. D. (2011) Dimerization-driven interaction of hepatitis c virus core protein with NS3 helicase. *J. Gen. Virol.* **92**, 101-111. PMC3052529

Appendix A: Details for the Material and Methods for the assays listed in Table 3.

Materials. Thioflavine S and primuline were purchased from Sigma (Cat. #T1892) and MP Biomedicals (Cat #195454), respectively. The Mechanistic Diversity Library was obtained from the National Cancer Institute (NCI, <http://ntp.cancer.gov/repositories.html>). All other reagents were purchased from commercial suppliers and used as received. All oligonucleotides were purchased from Integrated DNA Technologies (IDT, Coralville, IA). The partially DNA substrates used in MBHAs consisted of a helicase substrate forming 25 base pairs and consists of a 45-mer bottom strand 5'-GCT CCC CGT TCA TCG ATT GGG GAG C(T)20-3' and the 25-mer HCV top strand 5'-Cy5-GCT CCC CAA TCG ATG AAC GGG GAG C-IBRQ-3'. The 19-base pair RNA substrate used in MBHAs consisted of a 39 nucleotide long bottom strand 5'-AGU GCC UUG ACG AUA CAG C(U)20-3' and the 24 nucleotide long top strand 5'-Tye665-AGU GCG CUG UAU CGU CAA GGC ACU-IBRQSp-3'. Underlined areas denote hairpin-forming regions. DNA and RNA substrates were annealed and purified as described previously (14).

The cloning, expression, and purification of His-tagged recombinant HCV NS3 protein has been described previously (33, 40-42).

Helicase Assays [AID: 602275]. All assays were performed with helicase isolated from two different HCV genotypes (i.e. NS3h_1b(con1) and NS3h_2a(JFH1)). The genotype 1b is the basis for most HCV replicons (34) and genotype 2a(JFH1) is a unique strain capable of replicating in cell culture (43). All Molecular Beacon-based Helicase Assay (MBHAs) were performed as described before. (14, 42) For screening the NCI library, MBHAs contained 25 mM MOPS pH 6.5, 1.25 mM MgCl₂, 5.0 nM MBHA substrate, 12.5 nM NS3h_1b(con1), 0.05 mM DTT, 0.005 mg/mL BSA, 0.001% Tween20 with 20 μM each test compound (2% v/v final DMSO). In each flat black 384-well plate, 56 compounds were tested, in triplicate, along with 3 negative controls (DMSO only), 3 positive controls (500 nM dT20), and 2 wells with no enzyme. Fluorescence was read before ATP (F₀) addition and 30 minutes after ATP was added to 1 mM (F₃₀) using a Tecan Infinite M200 fluorescence microplate reader with excitation and emission wavelengths set to 643 and 670 nm, respectively. Percent inhibition was calculated with equation 1, and compound interference in the MBHA was calculated with equation 2.

$$\text{Inhibition (\%)} = \frac{\frac{Fc_0 - F(-)_0}{Fc_{30} - F(-)_{30}}}{1 - \frac{F(-)_0}{F(-)_{30}}} \cdot 100 \quad (\text{Equation 1})$$

$$\text{Interference (ratio)} = \frac{Fc_0}{F(-)_0} \quad (\text{Equation 2})$$

In equations 1 & 2, F_{c0} is the fluorescence of the reactions containing the test compound before adding ATP, F_{c30} is the fluorescence of the test compound reaction 30 minutes after adding ATP. F(-)₀ is the average of 3 DMSO-only negative control reactions before adding ATP and F(-)₃₀ is the average of three DMSO-only reactions 30 minutes after adding ATP.

To monitor helicase reaction kinetics and to calculate IC₅₀ values, MBHAs were performed in a volume of 60 µL in white ½ area 96-well plates and measured in a Thermo Varioskan Multimode reader (Thermo Scientific) using the 643 nm excitation wavelength and 667 emission wavelengths. Reactions were performed by first incubating all components except for ATP for two minutes, then initiated by injecting in 1/10 volume of ATP such that the final concentration of all components was as noted above. Initial reaction velocities were calculated by fitting first order decay equation to data obtained after ATP addition and calculating an initial velocity from the resulting amplitude and rate constant. The concentration at which a compound causes a 50% reduction in reaction velocity (IC₅₀) was calculated by fitting compound concentration to initial velocity using equation 3:

$$v_i = \frac{v_0}{1 + \left(\frac{[I]}{IC_{50}}\right)^h} \quad (\text{Equation 3})$$

where v₀ is the velocity observed in DMSO-only controls, h is the Hill slope coefficient, [I] is the concentration of test compound.

Reagent	Resource	Catalogue Number
NS3h_1b(con1) helicase	Frick Lab	N/A
NS3_2a(JFH1) helicase	Frick Lab	N/A
5'-Cy5-GCTCCCAATCGATGAACGGGGAGC-IBRQ-3'	Integrated DNA technologies	N/A
5'-GCT CCC CGT TCA TCG ATT GGG GAG C(T)20-3	Integrated DNA technologies	N/A

DNA Binding Assays [AID 623972 (ethidium bromide) and AID 623970 (SYBR Green I)]. Fluorescent intercalator displacement (FID) assays (22) were used to measure the ability of a compound to bind the MBHA substrate. The concentration at which half the ethidium bromide is displaced (EC₅₀), were determined using the different conditions as above to more closely mimic the conditions of a standard helicase assay. Each 60 µL reaction contained 25 mM MOPS pH 6.5, 0.32 µM MBHA DNA substrate (lacking Cy5 and IBQ-RQ modifications), 2 µM ethidium bromide, and various concentrations of test compound. Fluorescence of ethidium bromide was monitored using excitation and emission wavelengths of 545 and 595 nm, respectively, on a Cary Eclipse fluorescence spectrophotometer in white 96-well plates. The amount of ethidium bromide-DNA complex fluorescence was used to estimate the ability of compounds to bind DNA, and therefore displace the fluorescent intercalator (ethidium bromide).

$$\text{Binding}(\%) = \frac{F_c - F(+)}{F(-) - F(+)} \times 100 \quad (\text{Equation 4})$$

In equation 4, F_c is the fluorescence in the presence of the compound, $F(-)$ is the average DMSO-only negative controls, and $F(+)$ is the average positive controls (100 μ M berenil). EC_{50} values were from a normalized dose response curve.

A modified FID assay in which ethidium bromide was replaced with SYBR Green I (Invitrogen) was used to estimate a compound affinity for the MBHA substrate. Reactions were performed as described above except that the DNA substrate was present at 0.64 μ M, ethidium bromide was absent and SYBR Green I was present at 0.68 μ M. Data were normalized as described above and fit to dose response equation using GraphPad Prism software. Titrations with each compound were performed in triplicate and EC_{50} values from three independent titrations are reported \pm standard deviations. Average percent bound at 100 μ M is reported for compounds that did not decrease the fluorescence of SYBR green stained DNA more than 50% at the highest concentration tested.

Reagent	Resource	Catalogue Number
Ethidium bromide	Alfa Aesar	L07482
SYBR Green I	Invitrogen	S-7585
5'-GCT CCC CAA TCG ATG AAC GGG GAG C-3'	Integrated DNA Technologies	N/A
5'-GCT CCC CGT TCA TCG ATT GGG GAG C(T)20-3	Integrated DNA Technologies	N/A

ATP Hydrolysis Assays [AID 623973]. A modified “malachite green” assay was used to measure ATP hydrolysis(44). Reactions were 30 μ L and contained 25 mM MOPS pH 6.5, 1.25 mM $MgCl_2$, and 1 mM ATP. The colorimetric reagent was prepared fresh by mixing 3 volumes 0.045% (w/v) malachite green, 1 volume 4.2% ammonium molybdate in 4N HCl, and 0.05 volume of 20% Tween 20. For SAR profiling, reactions were performed in 10% DMSO with 8 concentrations of each compound ranging from 200 μ M to 1.6 μ M in the absence of RNA with 100 nM of NS3h_1b(Con1). Reactions were initiated by adding ATP, incubated for 30 minutes at 23 $^{\circ}$ C, and terminated by adding 200 μ l of the malachite green reagent, followed by 30 μ L of 35% sodium citrate. The color was allowed to develop for 30 minutes and absorbance at 630 nm was read. Percent inhibition was calculated by normalizing the data to reactions without enzyme (100% inhibition) and reactions with DMSO only (0% inhibition).

Reagent	Resource	Catalogue Number
NS3_1b(con1) helicase	Frick Lab	N/A
Poly(U)RNA	Sigma-Aldrich	P9528-100MG
Malachite green	ACROS	41349-0250

NS3 Protease Assay [AID 623964]. All protease assays were carried out using the AnaSpec Enzolyte 520 Protease Assay Kit according to the manufacturer’s protocol (AnaSpec, San Jose, CA). Each assay contained either the test compound, DMSO as a negative control or 20 μ M of the HCV protease inhibitor. Assays were carried out in a total volume of 20 μ L in black 384-well

plates with fluorescence measured using a BMG FLUOstar Omega fluorescence spectrophotometer. The protease enzyme used was 10 nM of “single chain” NS3-NS4A (scNS3-4A), where the portion of NS4A needed for protease activation tethered to its N-terminus of NS3 (33). IC₅₀ values were calculated from slopes of the initial reaction phases fit to compound concentration as determined with equation 3 (above).

Table A.4. Critical reagents for the NS3 protease assay		
Reagent	Resource	Catalogue Number
NS3-NS4A (scNS3-4A)	Frick Lab	N/A
AnaSpec Enzolyte 520 Protease Assay Kit	AnaSpec	71145

***E. coli* SSB DNA binding Assay [AID 623966].** Assays were performed in 60 µL in 384-well black microplates. All assays contained 5 nM Cy5-dT15 DNA (5'- Cy5 TT TTT TTT TTT TTT T - 3'), 20 nM *E. coli* SSB (New England Biolabs), 25 mM MOPS, pH 7.5, 1.25 mM MgCl₂, 0.0025 mg/ml BSA, 0.005% (v/v) Tween20, and 0.025 mM DTT. Compounds dissolved in DMSO were added at the indicated concentration, and Cy5 fluorescence polarization was read using a G-factor calculated from a well lacking SSB or test compounds. Percent displacement was calculated by first calculating percent binding as described above for the FID assay then subtracting percent binding from 100. Dose response curves were fit to the data to calculate IC₅₀ values.

Table A.5. Critical reagents for the <i>E. coli</i> SSB DNA binding assay		
Reagent	Resource	Catalogue Number
Cy5-dT15 DNA	Integrated DNA Technologies	Custom synthesis
<i>E. coli</i> SSB	New England Biolabs	M301A

HCV Subgenomic Replicon Assay [AID 623962]. An HCV Renilla luciferase (HCV RLuc) reporter construct was used to measure the effect of each compound on cellular HCV RNA levels. The replicon was a generous gift from Seng-Lai Tan. In HCV RLuc, the HCV internal ribosome entry site (IRES) drives the translation of the neomycin and Renilla luciferase genes while the HCV nonstructural proteins (NS3 to NS5B) are translated from the Encephalomyocarditis virus IRES (37). The plasmid DNA was cleaved with Sca I, purified by phenol/chloroform extraction followed by ethanol precipitation, and used as template for RNA transcription using MEGAscript™ T7 RNA transcription kit (Ambion, Austin, TX). The RNA transcripts were treated with 2 U DNase I (Ambion) at 37 °C for 30 min, purified by acid phenol/chloroform extraction, followed by isopropanol precipitation, and suspended in diethylpyrocarbonate-treated water. RNA concentration was determined by spectrophotometry by measuring the OD₂₆₀. RNA integrity and size was checked on 1% agarose gel. Transcribed RNA was stored in aliquots at -80 °C until needed.

Huh7.5 cells RNA were transfected with HCV RNA by electroporation. Briefly, subconfluent Huh7.5 cells were trypsinized, suspended in complete growth medium, and centrifuged at 1,000 x g for 5 min at 4 °C. The cell pellets were then washed twice with ice-cold phosphate-buffered saline (PBS) and suspended at 1.75 x 10⁷ cells/mL in ice-cold PBS. Replicon RNA (5 µg) was

mixed with 0.4 ml of cell suspension and transferred to a 2 mm gap width electroporation cuvette (Eppendorf AG, Germany) and pulsed with 5 times for 99 μ sec at 820 V over 1.1 sec intervals using the ECM 830 electroporator instrument (BTX Harvard Apparatus, Holliston, MA). After a 5 min recovery period at room temperature, cells transferred to 10 mL complete growth medium, and seeded into 10 cm diameter cell culture dishes. 24 Hours after transfection, the medium was replaced with fresh complete DMEM supplemented with 1 mg/mL geneticin (Invitrogen) and the medium was replaced every three to four days with fresh medium containing 1 mg/mL geneticin. Geneticin-resistant colonies were selected for a period of two weeks and expanded in the presence of 250 μ g/mL geneticin.

HCV RLuc replicon cells were seeded at a density of 10,000 cells per well in 96-well plates and incubated for 4-5 h to allow the cells to attach to the plate. The compounds dissolved in dimethyl sulfoxide (DMSO) were added at a final concentration of 10 μ M (DMSO solvent final concentration was 0.5%) and the cells were incubated for 72 h at 37 °C under 5% CO₂ atmosphere. The effects of compounds on HCV replication were then assessed by measuring the Renilla luciferase activity in compound-treated versus DMSO-treated cells. At the end of the incubation period, the medium was aspirated and the cells were washed with 1 x PBS. The Renilla luciferase reporter gene assay was performed using the Renilla luciferase assay kit (Promega, Madison, WI) according to the manufacturer's instructions. Briefly, the cells were lysed by addition of 50 μ L of Renilla luciferase lysis buffer (Promega) followed by two cycles of freeze/thaw. The luciferase activity content of the lysate was measured with a FLUOstar Omega microplate reader instrument (BMG Labtech, Germany) after injecting 50 μ L of luciferase substrate and reading for 5 s.

Reagent	Resource	Catalogue Number
HCV RLuc	Seng-Lai Tan	N/A
SCA I	New England Biolabs	R0122S
2 U DNase I	Ambion	2238G2
Huh-7.5 cells	Rice Lab (Rockefeller U)	N/A
DMEM	Invitrogen	11995
Geneticin	Invitrogen	10131
Renilla luciferase assay kit	Promega	E2820
MEGAScript RNA transcription kit	Ambion	AM1334

Cell Viability Assay [AID 623961]. To assess compound toxicity towards Huh-7.5 cells, cells were plated and treated as above and cell viability was assessed using the cellTiter-Glo luminescent cell viability kit (Promega) following the manufacturer's instructions. Briefly, at the end of a 72 h incubation period, the medium was aspirated and the cells were washed with 1x PBS, then an equal volume of growth medium and cellTiter-Glo reagent was added and the lysis was initiated by mixing on an orbital shaker. The plate was incubated at 23 °C for 30 min and the luciferase activity was measured for 1 s using the FLUOstar Omega microplate reader (BMG Labtech).

Reagent	Resource	Catalogue Number
Huh-7.5 cells	Rice Lab (Rockefeller U)	N/A
CellTiter-Glo luminescent cell viability kit	Promega	G7572

Cellular HCV RNA quantification Assays [AID 623968]. At the end of the treatment the cells were washed 2 times with ice cold phosphate buffered-saline and harvested by scraping and collected by low speed centrifugation at 1000 x g for 5 min at 4 °C. Total RNA was then extracted using TRizol total RNA extraction kit (Invitrogen) following the manufacturer's instructions and suspended in 30 µL of nuclease-free water. RNA concentration was determined by reading the absorbance at 260 nm and RNA samples were stored in aliquots at -70 °C until needed. Real time RT-PCR was performed with the TaqMan chemistry using 1 µg total RNA and the qScript™ One-step Fast qRT-PCR kit (Quanta Biosciences, Gaithersburg, MD) following the manufacturer's instructions. Reverse transcription was done at 50 °C for 20 min followed by one cycle at 95 °C for 5 min and 40 cycles at 95 °C, 15 sec and 60 °C for 1 min. HCV primers and probe target the HCV 5'UTR. The house-keeping gene rRNA was amplified in parallel for normalization. The expression levels of HCV RNA in each sample were determined by first calculating the ΔC_T of each sample which was obtained by subtracting the threshold cycle (C_T) of each sample including the DMSO-control sample to that of the corresponding housekeeping gene rRNA. The relative expression level was then determined by the $2^{-\Delta\Delta C_T}$ method where $\Delta\Delta C_T$ is the difference between the ΔC_T of each sample to that of the DMSO-control sample.

Reagent	Resource	Catalogue Number
TRizol reagent	Invitrogen	15596-026
qScript One-Step Fast qRT-PCR kit	Quanta Biosciences	95079-500

Indirect immunofluorescence staining. Huh-7.5/Rluc cells were plated on cover slips in a 24 well plate. The next day, compounds were added at a 10 µM concentration and after 48 h from the first addition, the medium was supplemented with 10 µM compound. Interferon alpha2a was used as control and 100 U/well was added at same time points as compounds were added. After 72 h of treatment, Indirect immunofluorescence staining was performed as described previously (45). Cells were fixed in 1% PFA for 40 min, washed thrice with 5 mL PBS, permeabilized with 0.05% saponin (Sigma Aldrich) and blocked with 3% BSA (PAA) in 1 x PBS for 1 h at 37 °C. Subsequently, cells were washed with 2 mL 1 x PBS three times, and the mouse monoclonal antibody 9E10 against NS5A (a kind gift from Charles Rice, Rockefeller University) (46) was added pre-diluted in blocking buffer, and was incubated for 1 h at room temperature. Cells were washed three times with 2 mL 1 x PBS and once with 3% BSA. The cells were then incubated with Alexa 546 goat F(ab')₂ anti-mouse immunoglobulin G (IgG)

(Invitrogen) for 1 h at room temperature. Cells were washed twice with 1 x PBS and then mounted on glass slides using ProLong Gold anti-fade reagent (Invitrogen). Appropriate controls were performed to rule out nonspecific binding of primary antibody and secondary antibody.

Reagent	Resource	Catalogue Number
Huh-7.5/Rluc cells	Frick Lab	N/A
Interferon alpha2b	PBL Biomedical Laboratories	11105-1
saponin	Sigma Aldrich	47036
Mouse monoclonal antibody 9E10	Charles Rice, Rockefeller University	N/A
Alexa 546 goat F(ab)2 anti-mouse immunoglobulin G	Invitrogen	A-11018
ProLong Gold	Invitrogen	P36934

Microscopy. Wide-field microscopy was performed with a Nikon Ti-E inverted fluorescence microscope using a 40 x/NA 1.4 objective. Compounds were imaged using DAPI filter 340/40 band-pass excitation and a 435/50 band pass emission filter. For Alexa 546, a 528/25 nm band pass excitation filter and 590/60 nm band-pass emission filter were used. Image acquisition was performed with a Q imaging Rolera camera and the NIS elements basic research imaging software (Nikon). Images were processed uniformly by using NIH Image J 1.45m image analysis software.

Appendix B: NMR Data and LCMS Data for Probe Compound for Probe CID 50930730/ML283:

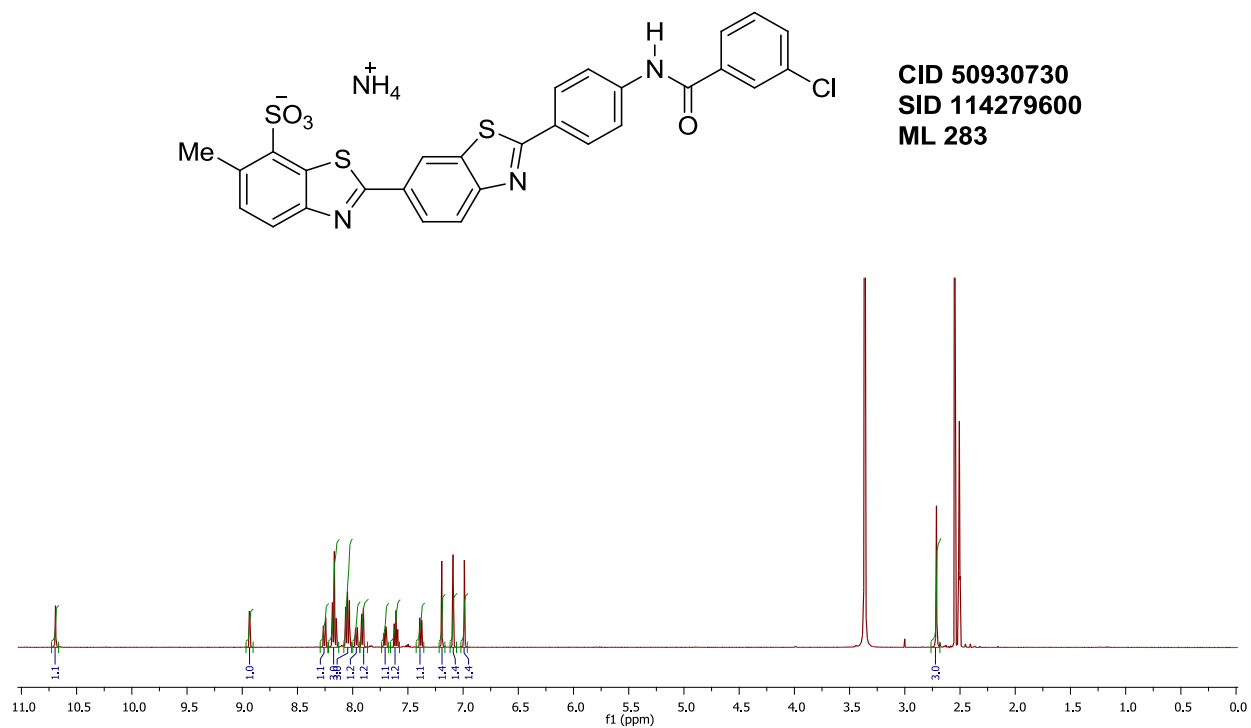


Figure B.1. Proton NMR spectrum for SID 114279600 (CID 50930730)

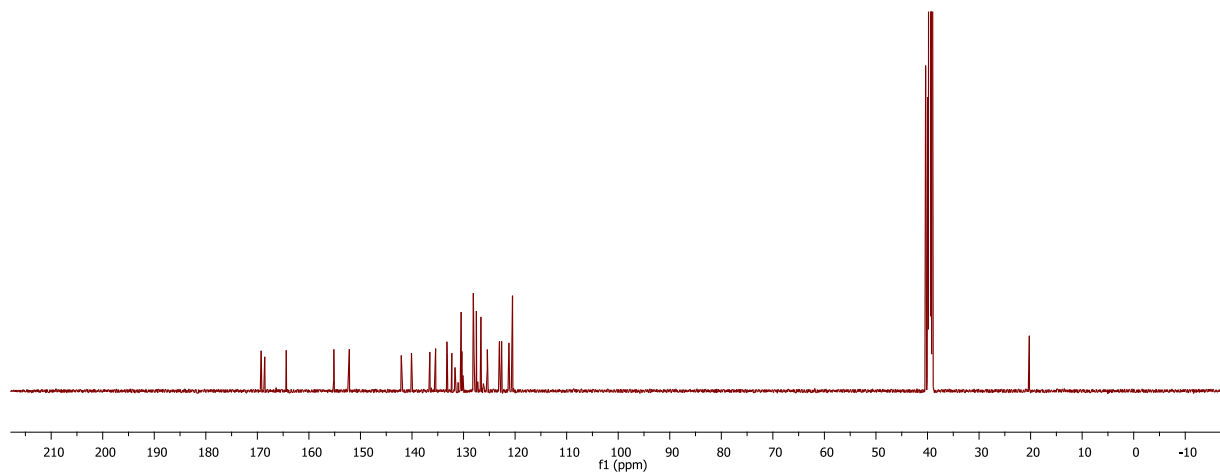
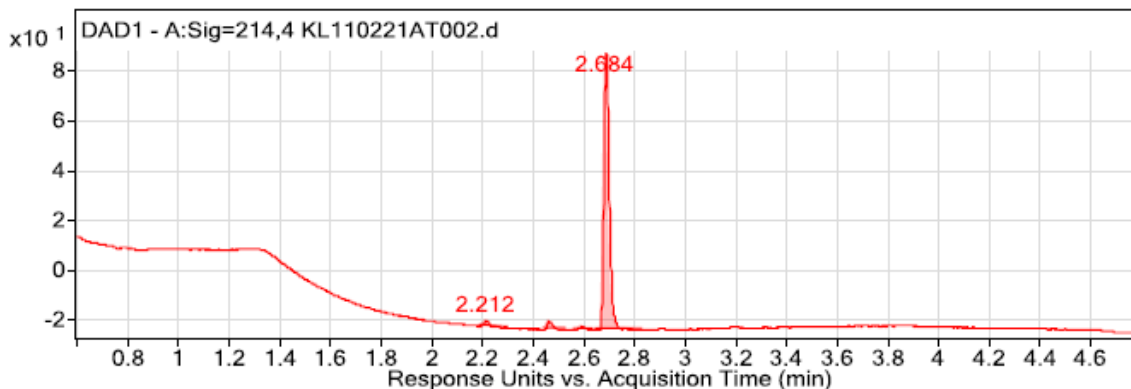


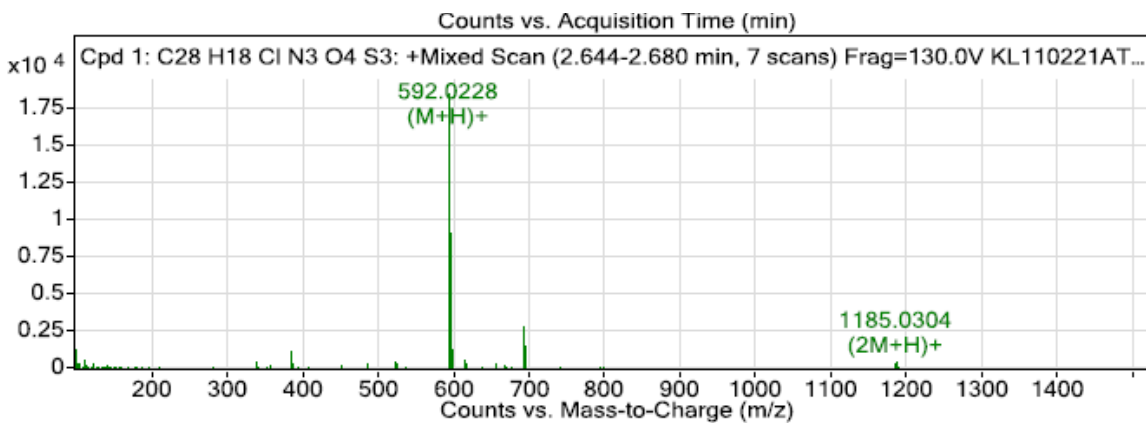
Figure B.2. Carbon NMR spectrum for SID 114279600 (CID 50930730)



User Chromatogram Peak List

Peak #	RT	Height	Height %	Area	Area %	Area Sum %	Width
1	2.212	2.37	2.15	4.02	2.42	2.27	0.025
2	2.459	3.14	2.85	5.12	3.08	2.88	0.025
3	2.59	1.33	1.21	2.3	1.38	1.3	0.027
4	2.684	110.25	100	166.02	100	93.56	0.024

Figure B.3. LCMS purity data at 214 nm for SID 114279600 (CID 50930730); LCMS retention time: 2.68; purity at 214 nm = 93.6%.

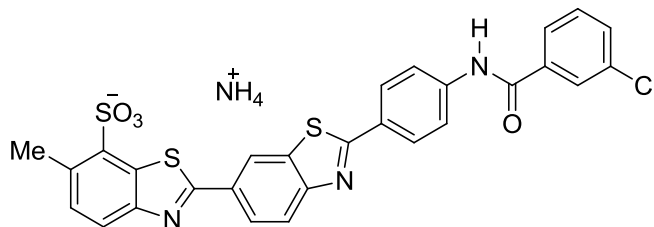


m/z	Calc m/z	Diff(ppm)	z	Abund	Formula	Ion
592.0228	592.0221	1.22		18444	C ₂₈ H ₁₉ ClN ₃ O ₄ S ₃	(M+H) ⁺
593.0243	593.025	-1.06		5723	C ₂₈ H ₁₉ ClN ₃ O ₄ S ₃	(M+H) ⁺
594.02	594.0199	0.27		9084	C ₂₈ H ₁₉ ClN ₃ O ₄ S ₃	(M+H) ⁺
594.4901				563		
595.0226	595.0221	0.69		2688	C ₂₈ H ₁₉ ClN ₃ O ₄ S ₃	(M+H) ⁺
596.0169	596.0185	-2.72		1326	C ₂₈ H ₁₉ ClN ₃ O ₄ S ₃	(M+H) ⁺
614.0038	614.004	-0.39	1	642	C ₂₈ H ₁₈ ClN ₃ NaO ₄ S ₃	(M+Na) ⁺
616.0004	616.0018	-2.25	1	417	C ₂₈ H ₁₈ ClN ₃ NaO ₄ S ₃	(M+Na) ⁺
1183.0355	1183.0369	-1.17	1	336	C ₅₆ H ₃₇ Cl ₂ N ₆ O ₈ S ₆	(2M+H) ⁺
1185.0304	1185.0355	-4.29	1	511	C ₅₆ H ₃₇ Cl ₂ N ₆ O ₈ S ₆	(2M+H) ⁺

Figure B.4. HRMS data for SID 114279600 (CID 50930730); HRMS (ESI) m/z calcd for C₂₈H₁₉ClN₃O₄S₃ ([M+H]⁺), 592.0226, found 592.0228.

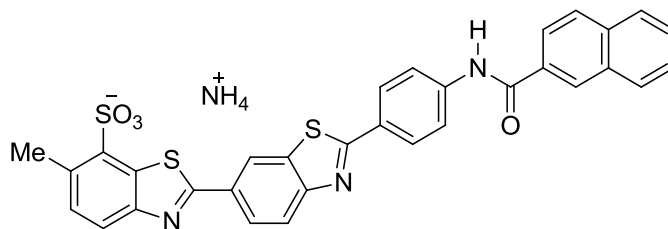
Appendix C: Continuation of Section 2.3, Probe Preparation.

Supporting information for supporting analogues submitted with the probe is detailed below.



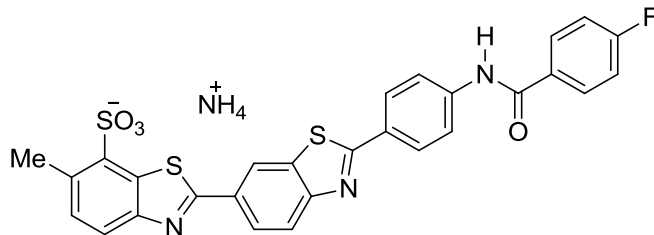
ML283
CID50930730

2'-(4-(3-chlorobenzamido)phenyl)-6-methyl-[2,6'-bibenzo[d]thiazole]-7-sulfonic acid. ^1H NMR (500 MHz, DMSO) δ 10.69 (s, 1H), 8.93 (d, $J = 1.8$ Hz, 1H), 8.26 (dd, $J = 1.8, 8.5$ Hz, 1H), 8.18 – 8.15 (m, 3H), 8.08 – 8.01 (m, 3H), 7.97 (d, $J = 8.2$ Hz, 1H), 7.91 (d, $J = 8.0$ Hz, 1H), 7.74 – 7.67 (m, 1H), 7.61 (t, $J = 7.9$ Hz, 1H), 7.38 (d, $J = 8.6$ Hz, 1H), 7.19 (s, 1H), 7.09 (s, 1H), 6.99 (s, 1H), 2.71 (s, 3H). ^{13}C NMR (126 MHz, DMSO) δ 169.3, 168.6, 164.4, 155.2, 152.2, 142.1, 140.1, 136.5, 135.4, 133.23, 133.17, 132.3, 131.7, 130.5, 130.3, 130.1, 128.1, 128.0, 127.5, 126.6, 125.4, 123.0, 122.6, 121.2, 120.5, 20.3. HRMS (m/z): calcd for $\text{C}_{28}\text{H}_{19}\text{ClN}_3\text{O}_4\text{S}_3$ (neutral $\text{M}+\text{H}$) 592.0226; found 592.0228.



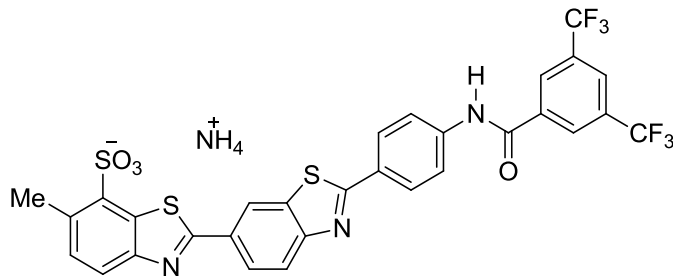
CID49849293

2'-(4-(2-naphthamido)phenyl)-6-methyl-[2,6'-bibenzo[d]thiazole]-7-sulfonic acid. ^1H NMR (500 MHz, DMSO) δ 10.79 (s, 1H), 8.94 (d, $J = 1.8$ Hz, 1H), 8.65 (s, 1H), 8.26 (dd, $J = 1.8, 8.5$ Hz, 1H), 8.20 – 8.16 (m, 3H), 8.15 – 8.02 (m, 6H), 7.91 (d, $J = 8.0$ Hz, 1H), 7.69 – 7.64 (m, 2H), 7.39 (d, $J = 8.5$ Hz, 1H), 7.19 (s, 1H), 7.09 (s, 1H), 6.99 (s, 1H), 2.72 (s, 3H). ^{13}C NMR (126 MHz, DMSO) δ 169.4, 168.6, 165.9, 155.2, 152.2, 142.5, 140.1, 135.4, 134.4, 133.2, 132.3, 132.0, 131.9, 130.3, 130.1, 129.0, 128.2, 128.13, 128.10, 128.0, 127.8, 127.7, 126.9, 125.4, 124.4, 123.0, 122.6, 121.2, 120.4, 20.3. HRMS (m/z): calcd for $\text{C}_{32}\text{H}_{22}\text{N}_3\text{O}_4\text{S}_3$ (neutral $\text{M}+\text{H}$) 608.0772; found 608.0760.



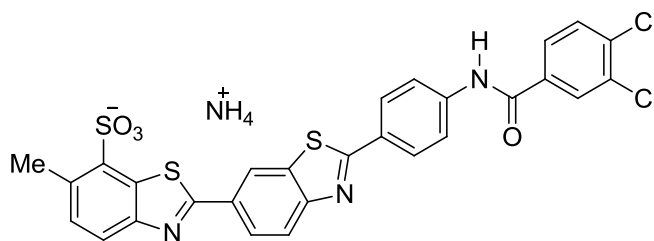
CID49849294

2'-(4-(4-fluorobenzamido)phenyl)-6-methyl-[2,6'-bibenzo[d]thiazole]-7-sulfonic acid. ^1H NMR (400 MHz, DMSO) δ 10.61 (s, 1H), 8.93 (d, $J = 1.8$ Hz, 1H), 8.26 (dd, $J = 1.8, 8.5$ Hz, 1H), 8.21 – 8.13 (m, 3H), 8.13 – 8.07 (m, 2H), 8.07 – 8.00 (m, 2H), 7.92 (d, $J = 8.0$ Hz, 1H), 7.43 – 7.38 (m, 3H), 7.22 (s, 1H), 7.10 (s, 1H), 6.97 (s, 1H), 2.72 (s, 3H). ^{13}C NMR (101 MHz, DMSO) δ 169.3, 168.6, 164.7, 163.0, 155.2, 152.2, 142.3, 140.1, 135.4, 133.2, 132.3, 131.04, 131.01, 130.6, 130.5, 130.3, 130.1, 128.1, 127.8, 125.4, 123.0, 122.6, 121.2, 120.4, 115.5, 115.3, 20.3. HRMS (m/z): calcd for $\text{C}_{28}\text{H}_{19}\text{FN}_3\text{O}_4\text{S}_3$ (neutral M+H) 576.0522; found 576.0509.



CID50930749

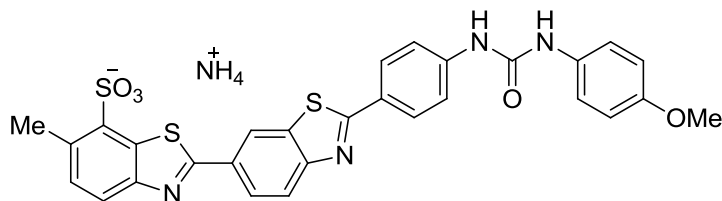
2'-(4-(3,5-bis(trifluoromethyl)benzamido)phenyl)-6-methyl-[2,6'-bibenzo[d]thiazole]-7-sulfonic acid. ^1H NMR (500 MHz, DMSO) δ 10.96 (s, 1H), 8.94 (d, $J = 2.2$ Hz, 1H), 8.66 (s, 2H), 8.41 (s, 1H), 8.26 (dd, $J = 1.8, 8.5$ Hz, 1H), 8.21 (d, $J = 8.8$ Hz, 2H), 8.16 (d, $J = 8.7$ Hz, 1H), 8.04 (d, $J = 8.8$ Hz, 2H), 7.91 (d, $J = 8.0$ Hz, 1H), 7.38 (d, $J = 8.5$ Hz, 1H), 7.19 (s, 1H), 7.09 (s, 1H), 6.99 (s, 1H), 2.71 (s, 3H). ^{13}C NMR (126 MHz, DMSO) δ 169.2, 168.6, 162.9, 155.2, 152.2, 141.6, 140.1, 136.8, 135.4, 133.2, 132.3, 130.9, 130.6, 130.4, 130.3, 130.13, 130.06, 128.7, 128.4, 128.2, 126.4, 125.4, 124.2, 123.1, 122.6, 122.0, 121.2, 120.7, 20.2. HRMS (m/z): calcd for $\text{C}_{30}\text{H}_{18}\text{F}_6\text{N}_3\text{O}_4\text{S}_3$ (neutral M+H) 694.0364; found 694.0340.



CID50930737

2'-(4-(3,4-dichlorobenzamido)phenyl)-6-methyl-[2,6'-bibenzo[d]thiazole]-7-sulfonic acid.

^1H NMR (500 MHz, DMSO) δ 10.71 (s, 1H), 8.92 (d, $J = 1.8$ Hz, 1H), 8.30 – 8.21 (m, 2H), 8.17 – 8.14 (m, 3H), 8.02 (d, $J = 8.8$ Hz, 2H), 7.98 (dd, $J = 2.1, 8.4$ Hz, 1H), 7.90 (d, $J = 8.0$ Hz, 1H), 7.84 (d, $J = 8.4$ Hz, 1H), 7.38 (d, $J = 8.6$ Hz, 1H), 7.20 (s, 1H), 7.10 (s, 1H), 7.00 (s, 1H), 2.71 (s, 3H). ^{13}C NMR (126 MHz, DMSO) δ 169.2, 168.6, 163.5, 155.2, 152.2, 141.9, 140.1, 135.4, 134.8, 134.6, 133.2, 132.3, 131.3, 130.8, 130.3, 130.1, 129.7, 128.2, 128.09, 128.06, 125.4, 123.0, 122.6, 121.2, 120.5, 20.3. HRMS (m/z): calcd for $\text{C}_{28}\text{H}_{18}\text{Cl}_2\text{N}_3\text{O}_4\text{S}_3$ (neutral $\text{M}+\text{H}$) 625.9836; found 625.9833.



CID53356656

2'-(4-(3-(4-methoxyphenyl)ureido)phenyl)-6-methyl-[2,6'-bibenzo[d]thiazole]-7-sulfonic acid.

^1H NMR (400 MHz, DMSO) δ 9.06 (s, 1H), 8.90 (d, $J = 2.3$ Hz, 1H), 8.64 (s, 1H), 8.24 (dd, $J = 1.8, 8.5$ Hz, 1H), 8.13 (d, $J = 8.9$ Hz, 1H), 8.08 (d, $J = 8.8$ Hz, 2H), 7.91 (d, $J = 8.0$ Hz, 1H), 7.69 (d, $J = 8.8$ Hz, 2H), 7.42 – 7.38 (m, 3H), 7.03 (s, br. 3H), 6.91 (d, $J = 9.1$ Hz, 2H), 3.74 (s, 3H), 2.72 (s, 3H). ^{13}C NMR (126 MHz, DMSO) δ 169.5, 168.6, 155.3, 154.7, 152.3, 152.2, 143.4, 140.1, 135.3, 133.1, 132.31, 132.25, 130.1, 128.3, 125.8, 125.3, 122.8, 122.6, 121.1, 120.2, 118.0, 114.0, 55.1, 20.2. HRMS (m/z): calcd for $\text{C}_{29}\text{H}_{23}\text{N}_4\text{O}_5\text{S}_3$ (neutral $\text{M}+\text{H}$) 603.0831; found 603.0831.

Appendix D: Description of the outcome for the screen of 827 compounds from the NCI DTP compound collection.

Compounds are ranked by their ability to inhibit HCV helicase catalyzed DNA unwinding as calculated from equation 1 (Appendix A). Assay interference was calculated with equation 2 (Appendix A).

NSC#	Inhibition (%)	Interference (Ratio)
363998	138.7	0.17
175493	136.8	0.57
273829	105.0	0.26
34391	100.6	0.24
69187	99.2	0.22
34931	89.2	0.90
70845	84.4	0.59
154890	79.4	0.29
640199	76.4	0.70
640506	71.1	0.91
337766	70.0	0.65
85561	68.8	0.90
71948	67.5	0.91
3053	67.5	0.55
627168	64.3	0.53
44690	61.5	0.66
166454	60.4	0.18
10010	56.7	0.23
208734	56.5	0.56
638352	56.2	0.89
87206	55.6	0.92
526417	55.2	0.86
14229	55.1	1.08
58514	54.9	1.04
622124	54.2	1.11
51148	53.4	0.94
15200	53.4	0.75
142982	53.1	0.75
136044	47.9	0.33
258812	46.4	0.64
338259	45.5	0.93
699479	45.1	0.38
276299	42.1	0.54
219734	41.8	0.26
98904	41.2	0.89
93419	38.9	0.91

265450	38.9	0.54
96932	38.8	0.59
5159	38.6	1.03
181486	38.3	0.50
637993	37.7	0.77
224124	37.7	0.93
245432	37.4	1.06
623135	36.6	0.87
316157	36.4	0.70
268986	36.0	0.81
24559	36.0	0.91
290205	34.9	1.03
73413	34.8	0.99
146397	34.3	0.67
70422	33.9	0.85
652174	33.4	0.87
667467	33.3	0.89
145366	33.1	0.53
329696	32.6	0.81
354844	32.6	0.93
70929	32.1	0.20
13973	31.8	0.28
255109	31.7	0.77
267229	31.5	0.49
18805	31.0	0.98
268242	30.6	0.88
14574	30.3	0.85
85700	29.7	0.46
641607	29.4	1.03
305782	28.4	0.87
288010	28.3	1.01
305819	28.1	0.99
668270	28.1	0.83
678917	28.1	0.89
326231	28.0	0.94
18268	27.6	0.61
622732	27.4	0.92
347466	27.4	0.89
184403	27.4	0.42
28002	27.1	1.08
600305	26.6	0.91
603169	26.2	0.22
53908	26.0	0.82

22992	25.9	0.86
304421	25.6	0.97
664327	25.5	0.82
635366	25.5	1.05
351306	25.4	0.92
119875	25.1	0.83
19990	25.1	0.96
600300	24.9	0.91
54650	24.7	1.11
243023	24.2	0.46
619179	23.8	0.44
647613	23.5	0.91
633001	23.2	0.89
68075	23.1	1.02
314622	23.1	0.70
639828	23.0	1.05
382007	22.9	0.85
167780	22.8	1.00
106408	22.7	0.94
363182	22.2	1.08
215989	21.9	0.82
361813	21.8	1.03
610744	21.5	0.83
49660	21.2	0.93
637680	21.2	0.91
14974	20.9	0.99
632536	20.7	0.84
328166	20.7	1.04
299879	20.5	0.94
632839	20.4	0.87
681744	20.4	0.98
7364	20.2	0.86
68093	19.5	0.90
407010	19.4	0.90
382766	19.2	0.90
614928	19.1	0.99
30916	19.0	0.93
529469	18.9	0.89
35489	18.7	1.04
86100	18.6	1.00
339004	18.5	0.89
45575	18.4	0.97
169676	18.3	0.87

269754	18.3	0.98
670224	17.9	0.88
400978	17.9	1.10
653012	17.7	0.91
45388	17.5	0.95
296961	17.5	0.92
653010	17.5	0.88
336628	17.4	0.90
233872	17.4	1.00
644735	17.3	0.94
363744	17.2	1.04
676561	17.1	0.96
620277	17.1	0.93
11779	16.8	0.89
403148	16.8	0.94
635441	16.7	0.92
37364	16.5	1.01
274893	16.2	0.88
33006	15.9	0.89
89303	15.8	0.93
125066	15.8	0.79
634658	15.7	0.85
20534	15.7	0.96
635436	15.6	0.89
632841	15.6	0.81
24817	15.4	0.99
35866	15.3	0.93
18804	15.2	0.97
670140	15.2	0.95
626120	15.1	0.97
269146	15.0	0.89
32982	15.0	0.90
643164	14.9	0.86
145669	14.8	1.14
165563	14.6	0.95
643774	14.6	0.90
662825	14.5	0.93
664181	14.5	0.84
635121	14.5	0.92
625590	14.3	0.95
118732	14.2	0.89
605756	14.1	0.33
65381	14.1	0.96

375294	13.9	0.87
118976	13.9	0.96
330516	13.8	0.92
60309	13.6	0.93
619165	13.6	0.89
47147	13.5	0.40
635824	13.5	0.91
180973	13.5	0.90
603577	13.5	0.93
163088	13.3	0.87
695218	13.3	0.99
172924	13.3	1.01
168415	13.3	0.95
183359	13.3	0.83
149765	13.2	0.94
46061	13.2	0.93
375575	12.9	0.93
9856	12.6	0.84
71669	12.4	1.06
667235	12.3	1.06
224131	12.3	0.86
305222	12.2	1.03
621889	12.2	1.08
330500	12.0	1.04
625483	12.0	0.93
129414	12.0	1.08
3970	11.8	0.95
749	11.7	0.89
697443	11.6	1.01
379531	11.6	0.89
164914	11.5	0.91
97911	11.5	0.95
376248	11.4	0.80
65380	11.3	1.03
607347	11.1	0.95
24113	11.0	0.81
265473	11.0	0.96
138429	10.9	1.09
405158	10.9	1.09
260610	10.7	0.27
323241	10.7	0.90
320846	10.7	0.90
118742	10.6	1.01

157389	10.6	0.88
640391	10.6	1.09
211500	10.6	0.89
5354	10.6	0.97
349438	10.5	1.01
76455	10.5	0.95
82025	10.4	0.94
19994	10.4	1.05
163501	10.3	0.91
71851	10.2	0.94
680506	10.2	0.92
99027	10.1	0.93
49842	9.9	0.98
633209	9.9	0.87
631160	9.9	0.91
664298	9.8	0.96
77021	9.8	1.00
169543	9.6	1.02
640584	9.6	0.90
261726	9.6	0.96
383468	9.4	0.98
140377	9.4	0.93
688795	9.3	1.02
345081	9.2	0.95
624158	9.2	0.90
177365	9.2	0.49
657722	9.1	0.93
126849	9.0	1.02
295156	9.0	0.99
635968	9.0	0.97
1026	9.0	0.90
119686	8.9	1.18
305884	8.9	1.04
265211	8.9	0.82
377	8.8	1.02
636786	8.8	0.91
659174	8.7	0.92
648419	8.6	0.90
72961	8.5	0.98
63878	8.3	0.89
132791	8.2	0.98
651084	8.1	0.95
41809	7.9	0.89

637578	7.9	0.97
95848	7.7	0.90
624169	7.7	0.96
757	7.7	1.00
154754	7.6	0.91
166381	7.6	0.82
157930	7.6	0.86
603624	7.5	0.92
79688	7.5	0.97
19857	7.4	1.05
115493	7.3	0.94
359463	7.3	0.45
4114	7.2	1.15
109444	7.2	1.01
157004	7.1	1.11
349644	7.1	0.91
352890	7.0	0.94
5200	7.0	1.02
1027	7.0	0.91
175274	7.0	1.09
338720	7.0	0.93
139105	7.0	0.98
635435	6.9	0.96
634928	6.8	0.97
185056	6.8	0.90
658494	6.7	0.95
267033	6.7	1.04
293015	6.7	0.96
310618	6.6	1.17
111119	6.3	1.16
659999	6.1	0.44
146604	6.1	1.12
174176	6.0	1.04
629738	5.9	0.97
116535	5.9	0.93
4728	5.9	1.07
635326	5.9	1.11
282880	5.8	0.85
657799	5.8	0.98
521777	5.8	0.90
3905	5.7	0.92
10447	5.6	1.06
253272	5.5	0.97

7521	5.5	0.94
204985	5.4	1.05
292663	5.1	0.95
373853	5.1	0.92
635321	5.1	1.01
631583	5.1	0.98
311153	5.0	0.29
622190	4.9	1.09
170984	4.7	0.95
78365	4.7	0.98
175296	4.7	0.90
635140	4.6	1.04
39202	4.5	0.91
12825	4.4	0.95
636132	4.4	0.90
320864	4.4	0.80
330515	4.3	0.95
63446	4.3	0.76
634473	4.2	1.01
755	4.2	0.93
349155	4.1	0.98
136037	3.9	1.00
602617	3.9	0.97
1011	3.7	0.87
32065	3.7	1.01
166464	3.7	1.00
407335	3.5	0.88
622116	3.5	0.97
36826	3.4	0.98
243928	3.4	0.87
196524	3.3	1.02
319726	3.2	1.02
374898	3.2	0.97
658285	3.1	0.90
140911	3.1	0.99
249992	3.0	1.08
98542	2.9	0.92
267213	2.9	1.05
369317	2.8	0.95
750	2.7	1.07
634224	2.7	1.17
357683	2.7	0.99
105808	2.6	1.14

168597	2.6	0.98
191392	2.5	1.10
635328	2.5	0.99
11897	2.5	1.05
606532	2.5	0.99
253995	2.4	0.78
645567	2.4	1.04
178249	2.4	0.87
634471	2.3	1.06
155595	2.3	1.17
337851	2.3	0.29
71300	2.2	1.12
66300	2.2	1.21
620261	2.2	0.99
21548	2.1	0.98
90636	2.1	0.84
48151	2.1	0.98
371846	2.1	0.86
65423	2.0	1.12
329279	1.9	0.94
353648	1.7	0.94
406021	1.7	1.10
18938	1.7	1.06
326397	1.6	1.06
647889	1.6	0.89
175634	1.5	0.93
56544	1.5	0.96
679527	1.5	0.98
22842	1.5	1.10
642033	1.4	0.99
117915	1.4	1.00
173904	1.4	1.09
306864	1.3	0.86
630374	1.3	0.89
653000	1.2	0.97
671136	1.2	0.90
80756	1.2	0.97
286193	1.1	1.13
278619	1.1	1.15
637916	1.1	0.97
40212	1.1	0.95
302358	1.1	1.05
654259	1.1	0.98

174280	1.1	0.90
102811	1.0	1.08
604535	1.0	1.08
208913	0.9	1.10
635448	0.8	0.93
629301	0.8	0.91
678932	0.6	1.05
105014	0.4	0.89
668260	0.4	0.94
85236	0.4	1.20
176655	0.3	1.08
38721	0.3	0.93
153858	0.3	0.95
146268	0.2	1.15
268251	0.2	0.96
1771	0.2	0.98
635437	0.1	0.92
624206	0.1	0.81
107412	0.0	0.83
169600	0.0	0.90
65346	0.0	0.92
284356	0.0	1.10
643031	-0.1	1.08
625487	-0.1	1.01
24819	-0.3	1.12
285116	-0.3	0.90
256927	-0.4	1.02
369318	-0.4	0.95
7210	-0.5	0.97
61805	-0.5	0.95
616232	-0.6	1.02
359892	-0.7	0.98
63984	-0.8	1.11
66914	-0.8	0.91
328477	-0.8	0.96
603578	-0.8	0.85
159935	-0.8	0.89
33004	-0.9	1.00
226080	-1.0	0.90
646189	-1.0	0.92
106995	-1.1	0.93
650792	-1.2	0.86
76747	-1.2	1.14

139109	-1.2	1.06
622684	-1.3	1.04
666526	-1.3	0.97
328587	-1.3	0.95
643834	-1.3	0.88
680516	-1.4	0.93
335142	-1.5	0.95
1906	-1.6	1.17
330770	-1.6	0.91
688363	-1.6	0.96
92339	-1.6	1.04
676963	-1.7	0.46
191384	-1.8	1.07
607316	-1.8	0.97
116693	-1.8	0.92
682864	-1.8	0.97
664331	-1.8	1.03
154020	-2.0	0.89
681730	-2.0	0.88
56817	-2.0	0.90
622608	-2.1	1.01
292147	-2.1	1.07
106997	-2.2	0.96
643162	-2.2	1.02
626433	-2.2	0.98
285166	-2.2	0.95
191389	-2.3	1.06
292684	-2.4	1.02
689872	-2.4	1.01
241509	-2.4	1.01
635975	-2.4	0.97
679524	-2.5	0.85
670226	-2.6	1.11
632233	-2.7	1.04
240419	-2.7	0.94
24818	-2.7	1.07
663996	-2.7	1.08
638504	-2.7	0.90
224117	-2.8	1.01
61811	-2.8	0.91
621094	-2.8	0.98
534	-2.8	1.24
307454	-2.9	1.08

40666	-2.9	1.09
328426	-3.0	1.00
640637	-3.0	0.86
1620	-3.0	1.06
638646	-3.1	0.76
653558	-3.1	0.98
128734	-3.1	0.91
642040	-3.2	0.90
620050	-3.3	0.96
192965	-3.4	0.89
7532	-3.4	0.89
262665	-3.4	0.95
623637	-3.5	0.97
627666	-3.6	0.87
646200	-3.7	1.14
281245	-3.7	1.08
637729	-3.8	0.97
675593	-3.8	1.04
313981	-3.8	0.93
63701	-3.8	0.98
643826	-3.8	0.89
95580	-3.8	0.93
18891	-4.0	0.89
284751	-4.0	1.05
673912	-4.0	1.04
403883	-4.0	0.93
54297	-4.0	0.96
269148	-4.1	0.71
143648	-4.1	0.99
208914	-4.1	1.09
623093	-4.2	0.87
640624	-4.2	1.11
11905	-4.3	0.80
128305	-4.3	0.99
634650	-4.4	1.12
651080	-4.4	0.85
624358	-4.4	1.05
4960	-4.5	0.90
662553	-4.6	1.02
614826	-4.8	1.06
29603	-5.0	0.99
684845	-5.0	0.91
175636	-5.0	0.96

73495	-5.1	1.01
106296	-5.2	1.23
687849	-5.2	0.93
118735	-5.2	0.96
15623	-5.2	1.06
147340	-5.2	1.01
333856	-5.2	0.95
129943	-5.2	1.13
637731	-5.3	1.07
652287	-5.4	0.98
671394	-5.4	0.86
282752	-5.5	1.00
76027	-5.5	0.85
658144	-5.5	0.78
697726	-5.6	0.90
202000	-5.7	0.99
603719	-5.7	1.20
643812	-5.7	0.91
248436	-5.7	0.84
89671	-5.9	1.04
90829	-5.9	1.16
266535	-5.9	0.87
107067	-6.0	0.90
654705	-6.0	1.02
657456	-6.1	0.85
74420	-6.1	1.10
400944	-6.2	0.84
241906	-6.2	0.88
191393	-6.3	1.05
618261	-6.4	0.95
235082	-6.4	1.02
26273	-6.4	0.89
40341	-6.4	1.09
622616	-6.5	0.95
659501	-6.6	1.06
82116	-6.7	1.10
635306	-6.8	0.96
176324	-6.8	1.02
635563	-6.8	0.92
301460	-6.9	0.93
667251	-7.0	1.09
80087	-7.0	1.17
645987	-7.0	0.88

640638	-7.0	0.93
56737	-7.2	1.12
635833	-7.3	0.93
376791	-7.3	1.08
631152	-7.3	0.94
682769	-7.3	0.96
34757	-7.4	0.98
624953	-7.5	0.90
674495	-7.5	0.98
98447	-7.6	1.05
163443	-7.6	0.88
601101	-7.8	0.97
658709	-7.9	0.90
683792	-8.0	0.93
4857	-8.0	1.07
611750	-8.1	0.94
51812	-8.1	0.99
624161	-8.2	1.03
636084	-8.2	1.01
186	-8.3	1.16
740	-8.3	1.11
302979	-8.3	0.89
257473	-8.4	1.08
99016	-8.6	1.10
69852	-8.6	1.06
603108	-8.6	1.03
623059	-8.7	0.94
263500	-8.7	1.18
343513	-8.7	0.91
36693	-8.8	0.76
218439	-8.9	0.46
148958	-8.9	0.99
35949	-8.9	1.25
95678	-9.0	0.98
97338	-9.0	0.96
62791	-9.1	0.93
4280	-9.2	1.01
669356	-9.2	1.08
109350	-9.3	0.92
97703	-9.3	1.11
169779	-9.4	1.12
104801	-9.5	1.00
67690	-9.5	1.16

673622	-9.6	1.08
643174	-9.6	1.07
59269	-9.7	0.96
31702	-9.7	0.92
126771	-9.7	1.12
65937	-9.8	1.01
265459	-9.8	1.00
627371	-10.1	0.92
327697	-10.2	1.22
349156	-10.2	0.95
690634	-10.3	0.82
625355	-10.4	1.05
621486	-10.4	1.16
689228	-10.4	1.04
640985	-10.5	0.97
620358	-10.5	0.91
7525	-10.5	0.96
80396	-10.6	1.12
664704	-10.6	0.98
623051	-10.9	0.92
605583	-10.9	0.89
9706	-10.9	0.98
637914	-11.0	1.01
407806	-11.1	1.00
642649	-11.2	1.05
642048	-11.3	0.99
145150	-11.3	1.12
292567	-11.3	0.85
353527	-11.3	1.04
627708	-11.4	1.03
329277	-11.4	1.08
672425	-11.4	0.89
102815	-11.4	0.76
100856	-11.6	0.98
687852	-11.6	0.94
52141	-11.6	0.83
103248	-11.6	0.92
25149	-11.6	0.93
625748	-11.6	0.94
332598	-11.7	0.98
321803	-11.7	1.02
404241	-11.9	1.06
79451	-11.9	0.98

283162	-12.0	1.08
173905	-12.0	1.11
687330	-12.1	0.91
173046	-12.2	0.93
47438	-12.2	1.18
643163	-12.3	1.09
2979	-12.5	1.00
616355	-12.6	1.01
168221	-12.6	0.96
4320	-12.6	0.95
115538	-12.6	1.02
24048	-12.7	1.11
635542	-12.7	0.91
11926	-12.8	1.14
617989	-12.9	0.96
643028	-13.0	0.96
174121	-13.1	0.91
118030	-13.1	0.92
641233	-13.1	0.91
90487	-13.2	1.18
308847	-13.3	1.05
93739	-13.3	0.81
622640	-13.4	1.10
32946	-13.6	1.07
641250	-13.6	0.95
641245	-13.7	0.89
376265	-13.7	1.02
26045	-13.7	0.92
139490	-13.8	0.95
167410	-13.8	0.87
4644	-13.9	1.32
135996	-14.0	1.07
13966	-14.1	1.13
624947	-14.2	0.86
92510	-14.2	1.00
165897	-14.2	1.20
126728	-14.3	1.03
650573	-14.3	0.86
267461	-14.4	1.01
697923	-14.4	1.07
686349	-14.4	0.85
657457	-14.5	1.06
634926	-14.5	0.92

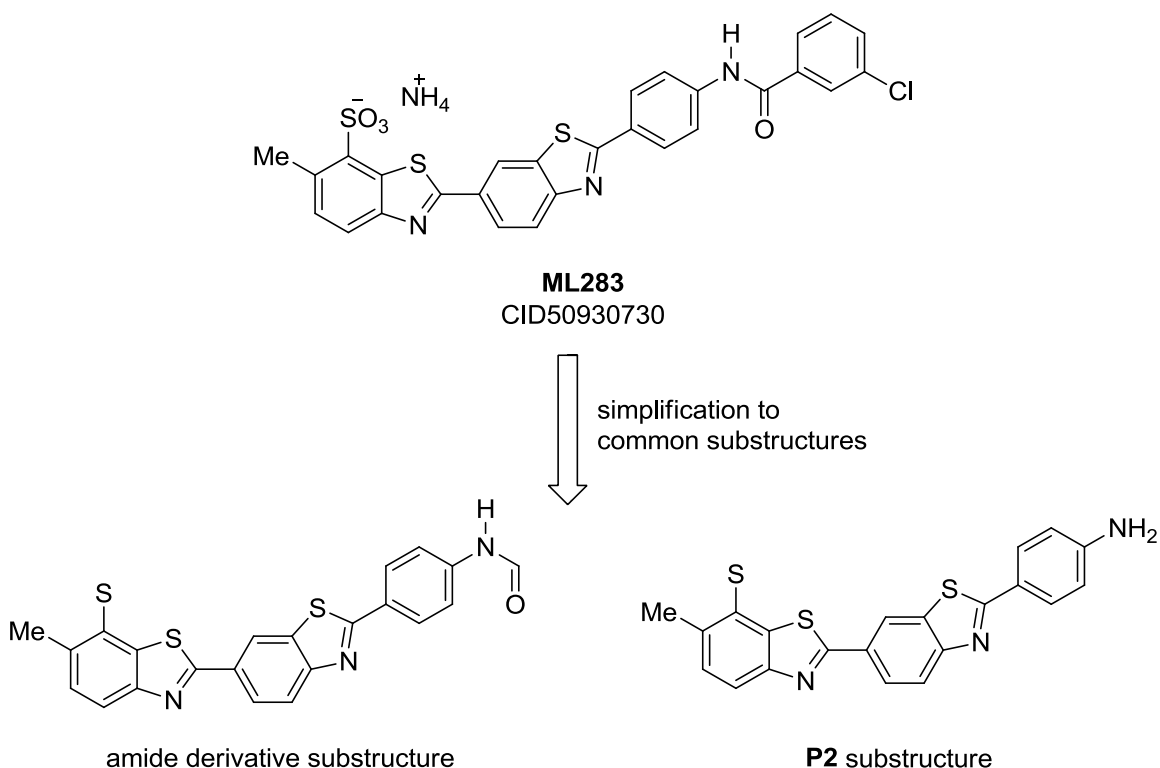
104117	-14.5	1.06
79456	-14.5	0.97
664329	-14.5	1.01
658139	-14.6	1.06
293927	-14.7	1.00
634568	-14.8	0.90
641240	-14.8	0.88
657598	-14.8	0.94
622586	-14.9	0.93
324368	-15.0	0.85
657603	-15.1	0.94
107415	-15.2	0.97
623095	-15.3	0.81
4810	-15.4	1.01
18298	-15.4	0.90
169774	-15.6	0.92
3852	-15.7	1.01
294577	-15.9	0.95
698031	-16.0	0.98
670225	-16.0	1.04
67574	-16.1	0.96
681741	-16.2	0.92
700582	-16.2	0.93
337612	-16.5	0.97
625873	-16.6	1.02
182986	-16.6	1.18
651079	-16.7	1.05
331757	-16.9	0.93
26040	-17.0	0.97
647363	-17.1	0.93
637833	-17.2	0.80
657298	-17.3	1.01
36437	-17.3	0.99
325319	-17.4	0.99
93135	-17.4	0.89
644794	-17.5	0.96
648422	-17.5	1.02
643175	-17.5	0.93
634396	-17.6	0.99
345647	-17.6	0.80
615593	-17.7	0.91
625639	-17.7	1.09
99733	-17.9	1.02

635312	-18.1	0.93
677392	-18.1	1.00
634863	-18.2	0.99
658350	-18.3	1.00
239375	-18.3	0.90
626734	-18.3	1.02
639754	-18.3	1.14
645033	-18.4	0.96
693053	-18.5	0.93
174163	-18.5	1.00
7833	-18.7	1.07
658388	-18.7	1.09
618332	-18.7	1.03
11930	-18.9	1.10
85998	-19.0	1.10
600681	-19.1	0.95
45383	-19.1	1.05
20514	-19.2	1.06
643001	-19.4	0.96
352876	-19.4	1.08
269142	-19.6	1.07
617570	-19.7	0.70
7530	-19.7	0.98
236657	-19.9	0.91
125176	-20.2	0.90
164909	-20.2	1.04
629713	-20.3	0.90
643148	-20.3	0.98
629971	-20.4	0.96
638634	-20.4	0.86
643351	-20.4	0.89
268965	-20.5	0.94
14975	-20.8	1.03
622589	-21.0	0.94
643186	-21.0	1.04
623527	-21.1	0.98
643910	-21.3	1.06
657446	-21.5	1.00
613009	-21.7	0.94
635544	-21.9	0.82
2186	-22.0	1.01
664286	-22.3	1.18
689857	-22.3	0.87

65104	-22.3	1.01
640342	-22.4	0.95
658293	-22.4	1.08
83265	-22.5	0.98
631521	-22.6	0.93
267712	-22.8	1.09
132493	-22.9	1.07
156215	-23.4	1.02
5890	-23.5	0.98
36354	-23.7	1.01
635438	-23.8	1.02
697468	-23.8	0.97
267700	-24.0	1.04
7522	-24.0	0.97
330753	-24.1	0.88
640335	-24.2	0.91
647418	-24.7	1.00
626551	-24.9	0.90
657449	-25.4	1.00
123115	-25.7	0.96
640499	-25.9	0.91
285223	-26.2	1.01
622627	-26.2	1.09
693632	-26.4	0.98
185065	-26.6	1.11
111041	-26.9	0.97
619907	-27.2	0.86
4170	-27.3	1.09
67580	-27.4	1.12
294961	-28.1	1.06
43321	-28.3	1.07
617540	-28.4	1.11
32992	-28.7	1.04
33410	-28.8	1.16
670229	-28.8	1.17
32944	-28.9	1.02
631529	-28.9	1.06
687667	-29.0	1.00
408120	-29.4	1.05
113090	-29.5	1.00
623746	-29.6	0.99
211489	-30.1	0.82
636817	-30.3	1.07

620280	-30.3	1.01
622690	-30.9	1.12
84074	-31.4	1.11
634503	-31.9	0.93
648320	-32.6	1.08
640580	-32.9	1.09
640974	-33.1	0.87
641253	-34.2	0.95
684480	-35.3	1.04
680509	-35.7	0.99
625641	-37.8	1.20
184398	-39.0	1.09
641228	-39.7	0.92
653016	-40.6	1.02
104129	-42.7	0.92
264880	-43.3	1.28
620279	-45.1	1.17

Appendix E: Results of SciFinder substructure searches for the ML283 chemotype.



While all analogues in the SAR tables are novel chemical entities, similar polycyclic benzothiazole-based compounds and mixtures have been investigated for over 60 years as potential dyes and stains. A SciFinder substructure search for any carbonyl derivatives of **P2** did not return any hits indicating that the amide and urea derivatization methods in the SAR tables have not previously been explored. To more fully access the novelty of the probe and analogues as inhibitors of the NS3 helicase, we conducted a SciFinder substructure search on the dimeric primuline component **P2**, which was the starting material for the majority of the analogues and was isolated from commercial material. The search results indicated that 116 substances or mixtures contained this substructure, as reported in 88 patents and references. Of these references and patents, 63 focused on the synthesis or use of the substances as inks or dyes for textiles, outside of a biological context. The 25 remaining references were largely focused on the interaction of these substances and mixtures with organisms and/or molecular structures. The remaining references, where these substances were associated with an enzymatic or phenotypic target or evaluated for therapeutic potential, were the exception and are summarized here (the full bibliography containing 88 entries follows). Most recently, thioflavine S (NSC71948) was singled out from the NCI DTP compound collection as an inhibitor of HSC70/BAG-1 protein-protein interactions (1 and 5). Independently, thioflavine S (NSC71948) was singled out from the NCI DTP compound collection as an inhibitor of the kinase CK2 (6). The dimeric primuline component, **P2**, was reported to selectively inhibit the triosephosphate isomerase of the parasite *Trypanosoma cruzi* (10 and 13). The diazonium dimer of **P2**, direct yellow 29 and related analogues were found to inhibit HIV-induced syncytia formation and the infectivity of CD⁺ cells (18). Finally,

P2 was reported to promote bone growth in the calvarial bone growth assay (20 and 21).

Full SciFinder bibliography:

1. Cichero, E.; Basile, A.; Turco, M. C.; Mazzei, M.; Fossa, P. (2012) Scouting new molecular targets for CFTR therapy: the HSC70/BAG-1 complex. A computational study. *Med. Chem. Res.* DOI:10.1007/s00044-012-9985-1
2. Isono, T.; Omura, N. (2012) Copper electroplating bath compositions and method for filling via holes and through holes by electroplating of copper. *Jpn. Kokai Tokkyo Koho JP 2012021202 A 20120202.*
3. Sheikh, Md. R. K.; Farouqui, A. N.; Yahya, R.; Hassan, A. (2011) Effect of acid modification on dyeing properties of Rajshahi silk fabric with different dye classes. *Fibers and Polymers* **12**, 642-647.
4. Hariharasuthan, R.; Nageswara R. A. (2011) Comparative studies of Sorel's cement on selected dyes. *Indian Journal of Science and Technology* **4**, 410-413.
5. Sharp, A., Crabb, S. J., Johnson, P. W., Hague, A., Cutress, R., Townsend, P. A., Ganesan, A. and Packham, G. (2009) Thioflavin S (NSC71948) interferes with Bcl-2-associated athanogene (BAG-1)-mediated protein-protein interactions. *J. Pharmacol. Exp. Ther.* **331**, 680-689.
6. Prudent R., Moucadel V., Lopez-Ramos M., Aci S., Laudet B., Mouawad L., Barette C., Einhorn J., Einhorn C., Denis J. N., Bisson G., Schmidt F., Roy S., Lafanechere L., Florent J. C., Cochet C. (2008) Expanding the chemical diversity of CK2 inhibitors. *Mol Cell Biochem* **316**, 71–85.
7. Stara, Z.; Krema, F.; Nejezchleb, M.; Skalny, J. D. (2008) Influence of solution composition and chemical structure of dye on removal of organic dye by DC diaphragm discharge in water solutions. *Journal of Advanced Oxidation Technologies* **11**, 155-162.
8. Anon. (2007) Ink-jet printing inks containing encapsulated pigments. *IP.com Journal* **7**, 9.
9. Mondal, Md. I. H.; Farouqui, F. I.; Salam, M. A. (2006) Graft copolymerization of acrylate monomers onto sulfonated jute-cotton blended fabric. *Journal of Applied Polymer Science* **100**, 4393-4398.
10. Espinoza-Fonseca, L. M.; Trujillo-Ferrara, J. G. (2005) Structural considerations for the rational design of selective anti-trypanosomal agents: The role of the aromatic clusters at the interface of triosephosphate isomerase dimer. *Biochemical and Biophysical Research Communications* **328**, 922-928.

11. Lewin-Kretzschmar, U.; Harting, P. (2004) The potential of surfactants modified supercritical fluids for dissolving different classes of substances. *Thermodynamic Properties of Complex Fluid Mixtures* 571-597.
12. Lewin-Kretzschmar, U.; Harting, P. (2004) The potential of surfactant modified supercritical fluids for dissolving polar dyes. *Chemical Engineering & Technology* **27**, 160-170.
13. Tellez-Valencia, A.; Avila-Rios, S.; Perez-Montfort, R.; Rodriguez-Romero, A.; Tuena de Gomez-Puyou, M.; Lopez-Calahorra, F.; Gomez-Puyou, A.. (2002) Highly specific inactivation of triosephosphate isomerase from *Trypanosoma cruzi*. *Biochemical and Biophysical Research Communications* **295**, 958-963.
14. Hipp, J. M.; Carlough, M. S.; Sherrill, W. T.; Stahala, P. J. (2002) Process and composition of sulfur dyes. U.S. Pat. Appl. Publ. US 20020069468 A1 20020613.
15. Klunk, W. E.; Mathis, C. A., Jr.; Wang, Y. (2002) Preparation of thioflavin derivatives for use in antemortem diagnosis of Alzheimer's disease and in vivo imaging and prevention of amyloid deposition. PCT Int. Appl. WO 2002016333 A2 20020228.
16. Miyazawa, T.; Maeda, S. (2001) Optical recording media recordable and/or regenerable by blue-emitting semiconductor lasers. Jpn. Kokai Tokkyo Koho JP 2001301329 A 20011031.
17. Zimnicki, J.; Krysiak, K.; Kazmierska, M. (2000) Dyes as a barrier to UV radiation. Part 2. Objective evaluation of protective properties of fabrics. *Barwniki, Srodki Pomocnicze* **44**, 17-32.
18. Singh, S. K.; Patch, R. J.; Pallai, P. V.; Neidhardt, E. A.; Palace, G. P.; Willis, K. J.; Sampo, T. M.; McDonald, K. W.; Shi, Z. (2000) Aldehyde-arom. sulfonic acid condensation polymers for inhibiting HIV infectivity. U.S. Patent Appl. Publ. US 6075050 A 20000613.
19. Hipp, J. M.; Carlough, M. S.; Sherrill, W. T.; Stahala, P. (2000) Process and composition of sulfur dyes for dyeing fibers. U.S. Patent Appl. Publ. US 6019800 A 20000201.
20. Orme, M. W.; Baidur, N.; Robbins, K. G.; et al. (1998) Compositions and methods for treating bone deficit conditions. PCT Int. Appl. WO 9817267 A1 19980430.
21. Petrie, C.; Orme, M. W.; Baidur, N.; Robbins, K. G.; Harris, S. M.; Kontoyianni, M.; Hurley, L. H.; Kerwin, S. M.; Mundy, G. R. (1997) Preparation of (hetero)aromatic compounds for treating bone deficit conditions. PCT Int. Appl. WO 9715308 A1 19970501.
22. Windsor, S. A.; Harrison, N. J.; Tinker, M. H. (1996) Electro-fluorescence studies of the binding of fluorescent dyes to sepiolite. *Clay Minerals* **31**, 81-94.

23. Sheikh, M. R. K.; Farouqui, F. I.; Hossain, M. I. (1994) Effect of sunlight on the tenacity and color fastness of Rajshahi silk. *Journal of Bangladesh Academy of Sciences* **18**, 209-16.
24. Fujita, H. (1994) Water-resistant ink compositions. Jpn. Kokai Tokkyo Koho JP 06228486 A 19940816.
25. Majumdar, S.; Chatterjee, S. K.; Dey, S.; Ghosh, B. L. (1994) Microbial susceptibility of bleached and dyed jute fabrics and their protection. *Indian Journal of Fibre & Textile Research* **19**, 269-76.
26. Carlson, J. D.; Weiss, K. D.; Bares, J. E. (1993) Polymer containing ionic dye-based electrorheological material for aesthetic visual effect. PCT Int. Appl. WO 9312192 A1 19930624.
27. Colorant-containing electrorheological materials.
28. Rashid, F.; Horobin, R. W. (1991) Accumulation of fluorescent non-cationic probes in mitochondria of cultured cells: observations, a proposed mechanism, and some implications. *Journal of Microscopy* (Oxford, United Kingdom) **163**, 233-41.
29. Rashid, F.; Horobin, R. W.; Williams, M. A. (1991) Predicting the behavior and selectivity of fluorescent probes for lysosomes and related structures by means of structure-activity models. *Histochemical Journal* **23**, 450-9.
30. Rapisarda, A. A.; Mantell, C. M. (1991) Detergent compositions with bleach-stable colorant. Brit. UK Pat. Appl. GB 2233662 A 19910116.
31. Farouqui, F. I.; Hossain, M. I. (1990) Dyeing of jute fiber with direct dyes and their fastness characteristics. *Indian Journal of Fibre & Textile Research* **15**, 65-72.
32. Shapiro, M.; Robertson, J. L. (1990) Laboratory evaluation of dyes as ultraviolet screens for the gypsy moth (Lepidoptera: Lymantriidae) nuclear polyhedrosis virus. *Journal of Economic Entomology* **83**, 168-72.
33. Akeyoshi, H.; Tamura, H.; Suzuki, R. (1989) Positive-charging electrophotographic photoreceptor. Jpn. Kokai Tokkyo Koho JP 01267555 A 19891025.
34. Malinowska-Grabos, Z. (1989) Evaluation of the suitability of some direct dyes for single-bath wool-cellulose blend dyeing. *Przegląd Włokienniczy* **43**, 355-6.

35. Freeman, H. S.; Hao, Z.; Kim, S. D. (1989) Design and synthesis of cellulose-substantive dyestuffs. *American Dyestuff Reporter* **78**, 15-16, 18-20, 22, 24, 48.
36. Bauer, W.; Steckelberg, W.; Ritter, J. (1989) Water-soluble yellow monoazo dyes for recording liquids. Eur. Pat. Appl. EP 311949 A2 19890419.
37. Westphal, J.; Traeubel, H.; Asbeck, H.; Fischer, A.; Goffin, R.; Mueller, W. (1988) Ecological and economical aspects of dyeing of small animal skins. Part 2. *Leder & Haeutemarkt* **40**, 4, 6-7, 10-15.
38. Traeubel, H.; Westphal, J.; Goffin, R.; Fischer, A. (1988) Ecological and economic aspects of dyeing small skins. Part 1. *Leder & Haeutemarkt* **40**, 138-44.
39. Westphal, J.; Traeubel, H.; Asbeck, H.; Fischer, A.; Goffin, R.; Mueller, W. (1988) Ecological and economic aspects of dyeing small skins. Part 2. *Leder & Haeutemarkt* **40**, 145-9.
40. Traeubel, H.; Woynar, H.; Mueller, H. W. (1987) Leather dyeing additives Ger. Offen. DE 3614280 A1 19871029.
41. Kuzmek, B.; Soljadic, I. (1986) Shortened methods for bleaching, finishing and dyeing of textiles. *Tekstil* **35**, 581-91.
42. Juarranz, A.; Horobin, R. W.; Proctor, G. B. (1986) Prediction of in situ fluorescence of histochemical reagents using a structure-staining correlation procedure. *Histochemistry* **84**, 426-31.
43. Faglia, G.; Martinelli, B.; Piccarolo, V.; Solunto, G.; Traubel, H.; Westphal, J.; Zampiva, F. (1985) Dyeing of small and large hides. Basic principles of dye selection for hides. *AQEIC Boletín Tecnico* **36**, 321-30.
44. Bujala, K.; Kawiorska, A. (1985) Color fastness of domestically produced dyes under various conditions for vulcanization. *Biuletyn Informacyjny: Barwniki, Srodki Pomocnicze* **29**, 8-17.
45. Dolezalova, L.; Solta, F. (1985) Study of the toxicity of some types of dyes to aquatic organisms. *Vodni Hospodarstvi: B* **35**, 49-53.
46. Gralinski, M. Dyes for one-bath dyeing of polyamide-cellulose fiber blends. From Zb. Prednasok - Medzinar. Konf. Text. Chem., 15th (1984), 203-9.
47. Trasch, H. F.; Endres, E.; Trost, A.; Rittersdorf, W. (1985) Erythrocyte retaining substrate. Ger. Offen. DE 3323973 A1 19850103.

48. No Inventor data available (1983) Recording inks. Jpn. Kokai Tokkyo Koho JP 58176279 A 19831015.
49. Smith, T. M.; Squires, R. F. (1983) Differential inhibition of brain specific [3H]flunitrazepam binding by several types of dyes. *Neurochemical Research* **8**, 1177-83.
50. Bujala, K.; Gralinski, M.; Jedrzejewski, J.; Salagacki, R.; Zawadzki, A. (1982) Azo dye complex mixture for blends of polyamide and cellulose fibers. Pol. PL 113404 B1 19801231.
51. Puchtler, H.; Waldrop, F. S.; Meloan, S. N. (1983) Application of thiazole dyes to amyloid under conditions of direct cotton dyeing: correlation of histochemical and chemical data. *Histochemistry* **77**, 431-45.
52. Bujala, K.; Kaurzel, Z. (1981) Jute - useful properties, processing, and upgrading methods. *Biuletyn Informacyjny: Barwniki, Srodki Pomocnicze* **25**, 86-92.
53. Pospisil, M.; Pastalka, K. (1980) Purification and isolation of dehydrothio-p-toluidinesulfonic acid. Czech. CS 187779 B1 19790228.
54. Bauer, W.; Bibka, J. (1979) Water-soluble monoazo dyes. Eur. Pat. Appl. EP 5449 A1 19791128.
55. Bauer, W.; Ribka, J. (1979) Water-soluble monoazo dyes and their use in dyeing and printing materials. Ger. Offen. DE 2821350 A1 19791122.
56. Ikeda, T.; Aisawa, T. (1976) Yellow developers for electrostatic imaging materials. Jpn. Kokai Tokkyo Koho JP 51094233 A 19760818.
57. Cowden, R. R.; Curtis, S. K. (1974) Interactions of fluorescent mercurial compounds and acidic fluorochromes with isolated living cells and nuclei. *Histochemistry* **40**, 253-62.
58. Waterkeyn, L.; Bienfait, A. (1971) Primuline-induced fluorescence of the first exine elements and ubisch bodies in Ipomoea and Lilium. *Sporopollenin, Proc. Symp.* 108-27.
59. Blackwell, J. (1972) Azo dyes for paper. Ger. Offen. DE 2151795 A 19720420.
60. Engelhardt, F.; Heid, C.; Dankert, H. (1972) Ger. Offen. DE 2044924 A 19720316.
61. Horobin, R. W. (1971) Analysis and purification of biological stains by gel filtration. *Stain Technology* **46**, 297-304.

62. Wright, R. S. (1971) Reagent for the nondestructive location of steroids and some other lipophilic materials on silica gel thin-layer chromatograms. *Journal of Chromatography* **59**, 220-1.
63. Szokol, M. (1971) Fluorochrome staining of granular cells of the juxtaglomerular apparatus. *Kiserletes Orvostudomány* **23**, 247-51.
64. Shatrov, V. D.; Gordon, E. B.; Ponomarev, A. N.; Tal'roze, V. L. (1971) Luminescence of solid organic dyes during bombardment with thermal hydrogen atoms. *Pis'ma v Zhurnal Eksperimental'noi i Teoreticheskoi Fiziki* **13**, 344-6.
65. Talipov, Sh. T.; Maksimycheva, Z. T.; Andrushko, G. S. (1969) Titrimetric determination of lead in the presence of primulin [sodium bis(dihydrothiitoluidenesulfonate)]. *Doklady Akademii Nauk UzSSR* **26**, 27-8.
66. Stepura, G. S.; Sidorenko, P. G. (1970) Use of fluorochromes for studies of cultures of living tissues and cells. *Kul't. Izolirovannykh Organov, Tkanei Kletok Rast., Tr. Vses. Konf., 1st* 187-91.
67. Kutsenova, A. V. (1970) Dye-sensitized photochemiluminescence of aqueous solutions of serum albumin. *Biofizika* **15**, 793-9.
68. Eirish, M. V.; Ivanova, A. A.; Pshenichnaya, N. F.; Tret'yakova, L. I. (1970) Nature of clay mineral reaction of organic dyes and luminophors. *Gliny, Ikh Mineral., Svoistva Prakt. Znachenie, Itogi Vses. Soveshch. Issled. Ispol'z. Glin, 2nd* 110-19.
69. Gomyo, T.; Yang, Y.; Fujimaki, M. (1968) Comparison of photosensitizing ability of dyes in oxidation of histidine. *Agricultural and Biological Chemistry* **32**, 1061-9.
70. Wallace, M. R.; Milliken, L. T.; Toner, S. D. (1967) Identification of dyes in paper by extraction and chromatographic analysis. *Tappi* **50**, 121A-124A.
71. Hayashi, K.; Kodaira, T.; Ogawa, Y.; Baba, K.; Kikuchi, K.; Tada, K.; Iwasaki, K. (1965) Substance affecting the episomic infective transfer system. I. Relation between the chemical structure of acridine derivatives and the inhibitory action on multiple-drug-resistance transfer. *Kyoritsu Yakka Daigaku Kenkyu Nenpo* **10**, 33-43.
72. Bowman, R. L.; Alexander, N. (1966) Ozone-induced chemiluminescence of organic compounds. *Science* **154**, 1454-6.
73. Villanua, L.; Carballido, A.; Olmedo, R. G.; Valdehita, M. T. (1964) Synthetic food colors. IX. Characteristics, properties, spectrophotometry, and chromatography of some water-soluble artificial dyes. *Anales Bromatol. (Madrid)* **16**, 377-94.

74. Lange, F. W. (1965) Pyridine derivatives as new types of oxidative hair dyes. *Fette, Seifen, Anstrichmittel* **67**, 222-7.
75. Puchtler, H.; Sweat, F.; Kuhns, J. G. (1964) Binding of direct cotton dyes by amyloid. *Journal of Histochemistry and Cytochemistry* **12**, 900-7.
76. Korson, Roy (1964) Silver stain for deoxyribonucleic acid. *Journal of Histochemistry and Cytochemistry* **12**, 875-9.
77. Zeidman, R.; Calin, C.; B., I.; Brenman, S.; Grindea, M. (1962) Stability of direct dyes at temperatures above 100°. *Buletinul Institutului Politehnic din Iasi* **8**, 445-50.
78. Horovitz, M.; Fehervari, M. M. (1962) Properties of some direct dyes in dyeing of polyamides. *Intern. Koloristenkongr., 4, Budapest* 50-6.
79. Barak, J. Edited By:Chukhrov, F. V (1961) Dyeing textiles of wool mixed with native or regenerated cellulose fibers. from No Corporate Source data available (1961), CS 100331 19610715, Language: Unavailable, Database: CAPLUS
80. Yamada, B. Edited By:Chukhrov, F. V. (1962) Azo dyes with s-triazine and urea bridges. *Yuki Gosei Kagaku Kyokaishi* **20**, 386-94.
81. Raju, N. A.; Neelakantam, K. (1960) Azo dyes as analytical reagents for aluminum and beryllium. *Current Science* **29**, 52-3.
82. Allan, Z. J.; Muzik, F. (1953) Aromatic diazo compounds. XII. Identification of primary aromatic amines by means of the absorption spectra of the corresponding azo dyes. *Chemicke Listy pro Vedu a Prumysl* **47**, 380-91.
83. Thaler, H.; Sommer, G. (1953) Dye analysis. IV. Paper chromatographic separation of water-soluble tar dyes. *Zeitschrift fuer Lebensmittel-Untersuchung und -Forschung* **97**, 345-65.
84. Diemair, W.; Boekhoff, K. (1953) Artificial colors and enzyme reactions. V. Effect upon catalase. *Fresenius' Zeitschrift fuer Analytische Chemie* **139**, 267-78.

85. Diemair, W.; Boekhoff, K. (1953) Artificial colors and enzyme reactions. IV. Effect on trypsin and the intestinal juices. *Fresenius' Zeitschrift fuer Analytische Chemie* **139**, 35-42.
86. Diemair, W.; Boekhoff, K. (1953) Artificial colors and enzyme reactions. III. Effect on pepsin and stomach juices. *Fresenius' Zeitschrift fuer Analytische Chemie* **139**, 25-34.
87. Akashi, H.; Oda, R. (1950) Reactions between furfural and diazonium salts. III. Synthesis of new dyestuffs from arylfurfural. *Chem. Soc. Japan, Ind. Chem. Sect.* **53**, 202-3.
88. Schubert, M. (1947) Identification of dehydrothiolutidine- and primulinesulfonic acid. *Justus Liebigs Ann. Chem.* **558**, 10-34.